DEVELOPMENT OF STANDARD METHODOLOGY TO MEASURE SULFATE IONS IN POST-TENSIONED GROUTS

FINAL REPORT

Project BDV29 977-43
(800002803)

Submitted To
FDOT Research Center
605 Suwannee Street
Tallahassee, FL 32399

Project Manager
Ron Simmons
Florida Department of Transportation, State Materials Office
5007 NE 39th Avenue
Gainesville, FL 32609

Principal Investigator: Kingsley Lau

Submitted By

Kingsley Lau
Florida International University
10555 W. Flagler Street
Miami, FL 33174

April 2021

Report Prepared by:
Samanbar Permeh
and Kingsley Lau

DISCLAIMER

This investigation was supported by the Florida Department of Transportation. The opinions, findings, and conclusions expressed here are those of the authors and not necessarily those of the Florida Department of Transportation or the U.S. Department of Transportation.

The contributions by Rutambara Sonawane to the work including the literature review and assistance with specimen assembly and data collection is acknowledged here. The assistance provided by Jonathan Hadad greatly appreciated.

Portions of the document were presented in conference proceedings, including:

1. S. Permeh, R. Sonawane, K. Lau, R. Simmons, and M. Duncan. “Update on the Evaluation of Grout Robustness and Corrosion by Accelerated Corrosion and Rapid Macrocell Testing.” NACE Corrosion/2021 (Virtual Conference)-2021 Digital Proceedings, Paper No. 16339.15pp.
2. R. Sonawane, S. Permeh, K. Lau, R. Simmons, and M. Duncan, “Review on the Determination of Sulfate Ion Concentrations in Deficient Post-Tensioned Grout” NACE Corrosion/2021 (Virtual Conference) - 2021 Digital Proceedings, Paper No. 16342.14 pp.
3. R. Sonawane, S. Permeh, D. Garber, K. Lau, R. Simmons, and M. Duncan, “Test Methods to Identify Robustness of Grout Materials to Resist Corrosion” NACE Corrosion/2020. 51320- Summer 2020 Digital Proceedings, Paper No. 14820.14 pp.

APPROXIMATE CONVERSIONS TO SI UNITS

SYMBOL	WHEN YOU KNOW	MULTIPLY BY	TO FIND	SYMBOL
LENGTH				
in	inches	25.4	millimeters	Mm
mils	mils	25.4	micrometers	Mm
ft	feet	0.305	meters	M
yd	yards	0.914	meters	M
mi	miles	1.61	kilometers	km

SYMBOL	WHEN YOU KNOW	MULTIPLY BY	TO FIND	SYMBOL
AREA				
in^2	squareinches	645.2	square millimeters	mm^2
ft^2	squarefeet	0.093	square meters	m^2
yd^2	square yard	0.836	square meters	m^2
ac	acres	0.405	hectares	ha
mi^2	square miles	2.59	square kilometers	km^2

SYMBOL	WHEN YOU KNOW	MULTIPLY BY	TO FIND	SYMBOL
VOLUME				
fl oz	fluid ounces	29.57	milliliters	mL
gal	gallons	3.785	liters	L
ft^3	cubic feet	0.028	cubic meters	m^3
yd^3	cubic yards	0.765	cubic meters	m^3
NOTE: volumes greater than 1000 L shall be shown in m^3				

SYMBOL	WHEN YOU KNOW	MULTIPLY BY	TO FIND	SYMBOL
MASS				
oz	ounces	28.35	grams	g
lb	pounds	0.454	kilograms	kg
T	short tons (2000 lb)	0.907	megagrams (or "metric ton")	Mg (or "t")

SYMBOL	WHEN YOU KNOW	MULTIPLY BY	TO FIND	SYMBOL
TEMPERATURE (exact degrees)				
^{o}F	Fahrenheit	5 (F-32)/9 or (F-32)/1.8	Celsius	^{o}C
SYMBOL	WHEN YOU KNOW	MULTIPLY BY	TO FIND	SYMBOL
ILLUMINATION				
fc	foot-candles	10.76	lux	lx
fl	foot-Lamberts	3.426	candela/m^2	cd/m^2

SYMBOL	WHEN YOU KNOW	MULTIPLY BY	TO FIND	SYMBOL
FORCE and PRESSURE or STRESS				
lbf	poundforce	4.45	newtons	N
lbf/in^2	poundforce per square inch	6.89	kilopascals	kPa

APPROXIMATE CONVERSIONS TO US. CUSTOMARY UNITS

SYMBOL	WHEN YOU KNOW	MULTIPLY BY	TO FIND	SYMBOL
LENGTH				
mm	millimeters	0.039	inches	in
µm	micrometers	0.039	mils	mils
m	meters	3.28	feet	ft
m	meters	1.09	yards	yd
km	kilometers	0.621	miles	mi

SYMBOL	WHEN YOU KNOW	MULTIPLY BY	TO FIND	SYMBOL
AREA				
mm^2	square millimeters	0.0016	square inches	in^2
m^2	square meters	10.764	square feet	ft^2
m^2	square meters	1.195	square yards	yd^2
ha	hectares	2.47	acres	ac
km^2	square kilometers	0.386	square miles	mi^2

SYMBOL	WHEN YOU KNOW	MULTIPLY BY	TO FIND	SYMBOL
VOLUME				
mL	milliliters	0.034	fluid ounces	fl oz
L	liters	0.264	gallons	gal
m^3	cubic meters	35.314	cubic feet	ft^3
m^3	cubic meters	1.307	cubic yards	yd^3

SYMBOL	WHEN YOU KNOW	MULTIPLY BY	TO FIND	SYMBOL
MASS				
g	grams	0.035	ounces	oz
kg	kilograms	2.202	pounds	lb
Mg (or "t")	megagrams (or "metric ton")	1.103	short tons (2000 lb)	T

SYMBOL	WHEN YOU KNOW	MULTIPLY BY	TO FIND	SYMBOL
TEMPERATURE (exact degrees)				
^{o}C	Celsius	1.8C+32	Fahrenheit	^{o}F

SYMBOL	WHEN YOU KNOW	MULTIPLY BY	TO FIND	SYMBOL
ILLUMINATION				
lx	lux	0.0929	foot-candles	fc
cd/m^2	$candela/m^2$	0.2919	foot-Lamberts	fl

SYMBOL	WHEN YOU KNOW	MULTIPLY BY	TO FIND	SYMBOL
FORCE and PRESSURE or STRESS				
N	newtons	0.225	poundforce	lbf
kPa	kilopascals	0.145	poundforce per square inch	lbf/in^2

Technical Report Documentation Page

1. Report No.	2. Government Accession No.	3. Recipient's Catalog No.
4. Title and Subtitle Development of Standard Methodology to Measure Sulfate Ions in Post-Tensioned Grouts		5. Report Date April 2021
		6. Performing Organization Code
7. Author(s) Samanbar Permeh, Kingsley Lau, and Berrin Tansel		8. Performing Organization Report No.
9. Performing Organization Name and Address Florida International University 10555 W. Flagler St. Miami, FL 33174		10. Work Unit No. (TRAIS)
		11. Contract or Grant No. BDV29 977-43
12. Sponsoring Agency Name and Address Florida Department of Transportation 605 Suwannee St. MS 30 Tallahassee, FL 32399		13. Type of Report and Period Covered: Final Report March 2018 – July 30, 2021
		14. Sponsoring Agency Code
15. Supplementary Notes		

16. Abstract

Steel corrosion in the deficient grout however was associated with elevated concentrations of sulfate ions stemming from the adverse influence of excess mix water and grout pre-hydration. There has been discussions for appropriate ways to address sulfate levels in grout including sulfate limits. Various test methodologies can include varying material conditioning procedures including heating, drying, and chemical reactions that can influence the level of sulfate ion aggregation in the test leachate from the initial bulk material. The research sought to identify ion transport mechanisms in and to identify the effects of grout sampling methodologies for deficient grouts. Testing included a proposed inverted-tee test (INT) and a modified incline-tube (MIT) test. It was shown that the different grout products have widely different propensity for segregation and accumulation of sulfate ions, but adverse grout mixing practices such as the addition of 10% mix water above the manufacturer's recommendation and pre-hydration promoted the development of grout deficiencies including the accumulation of sulfate ions even without external sulfate ion sources. Testing considered the effect of leaching heating, heating time, leaching volume, grout sample mass, and drying temperature. Leaching of larger grout sample mass can yield higher leachate sulfate concentrations, but the concentrations were not commensurate to the larger grout mass. Larger mass to water ratio (1:40) yielded higher leachate and normalized grout mass sulfate concentrations. The sulfate limits expressed as mass relative to the grout sample mass can be implemented to normalize leaching volume and mass size. Current FDOT specifications (30 ppm following current FM 5-618) can be expressed as 3 mgsulfate/ggrout. Assessment of this limit to the corrosion data set developed is consistent with historic data from previous research.

17. Key Word Grout, Post-Tension, Sulfate, Sulfate testing, Leaching, Corrosion, Pore water,	18. Distribution Statement		
19. Security Classif. (of this report) unclassified	20. Security Classif. (of this page) unclassified	21. No. of Pages 99	22. Price

EXECUTIVE SUMMARY

The severe corrosion of steel strand in posttensioned (PT) tendons containing segregated thixotropic grout in Florida bridges was not consistently associated with the typical causes of corrosion of PT structures such as chloride ion contamination, bleed water/grout void formation, and grout pore water carbonation. Steel corrosion in the deficient grout however was well associated with elevated concentrations of sulfate ions stemming from the adverse influence of excess mix water and grout pre-hydration. There, the sulfate ion concentrations can be locally elevated without external sources due to the segregation and transport processes.

There has been discussions for appropriate ways to address sulfate levels in grout. The suggestion to implement material sulfate limits would bring into question, for practical quality testing, when and where it would be appropriate to test sulfate concentrations. Material robustness testing can be considered as part of the material selection process. Difficulty arises due to the inconsistent reproducibility and variability of deficient grout modality, stability, and volume. Furthermore, various test methodologies can include varying material conditioning procedures including heating, drying, and chemical reactions that can influence the level of sulfate ion aggregation in the test leachate from the initial bulk material that may not well represent actual sulfate ion concentrations in the initial pore water.

The major research objectives sought to identify ion transport mechanisms in grouts in tendons with vertical deviation and to identify the effects of grout sampling methodologies on deficient PT grout for sulfate levels. An excess of mix water, 10% above the manufacturers' recommended limit was added for all test specimens. Test grout specimens were cast following a proposed inverted-tee test (INT) that incorporated a large change in the vertical axial cross-section to facilitate the displacement of water during the pumping stage of the grout installation as well as a modified incline-tube (MIT) test involving the pumping of grout in a 3-inch diameter pipe, along a 15-foot length at a 30 degree incline. Grout test conditions included the grout product, tee-stem height (1 ft to 5 ft), space constriction (with filters), grout pre-hydration (using expired grouts), and influence of external ion contamination (sulfate and chloride ions).

It was shown that the different grout products have widely different propensity for segregation and accumulation of sulfate ions, but adverse grout mixing practices such as the addition of 10% mix water above the manufacturer's recommendation and pre-hydration promoted the development of grout deficiencies including the accumulation of sulfate ions even without external sulfate ion sources. Sulfur content in the grout raw material showed modest correlation to the stratification of sulfate ions. Grout flow restriction did not show appreciable effects on the accumulation of sulfate ions and the mobilization of the sulfate ions was enhanced by moisture transport.

Six leaching methods were employed to assess the effect of leaching heating, heating time, leaching volume, grout sample mass, and drying temperature. Leaching of larger grout sample mass can yield higher leachate sulfate concentrations, but the concentrations were not commensurate to the larger grout mass. Leaching of a larger grout sample mass with a mass to water ratio of 1:10 was not shown to be efficient in the dissolution of sulfate ions. Larger mass to water ratio (1:40) yielded higher leachate and normalized grout mass sulfate concentrations. Pre-drying of grout samples to 100^{o}C for 24 hours was shown to incur losses in sulfate content.

The corrosion potentials and corrosion current densities for the steel embedded in the INT and MIT specimens were correlated to the grout sulfate content and the values produced from the test program here were consistent with historical data from earlier research, further verifying the adverse effects of elevated sulfate ion concentrations in the segregated grout. The expired grouts developed the highest sulfate ion concentrations and showed the greatest susceptibility for corrosion development. The sulfate limits expressed as mass relative to the grout sample mass can be implemented to normalize leaching volume and mass size. Current FDOT specifications (30 ppm following current FM 5-618) can be expressed as 3 $mg_{sulfate}/g_{grout}$. Assessment of this limit to the corrosion data set developed is consistent with historic data from previous research.

The sulfate content associated with severe corrosion was associated with deficient grout materials with high moisture content. As such, it is recommended that the sulfate testing be incorporated into material testing to assess the susceptibility of grout materials to segregate. Test methods such as the modified incline tube test incorporating overwatering in the grout mixing or alternative testing to facilitate the capturing of displaced water such as the inverted-tee test should be considered for grout material sampling. In the field, extraction of grout materials from locations typically associated with moisture and/or bleed such as at high points, points of deviation, and at joints should be considered.

TABLE OF CONTENTS

LIST OF FIGURES

LIST OF TABLES

CHAPTER 1. INTRODUCTION

The severe corrosion of steel strand in posttensioned (PT) tendons containing segregated thixotropic grout in Florida bridges was not consistently associated with the typical causes of corrosion of PT structures such as chloride ion contamination, bleed water/grout void formation, and grout pore water carbonation. Steel corrosion in the deficient grout however was well associated with elevated concentrations of sulfate ions. Findings from earlier research (BDV29-977-04) indicated possibility for steel corrosion activation in the presence of sulfate ions. The extent of corrosion is largely affected by the pore water pH and by the early presence of sulfate ions to impair initial passive film grout. Research findings identified possible mechanisms for grout segregation and corrosion initiation. Outcomes from those research efforts identified the negative influence of excess mix water and grout pre-hydration, posited test methods to identify grout segregation, identified the plausibility of steel corrosion initiation in sulfate grout solutions, and identified enhanced corrosion in the presence of sulfate ions combined with low-level chloride ion concentrations. The continued dissemination of information on grout material deficiency and corrosion development led to national and international attention to this durability concern.

There has been discussions for appropriate ways to address sulfate levels in grout, but ratification of standardized specification language remains open due to several unresolved technical issues. The major overarching question concerns the source of the elevated sulfate ions. Anecdotally, it was thought that gypsum would be the major source for sulfate ions. lt was also posited that the sulfate source may be related to kiln dust with contamination of alkali sulfates. Nevertheless, the high concentrations of sulfate ions in the field extracted deficient grout after construction indicated dissolution of sulfur bearing species into free sulfate in the grout pore water.

The early development of steel corrosion indicated fast transport of sulfate ions through the tendon. Previous research observations showed that the development of segregated grout was largely enhanced with large test sample casting with physical material segregation occurring after the tendon was already filled with grout and where significant air, water, and solid materials rapidly moved through the tendon. There, the sulfate ion concentrations can be locally elevated without external sources due to the segregation and transport processes.

The suggestion to implement material sulfate limits would bring into question, for practical quality testing, when and where it would be appropriate to test sulfate concentrations. Testing of the raw grout product would ideally provide early indicator of elevated incipient sulfate presence. However, the localized sulfate ion accumulation that can occur due to segregation after casting would indicate that additional testing would be needed to identify the in-situ sulfate levels. Testing of deficient grouts or excess moisture possibly from tests such as wick-induced bleed, schupak pressure, or inclined tube test may be useful for laboratory sampling of

grouts to identify sulfate ion accumulation. Material robustness testing can be considered as part of the material selection process. Testing after casting at various field tendon locations (especially tendons with vertical deviation) may be implemented as part of quality checks.

The next unresolved issue includes identifying appropriate methodology to sample and analyze deficient grout materials. Chemical analysis of sulfate ion concentrations in aqueous solution including ion chromatography, turbidity measurements, and chemical titrations is well established. ln the solid form, material analytical techniques including x-ray fluorescence and powder x-ray diffraction may be of interest as well. However standardized methods to sample sulfate ions in the grout pore water from hardened grout has not been well disseminated. Some investigators have modified standard test methods to identify sulfate ions in soil, but the material chemistry and solid properties of soils and cementitious materials are widely different. Several sampling methods have been proposed for hardened concrete including ex-situ and in-situ leaching as well as pore water expression. Difficulty arises due to the inconsistent reproducibility and variability of deficient grout modality, stability, and volume. Furthermore, various test methodologies can include varying material conditioning procedures including heating, drying, and chemical reactions. These steps would influence the level of sulfate ion aggregation in the test leachate from the initial bulk material that may not well represent actual sulfate ion concentrations in the initial pore water. lndeed, earlier testing implementing various sample pre-treatments yielded different levels of sulfate ions. There are several important questions to be addressed to determine appropriate test methods to specify sulfate ions in PT grouts.

The major research objectives to be explored include:
1. To identify the extent that vestigial sulfur-bearing cement or grout constituents contribute to sulfate ion levels in hardened and deficient grout pore water.
2. To identify ion transport mechanisms in grouts in tendons with vertical deviation.
3. To identify if sulfate content in raw grout materials or from laboratory bleed water tests can be used to characterize corrosion sulfate limits.
4. To identify the effects of grout sampling methodologies on hardened and deficient PT grout for total and water soluble sulfate levels.

Findings addressing these objectives will allow recommendation and validation of methodologies to test sulfate levels in PT grouts including feasibility to address sulfate limits as material specification, quality control, and durability assessment. importantly, findings will provide recommendation for testing procedures to sample hardened and deficient grout. Efforts to address these items are needed to allow appropriate development of standard methodologies to test PT grouts for remediation and maintenance decisions.

The intent of the research is to identify/develop test methodologies to measure sulfate ion content in PT grout for possible material specification of sulfate limits. However, any future specification language will have to not only provide clear indication of a quantifiable limit value, but also how to sample and analyze the grout as well as clarify the time and place for appropriate testing. Development of standard test methods must consider the intent of the testing that may include raw material specifications for material selection and compliance, quality control of construction, and assessment for corrosion durability.

The following objectives and approach were proposed:

1. ldentify the extent that vestigial sulfur-bearing cement or grout constituents contribute to sulfate ion levels in hardened and deficient grout pore water. Commercial PT grout products have proprietary mixes and cement components are typicaliy provided by external suppliers, thus the vestigial sulfate content in the raw grout product can vary. Identification of the level of dissolution of sulfate into solution is required to address possible initial sources of sulfate ion in segregated grout.

2. ldentity sulfate ion transport mechanisms in grouts in tendons with vertical deviation. Localized accumulation of sulfate ions in grout pore water solution can occur due to various ion mobilization and transport mechanisms such as hydraulic and capillary action and diffusion. Mobility of ionic species in grout pore water is also pertinent in relation to ionic strength. Understanding of these transport mechanisms is required to identify how sulfates may be temporally and spatially distributed in deficient grout.

3. ldentify the effects of grout sampling methodologies on hardened and deficient PT grout for total and water soluble sulfate levels. Sampling procedures, sample conditioning, and analysis techniques can affect the yield sulfate content. As further complication, sulfur bearing species are innate to cement constituents and do not necessarily play a role in corrosion. Thus, test procedures must appropriately address only sulfate levels that can diminish material durability. Furthermore, some analytical techniques require sufficient material quantities that may not be easily obtainable in practice and as observed in the field, deficient grouts are not easily preserved. Consideration of sample size (mass and volume), sample preservation, physical, chemical and environmental conditioning to promote extraction or leaching, dilutions, and constraints of analytical techniques should all be considered.

CHAPTER 2. LITERATURE REVIEW

2.1 CORROSION DURABILITY PROBLEMS OF STEEL STRAND EMBEDDED IN GROUTED TENDONS

Prestressed concrete bridge construction in the United Stated became widely used in the twentieth century. It allows the construction of large bridges with longer spans and opens up the range of design possibilities. The term prestressing is used to describe the process of introducing internal forces in a concrete structural element during the construction process in order to resist the external loads that will be applied when the structure is put into use [1]. When the steel is tensioned after concrete placement the process is called post-tensioning (PT). The prestressing strand, duct, and filler material are collectively referred to as a tendon. The tendon can be embedded or placed within the open spaces of an enclosed concrete structural elements. There has been a concern over the inspection of tendons in post-tensioned concrete bridges because of the difficultly of detection and quantifying the extent of deterioration [2].

Corrosion damage to the prestressed steel of PT concrete components can occur by different mechanisms depending on the prestressing conditions and environmental exposure. PT tendons are differentiated as being bonded or unbounded. The unbonded PT tendons typically rely on fillers (i.e., grease and wax) to provide encapsulation of the steel and act as a barrier to environmental exposure. The prestress steel is set in an injected cementitious grout in bonded PT systems. The systems used for bonded PT concrete typically consist of the concrete structural element, pre-stressing steel (in the form strand, wire, or bar), duct that houses the pre-stressing steel, cementitious grout, and the anchorage system [2]. Concrete is cast in a mold and allowed to reach a predetermined strength before the prestressing steel is tensioned. The alkaline cementitious environment in the grout of bonded PT concrete provides stable steel passivation that prevents any significant corrosion; however, occurrence of steel corrosion has been documented for some cases. For example, corrosion failures of PT tendons in a Florida bridge utilizing pre-packaged thixotropic grout products were recently documented [3-15].

The localized occurrences of severe corrosion of the steel strand were not always consistent with the presence of voids in the tendon but the locations of severe corrosion were well associated with the development of deficient grout that was generally characterized as having poor cohesive bulk properties and high moisture content [10]. Earlier work by Lau et al. presented field observations and material assessment of deficient grout [4-9]. There was good correlation between the occurrence of deficient grout conditions, corrosion development, and enhanced sulfate ion levels. The data from the field inspections showed that corrosion development of steel strand in the presence of enhanced sulfate ion concentrations predominantly occurs when the grout has significant physical material degradation.

The data available in the literature indicate that enhanced sulfate ion concentrations can lead to corrosion development in environments relevant to grout systems [16-28].

Deficient grouts exhibit nonuniform segregation of materials. Conditions that cause grout degradation and grout deficiency depend on parameters such as the amount of moisture added during mixing, ion composition, adequacy of mixing, temperature, and quality of water used in grout preparation. Grout segregation creates differences in pore water chemistry and physical properties (i.e., porosity, texture). Moisture affects the grout conditions and grout hydration significantly, resulting in deficient grouts during the hardening process [9-10, 29]. In laboratory studies conducted with deficient grouts promoted by non-ideal mix conditions (i.e., addition of excess mix water and using grout past expiration date), it was observed that excess moisture can promote grout deficiency, although the level of deficiency can vary by the grout product used [10-11]. It was observed that high sulfate concentrations can occur (at levels associated with severe corrosion of tendons in Florida) in the deficient grout without any added sulfate [10, 25]. The source of sulfate ions was not identified and has only anecdotally been attributed to the cementitious component of the grout [30]. As a result of the corrosion in bonded PT systems, work to develop material specifications relating to the deficient grout (including limits on sulfate ion levels) have been ongoing for the past several years [31-36].

Mobilization and stratification of ions and moisture in tendons during grout hydration can result in deficient grout conditions. Such stratification of ions in tendons can create favorable conditions that promote chemical and/or biochemical corrosion processes.

Oxidation of iron (Fe2+), under anaerobic conditions is a critical pathway in the biogeochemical cycles. Chloride ions also play an important role in initiating the corrosion process. The pitting corrosion in stainless alloys occurs in neutral-to-acid solutions by chloride ions [37]. Although the initiation mechanisms of corrosion by chloride ions are not well understood, one hypothesis is that chloride ions reduce the resistance of iron by incorporating into the passive film and resulting in establishment of an anodic area where corrosion continues (i.e., chloride induced passive corrosion) [38]. A second hypothesis is the interaction of chloride ions with Fe^{2+} to form soluble complexes (i.e., a passive film is not formed) which stimulates further dissolution of Fe^{2+} (i.e., chloride induced active corrosion) [38].

Although there is increased use of post-tensioned (PT) bridge constructions, several challenges with their use have come to the light. There have been recent changes in material and construction specifications for PT bridge construction due to documented corrosion of steel tendons in several bridges in the past three decades. The collapse of the Bickton Meadow bridge in Hampshire (UK) in 1967 and then the

Ynys-y-GWAS in West Glamorgan (UK) in 1985 led to prohibition of the prestressed bridge construction in the British Ministry of Transportation [39]. It was identified that the ineffective corrosion protection of prestressing steel at concrete segment joints was the reason behind the failure of the Ynys-y-GWAS bridge where moisture and chloride penetrated through the joints. Corrosion of tendons in post-tensioned structures due to improper duct filling, chloride penetration through defected ducts or hydrogen embrittlement are well documented. In the last 25 years, use of fluid grouts in France facilitated the injection of the prestressed ducts. In 1994, anomalies were detected at the upper point of the sheaths in an investigation of external prestressing tendons of a box girder bridge under construction. After opening of some of these, an incomplete grout filling was observed along with the presence of a product having consistency of a wet and soft paste. The Walnut Lane bridge in Philadelphia (1949-1950) was replaced in the mid of 1980 due to grouting problems which led to significant corrosion damage to the post-tensioned tendons.

Other cases of tendon corrosion include the Nile Channel Bridge in the Florida Keys after 18 years of service and the Mid Bay Bridge after 7 years of service in 2000. The Sunshine Skyway Bridge and Varina-Enon in the USA are other examples of the failure of the post-tensioned system after less than 2 decades of service. In May 2018, the westbound span of Charleston's James B. Edwards Bridge closed for several weeks because of the cable inside was snapped and the routine inspection showed damage to the cable inside the box-girder span. Corrosion of PT tendons have conventionally been associated with the development of bleed water and voids in PT grout. Subsequent material specifications required thixotropic grouts to prevent bleed water formation. However, corrosion failure of external PT tendons were documented in 2011 in a Florida bridge after being in service for 8 years. The corrosion there was associated with deficient grout having high moisture content, high free sulfate ion concentration, high pore water pH, and low chloride ion content.

Earlier research of Bertolini and Carsana, 2011 [40] has shown that the segregation of injection cement grout for prestressing cables may lead to the formation of a whitish phase with plastic consistency, characterized by high content of alkalis and sulfate ions. It has been observed that the concentration of chloride was lower than the conventional threshold, but the concentration of sulfate was higher [8]. The high sulfate concentration can be accumulated in deficient grouts without external sources [25].

2.2. DEVELOPMENT AND DESIGN OF PT GROUT

The concrete sections can minimize exposure of the external tendons by providing clear cover over internal strands in pre-tensioned systems and internal tendons in post-tensioned system from aggressive chemicals such as chloride ions and carbon dioxide as well as moisture from the external environment. The grout material likewise is an important aspect of overall bridge corrosion durability as it

provides additional barrier to protect the steel strand from environmental exposure. Furthermore, the cementitious grout provides an alkaline environment which passivates the surface of steel to control the corrosion process. The steel strand should be full surrounded and bonded with the grout to protect it from corrosion. The successful grouting operation depends on pumping and mixing of grout materials.

2.2.1. Grout Material

The Post-Tensioning institute (PTI) classifies grout materials in four different classes based on material specifications and field requirements:

Class A- Nonaggressive: indoor or nonaggressive outdoor.
Class B- Aggressive: subject to wet/dry cycles, marine environment, deicing salts.
Class C- Non-Aggressive or aggressive (Pre-packages)
Class D- Determined by Engineer.

Grout A does not have thixotropic properties. Group B, C, and D grouts may or may not exhibit thixotropic properties due to different combination of admixtures (PTI M55.1-12, Specification for Grouting of Post-Tensioned Structures, Section 3.3). Primarily, grout is made of Portland cement (type I or II) conforming to the requirements by ASTM C150/C150M. Resistance to aggressive environment can be achieved by adding other cementitious material such as silica fume.

2.2.2. Cement Chemistry

Cement is normally made up of limestone, shells, and combination of shale, clay, slate, blast furnace slag, silica sand and iron ore. The Portland cement is made by heating a mixture of limestone and clay and partial fusion produced clinker. ASTM C150/C150M (2012) stated that Portland cement can be composed of 5% limestone filler material. The clinker is mixed with a few percent of calcium sulfate to make the cement. The clinker is made up of 67% Cao, 22% SiO_2, 5% Al_2O_3, 3% Fe_2O_3 and 3% other components. The clinker has four major phases such as alite, belite, aluminate, and ferrite. The other phases of clinker, such as alkali sulfates and calcium oxide are normally present in minimum amounts. The term hydration means the changes which occurs when anhydrous cement is mixed with the water. The cement has certain physical properties such as settling time, soundness, fineness, consistency, compressive strength, heat of hydration, loss of ignition, and specific gravity that must be conform to ASTM C150.

In the chemical process of the cement, the chemical reactions taking place are generally complex conversions of anhydrous compounds into corresponding hydrates. Various hydration products form such as C-S-H gel, calcium hydroxide, ettringite, monosulfate or monocarbonate when portland cement comes in contact with water [41]. The important mineral of portland cement is tricalcium aluminate which is formed when appropriate proportion of calcium oxide and aluminium oxide are heated together above 1300°C. Tricalcium aluminate releases a large amount of

heat and provides some early strength to cement. The gypsum is added to delay the tricalcium aluminate hydration process otherwise, without gypsum the portland cement will set almost immediately after adding water. Calcium chloride should be added at the same time to accelerates the process of settling and hardening of portland cement [42]. The dissolution of sulfate and alkali constituents react with tricalcium aluminate in cement hydration process which form tri sulfoaluminate hydrate (ettringite). The ettringite transforms into monosulfates that contain relatively less sulfate which shows imbalance of sulfate in cement [43]. The hydration process can continue for extended period of time even last for years after the initial cement hydration [44].

2.2.3. Admixtures

Chemical admixtures are the ingredients which are added to the mix before or during mixing. Admixtures are classified into five different functions: water-reducing admixtures, retarding admixtures, accelerating admixtures, superplasticizers, corrosion-inhibiting admixtures. There are many types of grout admixtures available in the market such as superplasticizer, expansive, anti-bleed, corrosion inhibitors, fly ash, and silica fumes.

Chemical admixtures can serve multiple roles and can help with pumpability by reducing the viscosity of the grout, while also helping with controlling the time it takes for the grout to set. Researchers investigated the use of mineral and chemical admixtures in developing high-performance grouts and at the same time, grout manufacturers developed various prepackaged cementitious grouts [45-46]. The grout in current practices is primarily Portland cement and can include supplemental cementitious material, admixtures, and fine-sized aggregates. Prepackaged grouts claim to have improved volume stability, strength, and fluidity. The proper use of admixtures depends on the use of appropriate methods of concreting and batching. The effectiveness of the admixture depends on the cement, water content, mixing time, slump, and temperature of the concrete and air.

Set-controlling admixtures have been widely used for many years with portland cement concrete. These admixtures used in grout conform to ASTM C494 and are permitted in PTI section 2.4.1 through 2.4.5. As per PTI M55, Type D-G set-controlling admixtures in grouts are permitted (PTI, M55.1-12(13), specifications, set-controlling admixtures):

Type D: Water-reducing and retarding admixtures
Type E: Water-reducing and accelerating admixtures (only non-chloride type admixtures are permitted in grout for PT)
Type F: Water-reducing, high-range admixtures
Type G: Water-reducing, high-range, and retarding admixtures.

2.2.4. Pozzolanic materials

Silica fume is by-product from the manufacturing of silicon and research has been shown that the addition of silica fume can increase compressive strength, reduce bleed and reduce permeability. The addition of silica fume results in an increased water demand thus, the superplasticizer must be added in grout in order to maintain workability. The amount of superplasticizer depends on the use of silica fume. The silica fume has been found to be thixotropic in nature as they remain sticky and cohesive at rest but remain their fluidity when agitates. Silica fume grouts tend to have lower pH than plain grouts, and the concentration of chlorides necessary to breakdown the passive layer on the steel may be reduced.

Two classes of the fly ash commonly used such as class F and class C. Fly ash tends to reduce bleed and reduce permeability, in addition of fly ash reduces the dosage of superplasticizer needed to maintain adequate fluidity in grouts.

2.2.5. Inhibitors

Corrosion inhibitors are intended to slow the corrosion process of steel. Corrosion inhibitors can be divided into three basic types by method in which they slow the corrosion process. Anodic inhibitors react with the steel to form protective layer and proper dosage depends on the amount of chloride penetration. Cathodic inhibitors form a barrier around the cathodic site to reduce chloride ingress. Mixed Inhibitors are a combination of both the anodic and cathodic type inhibitors. Calcium Nitrite is one of the corrosion inhibitors and it slows down corrosion process.

2.3 EXISTING QUALITY CONTROL TO MITIGATE CORROSION IN GROUTED PT

2.3.1. Material Specifications

2.3.1.a. Bleed

The quality control of each material is necessary during production. The purpose of the testing is to ensure suitability of the material to achieve the aim of full protection and the bond. The testing may include field test, lab test, and material acceptance tests for specific job. An inclined tube test, wicked induced inclined tube test, and the Schupak pressure bleed test are examples of methods to assess grout bleeding.

2.3.1.b. Fluidity and Viscosity

The fluidity and viscosity of the grout material can be measured. Fluidity tests during mockups are used to establish a target range of flow times that are preferable for the grout and conditions before pumping grout into tendons.

In the cone method, the time for a grout to flow through a cone is measured. The flow cone method is specified by PTI M55 4.4.5 and conform to a modified ASTM C939. In the modified test, the flow cone is filled to the top of the flow cone instead of the standard level (1,725 mL). The efflux time of grout, when thoroughly

mixed, is measured as the time to fill a 1 L container. Per PTI M55, a working time is measured after 30 minutes and then remixed for 30 seconds, and the flow is measured within 10 seconds of the originally established flow.

The dynamic viscosity of chemical grouts is measured from the torque of an immersed rotating disc of a rotating viscometer. The relative viscosity factor, RVf, is needed to determine if grouts can be used as filler material for PT structures as specified in Section 938 of FDOT specifications. FM 5-605 specifies a procedure to determining the relative viscosity. In general, the method describes testing of grout samples mixed with a high speed mixer at elevated temperature with a dynamic shear rheometer to calculated RVf as a quotient of viscosity measurements made at 45 and 60 minutes.

2.3.1.c. Temperature:

As per FDOT specifications Section 938, ASTM and FM test methods should be conducted at laboratory temperature of 65^{o}F to 78^{o}F. As per PTI M55 5.8.1, to produce or keep grout cool, a thermal insulation or cooling circulation system may be installed. If it is unavoidable to keep the grout in the required temperature ranges, then special precautions, such as the use of suitable admixtures, should be taken to control flash set. Cold climate conditions are considered whenever the ambient temperature is 40oF and falling. At 32^{o}F, ducts should be kept free from water and moisture to avoid damage due to freezing. PTI M55 5.8.2 mentions that dry ice or liquefied carbon dioxide must not be used for cooling purposes.

2.3.1.d. Wet Density

As per PTI M55 4.7.8, a range of wet density should be used for the optimized grout using the mud balance test at minimum and maximum water dosage. ANSI/API mud balance test can be monitored in the field to verify the water cement ratio and the compactness of the grout. Generally, the mud balance instrument is used to measure the fluid density per ANSI/API, 2017. FDOT Section 938 requires maximum and minimum wet density measurements made in the field and in the lab conforming to ASTM C185 and ASTM C138.

2.3.1.e. Mixing

As per FDOT, the grout should be mixed and pumped as per the grout manufacturer’s recommendations. The batch water shall be metered to accurately measure the water added and water shall never be added in excess of the manufacturer’s recommendations. The mixing following manufacturer’s directions should allow for a homogenous grout free of lumps. The grout should be continuously agitated until pumped and should be used within 30 minutes of the first addition of water. According to PTI’s specification 4.6.2 for grouting of Post-Tensioned Structures water content could be determined by mixing and testing modified flow after 16-25 seconds exactly after mixing.

2.3.2. Hardened Grout

2.3.2.a Setting Time

PTI M55 4.4.1 and ASTM C953 specified setting time tests of grout which is determined using the Vicat apparatus. The Vicat conical ring and base plate is warmed to 100o C and a thin layer of paraffin wax is applied to the base of the conical ring. After cooling the conical ring and base plate to room temperature, the conical ring apparatus should be filled with grout within 2 minutes after mixing. The top of the grout is smoothened, and the specimen stored in a moist room. Procedures following ASTM C191 are followed to determine the setting time by a penetration test with a 1 mm needle after 30 min molding until 25 mm or less penetration obtained.

2.3.2.b. Strength:

Strength of the grout material can be measured and tested in accordance with ASTM C942 on cubes or cylinders using molds compliant with ASTM C109. ASTM C942 strength test for cubes mentions that the mold should be filled halfway and prodded for consolidation until the mold is filled with grout. Molds are placed in the moist room and cured conforming to ASTM C109/C109M. Compressive strength should be measured at age of 7 days and 28 days using compressive strength testing machine following ASTM C109/C109M. As per PTI M55 4.4.2, The compressive strength of cubes should exceed 21 MPa after 7 days.

2.3.2.c. Permeability Test

PTI M55 4.4.3 referred that the permeability test should be performed according to ASTM C1202. Per ASTM C1202, the test method monitors the amount of electric current passing through cylinders during a period of 6 hours. One end of the specimen is immersed in a sodium chloride and another one in a sodium hydroxide solution. The potential difference is continued at 60 V dc and the total charge is measured in coulombs and found to be correlated to the resistance of specimen to chloride ion penetration.

2.3.2.d.Chloride testing:

ASTM C1152/C1152M describes a standard test method for acid soluble chloride in mortar and concrete. The samples are digested in diluted nitric acid. Hydrogen peroxide can be added if a smell of hydrogen sulfide is strong. pH is typically monitored and controlled. After acid digestion, the solution is filtered through filter paper. Potentiometric titrations using 0.05N silver nitrate as a titrant are made to measure the equivalence point.

2.3.2.e Volume Change

The volume change test per PTI M55 4.4.4 follows ASTM C1090. Per ASTM C1090, the grout material should be filled in to the mold and then tapped along the sides of the mold to release air. A coated glass plate is placed at the top of the specimen and then a plunger is lowered. The change in height after 1 to 28 days is

measured as a percentage of the difference in height after the time of test and the original specimen height.

2.3.3. Inspection

2.3.3.a. Corrosion

Corrosion is major issue of the long-term durability of post-tensioned systems. Post grouting inspections include identifying grout quality within the duct, for example sampling grout from vents. Identification of the presence of voids, proper capping of vent caps, and moisture levels are all measures that can be made after grouting.

Hammer soundings, although subjective by operator, can be useful to identify voids in the tendon and other grout anomalies. Field testing by ultrasonic/sonic testing has been shown to be useful to identify presence of grout defects and presence of runoff water within ducts. Post grouting testing of the grout material to identify grout deficiencies including accumulation of ions such as chlorides and sulfates due to segregation may be considered as well to ensure homogeneity of the grout at the injection inlet and outlet of the duct and identify corrosive conditions. In-situ monitoring of relative humidity levels within the duct may also provide indication of moisture levels within the duct.

Magnetic non-destructive testing including magnetic flux leakage (MFL) methods were shown to be useful to identify loss of steel cross-section within the PT duct. However, this testing would only be useful after some level of corrosion has already occurred and not necessarily a means to identify quality of the construction.

2.3.3.b.Void and Segregation

Incomplete grouting and trapped air pockets can cause voids within the post-tensioning duct. Procedures of grouting and proper venting of the post-tensioning duct are very critical. The space between the tendon and the post tensioning duct is very complex and the voids geometry can vary in shape and size. These voids may separate water, cement in the grout and form bleed lenses. This problem can be accented in the interstitial spaces of braided steel wires. The interstitial spaces of 7-wire strand for examples would allow water transport by mechanisms such as capillary action. Vertical ducts with vertical rises typically cause more bleeding due to increased pressure within the grout column.

The presence of voids in the grout of ducts can provide conditions where corrosion development may occur. The voids have been associated with development of grout bleed water at the time of the grouting and then reabsorption into the grout. After void formation, the grout at the steel/void interface would have dissimilar chemical composition as the bulk grout. The region would also be susceptible to moisture, oxygen, and carbon dioxide presence resulting in carbonation, accumulation of chloride ions, galvanic interaction with the metal ducts and anchorages and possible enhanced microcell and macrocell corrosion.

Environmentally assisted corrosion processes such as stress crack corrosion cannot be eliminated.

Segregation is the tendency in which course particles separate from the finer particles. Segregation of grout in tendons in a Florida bridge created regions of material with high water content, low cement content, high pore water pH, accumulation of filler material, silica fume, and sulfate ions. It was thought that high points of the tendon would be most susceptible to grout segregation, but field inspections revealed that similar grout segregation accompanied by severe steel corrosion also occurred at low point anchor sites.

Testing by the modified incline tube test and a proposed inverted tee test showed that regions with higher vertical deviations due to material and water displacement created regions of grout with greater moisture content that contained elevated levels of sulfate ions.

2.3.3.d. Chemical, pH

The pH value of the hydrated grout is high (ie up to pH 13) and mature grouts typically have pH greater than 12. Access to atmosphere in tendons with improper sealing would allow for carbonation resulting in pH drop and carbonation-induced corrosion. Research by Carsana and Bertolini [40] suggested that corrosion of PT strands can be accounted if the grout pore water pH exceeded 14.

2.3.4. Current FDOT Specifications

FDOT section 938 provides specifications for duct filler for PT structures. The department's approved product list should be used for post-tensioned grouts and flexible filler materials. Grout material should be pre-packaged and clearly labeled in moisture proof containers. Grout bags shall indicate application type, date of manufacture, LOT number and mixing instructions. A copy of the Quality Control Data Sheet for each lot number and shipment sent to the job site shall be provided to the Contractor by the grout supplier and furnished to the Engineer. Table 2.1 lists some standardize method for filler materials. Table 2.2 lists FDOT approval product list for the filler material.

Table 2.1. Standardized test methods for filler materials

No	Test Methods	Property	Filler	Values
1	FM 5-516	Total Chloride Ions	Grout	Max. 1.0 lbs/yd^3
2	ASTM C136	Gradation	Grout	99% passing the No. 50 95% passing the No. 100 90% passing the No. 170
3	ASTM C1090	Hardened Height Change @24 hours and 28 days	Grout	0.0% to +0.2%
4	ASTM C940	Expansion Bleeding @ 3 hours	Grout	≤2.0% for upto 3 hours 0.0%
5	ASTM C138 Or ASTM D4380	Wet Density- Laboratory Wet Density- Field	Grout	Report maximum and minimum obtained test value lb/ft^3
6	ASTM C942	Compressive strength 28 day	Grout	≥7,000 psi
7	ASTM C953	Initial set of filler	Grout	Min. 3 hours Max. 12 hours
8	ASTM C939	Time of Efflux immediately after mixing	Grout	Max. 12 hours
9	ASTM C1741	Pressure Induced bleeding	Grout	0.0%
10	FM 5-578	Surface Resistivity @28 days	Grout	16KOhms-cm
11	FM 5-605	Relative Viscosity	Grout	<1.15
12	ASTM B117	Salt Fog – 168 hours @35°C	Microcrystalline Wax	No corrosion
13	ASTM D512 And ASTM D3867	Corrosive Constituent Concentration Chloride, Sulfides, and Nitrates	Microcrystalline Wax	≤ 50 ppm (Total)
14	ASTM D516	Sulfate	Microcrystalline Wax	≤ 100 ppm
15	ASTM D938	Congealing Point	Microcrystalline Wax	≥ 65°C
16	ASTM D937	Cone Penetration at 25°C	Microcrystalline Wax	≤ 260 d-mm
17	ASTM D6184	Bleeding at 40°C	Microcrystalline Wax	≤ 0.5%
19	ASTM D445	Kinematic Viscosity at 100°C	Microcrystalline Wax	10-30 mm^2/s s
20	ASTM D942	Resistance to Oxidation 100 hours at 100°C	Microcrystalline Wax	≤ 0.03 Mpa

Table 2.2. FDOT filler material approval product list

No	Name	Type	APL Certification	Features	Pumpable	Uses and Applications
1	Euco Cable Grout PTX	Horizontal Vertical Repair only	934-000-004 934-001-001 934-002-002	Non-shrink Aggregate-free High fluidity Exceptional strength	2 hours @ 90°F	Post-tensioned cables and ducts Grouting of tight clearances
2	MasterFlow 1205	Horizontal Repair only	938-000-001 938-002-002	High compressive strength Bleed-free	1 hour @ 90°F	Post-tensioned cables, ducts, and high steel rods Grouting of unanchored cables and rods
3	MasterFlow 1206	Horizontal Vertical	938-000-007 938-001-002	Bleed-free High compressive strength	1 hour @ 90°F	Horizontal, vertical, and inclined post-tensioned tendon configuration Vertical bridge components and other vertical ducts
4	Special Grout 400	Horizontal Vertical	938-000-009 938-001-004	Bleed-free Non-shrink Non-metallic	2 hours @ 90°F	Corrosion protection of bridge cables Grouting of anchorages Pressure placement in tendon ducts
5	CIRINJECT CP	Microcrystalline wax	938-003-001	Anti-wear Anti-corrosion Resistance to oxidation	Application temperature 100°C	Post-tensioned cable filler
6	Fill-Flex 100	Microcrystalline wax	938-003-002	Resistance to oxidation Moisture and another compound preventative	Application temperature 80°C to 100°C	Post-tensioned cable filler
7	Fill-Flex 200	Microcrystalline wax	938-003-001	Resistance to oxidation Moisture and another compound preventative	Application temperature 80°C to 100°C	Post-tensioned cable filler
8	Renolin CL 4 RO	Microcrystalline wax	938-003-002	-	-	Post-tensioned cable filler
9	Strand Shield Flex Filler	Microcrystalline wax	938-003-001	-	-	Post-tensioned cable filler

2.4. CORROSION MECHANISM

Degradation of steel integrity and strength due to the electrochemical interaction with the environment is known as corrosion. Rust on steel exposed in outdoor atmosphere is an example of general corrosion. In cementitious materials, general corrosion of steel can develop when the passive film is not stable or is destroyed. Conventionally, depassivation of steel in cementitious materials occurs due to carbonation of the cement pore water or presence of chloride ions.

Steel in the prestressed concrete is covered with the grout material to protect it from corrosion due to the beneficial effect of the alkaline environment that cementitious materials can provide to promote steel passivation. An ideal grout for the post-tensioned structure has good strength, workability, and provides good corrosion protection. If the duct is partially filled with the grout material, then grout protection is less effective. The presence of the voids may allow the movement of moisture and chlorides along the length of the tendon. Fluidity, bleed resistance, volume change, and set time are important properties of fresh grout. These properties are controlled by the water-cement ratio, chemicals and mineral admixtures used, and type of the cement.

High chloride content in pre-packaged PT grout in a construction project in Texas in 2010 led to inquiries by TxDOT and the Federal Highway Administration (FHWA). The chloride content in early testing was as high as 5% by weight (Merrill, 2010), well exceeding conventional chloride limits. For example, FDOT specifications allows maximum of 0.4 lb/yd^3 chloride content and PTI specification allowed a maximum chloride of 0.08% by weight of cementitious material [47]. Research by Lee et al, consisted for mockup tendons with steel strand cast in ducts using pre-packaged grout products [48]. Corrosion developed at chloride levels greater than 0.2% chloride concentration. Steel strand corrosion was also observed at small regions of the tendon with deficient grout containing elevated sulfate concentrations indicating that further work on addressing corrosion associated with deficient grout was needed.

Severe corrosion was seen in the presence of segregated grout consistently characterized by high moisture content, high pH, low chloride concentrations, and enhanced concentrations of sulfur-bearing species

The high concentration of free sulfate ions in the deficient grout was suspected to be related to the corrosion. Indeed, in the 1970s, Gouda [16] examined the corrosion behavior of steel in alkaline solutions and that work showed that the sulfate ions in saturated calcium hydroxide solution could allow for corrosion initiation. Also, accumulated data from analysis of grout from Florida bridges corroborated with initial observations of enhanced sulfate content in deficient grout in 2011.

In laboratory testing in solution, significant corrosion activity was noticed in samples initially exposed to pore solution with high concentration of sulfates in very short periods of time after exposure. However, in complementary testing, samples initially exposed to alkaline pore solution free of chloride and sulfate ions for up to 60 days, did not show subsequent corrosion activity after sulfate was later introduced into the solution. The results showed that early exposure to sulfates in the deficient grout is among conditions where the development of a stable passive layer can be compromised.

Previous research showed that the role of sulfates in hardened grout and its interaction with solid phases in the grout need further examination. High level of sulfate ions in the field extracted deficient grout after construction indicated dissolution of sulfur bearing species into free sulfate in the grout pore water. A major overarching question concerns the source of the elevated ions. Gypsum would be the major source for sulfate ions. It was posited that the sulfate source may be related to kiln dust with contamination of alkali sulfates. The early development of steel corrosion indicated fast transport of sulfate ions through the tendon. Furthermore, practical concerns include identifying appropriate methodology to sample and analyze deficient grout materials.

2.5 SULFATE CONTENT IN DEFICIENT GROUT

There is no standardized method for measuring the free-sulfate content of cement material but leaching procedures can be used for the samples. Grout cylinders, modified inclined tube test, and inverted tee test were used in recent studies..

2.5.1 Test Setup

2.5.1.a. Grout Cylinders

The research by, Permeh et al. used pre-exposed grout samples to be analyzed by ex-situ leaching method. Exposing the material in high humidity for a prolonged duration can promote development of grout deficiencies. Two commercially available pre-packaged PT grout products were used and placed in containers within a 100% RH chamber for 3-7 days prior to casting. The grout was cast with 20 % excess water in cylinder molds and then placed in 100 % RH for 60 days. Grout pore water pH measured by an ex-situ leaching method as well as applying a pH spray indicator on a freshly fractured grout surface indicated that alkaline conditions pH>12.6 was typically maintained even when grout deficiencies developed. The free sulfate concentrations in the grout leachate, measured by ion chromatography, were not well differentiated even though various levels of grout segregation developed for the different grout products. However, samples from grout with significant grout deficiencies consistently showed elevated free sulfate concentrations relative to complimentary well hardened grout.

2.5.1.b. Modified Inclined Tube Test

Corrosion behavior of steel in expired grout was measured in large mock up tendons and samples were cast in non-ideal conditions in order to promote grout deficiencies. Fifteen-foot-long tendons with 4-inch diameter PVC mockups were cast at 30-degree incline with expired grout and 15 % excess mix water. Steel corrosion test probes were placed along the length of the tendon. This test provided the benefit to assess the extent of corrosion with varying degrees of grout deficiencies. The corrosion potential was measured with copper/copper-sulfate reference electrode via access points along the length of the tendon. Linear polarization resistance measurements were made with a Gamry Ref600 potentiostate. At the end, tendons were opened to conduct chemical analysis to qualify the levels of sulfates. Corrosion consistently developed on the steel test probed places at the upper 1 foot elevation of the tendon where deficient grout (>20% moisture and >0.001g/g sulfate) developed.

2.5.1.c. Inverted Tee Test

The inverted tee test is a small laboratory test where displaced water and less dense deficient grout developed by grout segregation can be accumulated. Test specimens consisted of a PVC tee (2×2×1½ ‘’ ø, 4 ¾ “length) filled with grout mixed with 20% excess water and varying concentrations of sulfate additions. Steel corrosion probe were placed in the tee base and tee head to differentiate corrosion behavior of steel in the deficient grout. An activated titanium rod, routinely calibrated with a copper/copper-sulfate reference electrode, was used as the reference electrode and stainless-steel rod was used as the counter electrode. The corrosion potential and polarization resistance of the embedded steel probes were routinely measured. In the testing described by Permeh [25], deficient grout of varying levels formed in the tee header. The grout in the tee header consistently showed higher sulfate concentrations relative to the grout in the tee body, however, significant corrosion was not always distinguished in the former. Grout pore water chemistry including chloride and sulfate levels that develop in the deficient grout was found to be important

2.5.1.d. Other Testing

Industry standard testing including grout bleed tests are already required to specify and approve application of grout materials. These tests collect bleed water from the fresh wet grout material. It was posited that grout chemical deficiencies including accumulation of aggressive ionic constituents in the bleed water could be quantified by these already existing test methods.

Pore expression of cementitious materials have also been used in cement and concrete research. Barneyback and Diamond, 1981 [49] developed device which has been used for extraction of pore solution from hardened cement, grout, and mortars. Compressed gas or vacuum can be used to get pore fluid from the

device with maximum pressure of 80000 psi. Grout pore water pH can be determined from the extracted pore water. Table 2.4 shows the different grout testing.

Table 2.3. Grout testing list

No	Test	Specification	Reference	Year	Findings
1	Inclined tube test	ASTM	D516-16	2016	Bleed test, accelerated test, sulfate test
		British Standard	EN 445:2007	2007	
		FDOT	Section 938	2012	
2	Wick-induced inclined tube test	British Standard	EN 445:1996	1996	This test does not represent the true conditions as strands are not considered.
		ASTM	Updated EN 447:2007	2007	
			C940-16	2016	
		FDOT	Section 938	2002	
3	Modified inclined tube test	FDOT	Hamilton, R., et al., 2002	2002	Bleed test, accelerated test, sulfate test
4	Pressure bleed test	ASTM	C1741	2018	This test is revised in 2018 and it is based on Schupak pressure test
5	Schupak pressure test	PTI	M-55 Sect. 4.4.6.2	2002	Identifies grout bleeding.
		FDOT	Section938		
		ASTM	C1741	2018	
		PCI	V 19 No. 6, pp 28-39	1974	
6	Fluidity test	TxDOT Item 426	Tex-437-A	2008	Identifies material and proportions
7	Inverted Tee test	-	Permeh, S., et al., 2016	2016	Identifies accelerated corrosion and sulfate content
8	Grout Cylinder Test	-	Permeh, S., et al., 2016	2016	Identifies sulfate content

2.5.2. Sulfate Analysis

The following summarizes methods have been used in analysis of sulfates in soils, water, and cementitious materials. Table 2.5 and 2.6 showes the methods list for total sulfate content in soil, water and groundwater, respectivley.

2.5.2.a. Ion Chromatography

EPA Method 300.1 describes a standard method to determine sulfate levels of drinking water by ion chromatography. This method is applicable to water, chemical, and pharmaceutical industries. In the chromatographic phase, samples go through a

pressurized chromatographic column where ions are held by due to the ionic interactions and eventually reach the detector. Based on the retention time, ions of interest can be identified on the detector response to those ions.

2.5.2.b. Digestion-Distillation Test

Johnson And Nishita [50] developed testing to measure sulfur levels in plant materials, solid, and irrigation water using digestion-distillation test. In this method, sulfate is digested at 115^{o}C with a reducing mixture composed of hydriodic acid, formic acid, and red phosphorus. The resulting hydrogen sulfide is determined spectrophotometrically. A modified method was published in 1952 with addition use of methylene blue solution for sulfate extraction.

2.5.2.c. Gravimetric Method

A gravimetric method described in Texas DOT, Tex-620-J based on the Johnson and Nishita digestion test, explained determination of chloride and sulfate content in soils in 1999. The sample materials are kept for digestion and then filtered using a Whatman filter paper. An aliquot is pipetted from the filtrate and the sulfate and chloride content according to test method Tex-619-J. Tex-619-J described analysis of water for chloride and sulfate ions by ion chromatography.

2.5.2.d.. Conductivity Test

Tex-146-E explained in detail a conductivity test for field detection of sulfates in soil. Calibration conductivity meter should be used for determining sulfate content. Soil samples can be obtained by drying in an oven and mix with deionized water. Conductivity should be measured immediately and after 12 hours using meter.

2.5.2.e. Turbidity

ASTM D516-16 describes a standard test method for sulfate ion in water. In this method, sulfate ion is reacted to a barium sulfate suspension in controlled conditions. A solution containing glycerin and sodium chloride is combined and mixed with the sample to stabilize the suspension. Then, the solution turbidity can be determined by a nephelometer, spectrometer, or photoelectric colorimeter. Florida method 5-553 approved turbidity test to determine sulfate in soil and water using either a screening approach based on sulfate reagent system or an analytical approach found in the standard methods for examination of water and waste water section 4110 B(SMEWW).

TxDOT 145-E determines the soluble sulfate content of soil by using turbidimetric techniques. Oven dried soil is mixed with distilled or deionized water solution and is shaken vigorously for about 1 min. Leaching of ions from the soil is made for 12 hours, and subsequently filtered and tested. This test method is mentioned in ASTM C1580-05 for soil and water. ASTM C1580-05 test method was developed for concentrations of water-soluble sulfate in soils. In this test method, soil samples are be collected, oven dried for 24 hours, and mixed with 250 ml of

deionized water. The sample is stirred and filtered. Hydrochloric acid is used as conditioning reagent and added into the sample. Turbidity is measured with a photometer. ASTM C938-16 described same turbidity test method for proportioning grout mixtures for preplaced-aggregate concrete.

FM 5-618 updated turbidity test for sampling of PT tendon grout in May 2018. This method describes procedures for obtaining a proper sample and sample preparation of PT tendon grout to determine sulfate content. FM 5-618 conform FM 5-553 to obtain sulfate level from sample. Sample should be crush approximately ¾" size using crusher and spread on tray in a thin layer under ambient condition, or dry in an oven not higher than 140^{o}F for 24 hours. Dry grout sample should be mix with deionized water to obtain 1:10 leaching volume and place the sample on hot plate and remove the sample after digestion time of 18-24 hours. Using no. 42 size filter paper filter water and follow sections 2,3 and 6 of FM 5-553.

Table 2.4. Sulfate content in soil test methods

No	Test	Type	Approved by	Reference	Note
1	Gravimetric Method	Chemical	US Army	TM 5-822-14/AFJMAN	Interference from other soil constituents due to boiling.
			Texas DOT	Tex-620-J	
			AASHTO	T290-95 Method(A)	
			British Standard	1377:1975, Test 9 (A)	
			ASTM	D516-02 11.01, 1988	
2	Conductivity Method	Chemical	Texas DOT	Tex-146-E	Differentiation is not possible between ionic types
			AASHTO	T-290	
3	Turbidity /Calorimetry Method	Chemical	Colorado DOT	CP-L-2103	-
			Texas DOT	Tex-145-E	
			AASHTO	T-290-95 Method(B)	
			ASTM	D516-16	
			FDOT	FM 5-618	
			ASTM	C1580-05	
4	Modified Digestion-Distillation Test	Chemical	University of California	California, Berkeley	Acid concentration must be done carefully
5	Method of Testing Soils for Sulfate Content	Chemical	Department of Transportation	State of California California Test 417 March 1999 March 2013	Alternative tests: ASTM D516-16 and Gravimetric Method

Table 2.5.Sulfate content for water and groundwater test methods

No	Test	Type	Approved by	Reference	Note
1	Turbidity Test	Chemical	ASTM	D516-16	-
			TxDOT	145-E	
2	Gravimetric Method	Chemical	ASTM	D516-02 Volume 11.01,1988	-
			British Standard	1377:1975, Test 9(A)	
3	Method of Testing Soils for Sulfate Content	Chemical	Department of Transportation	State of California California Test 417 March 2013	Alternative test is ASTM D516-16 and Gravimetric Method from soil test
4	Ion Chromatography	Chemical	EPA	Method 300.1	Ions can be identified with any liquids
			AASHTO	T-290	

2.5.3 Grout Segregation

It was documented in earlier works that tendon locations with deficient soft grout (that was associated with severe steel strand corrosion) typically also contained high sulfate ion concentrations. Identifying the extent of sulfate ion accumulation in deficient grout was of importance to elucidate the role of sulfate ions in the corrosion process, to assess corrosion risk in other grouted tendons, and to provide recommendations for material specifications.

As the source of the sulfate ions in the pore water of the field extracted grout materials has not been completely verified, early lab testing incorporated intentional sodium sulfate contamination in the grouted specimens. Methodologies to gage the extent of sulfate ion accumulation roughly followed ex-situ leaching procedures for soil testing that included conditions to promote extraction of sulfate ions from the grout into the leachate. Test conditions included increasing the leaching volume of water and heating.

In the project entitled “Simulation of Prepackaged Grout Bleed under Field Conditions” Hamilton et al., 2014 [51] investigated the role of moisture and grout filler materials on the formation of soft grout. Laboratory-cast tendon specimens were made following a modified version of the Euronorm EN445 inclined tube test (MIT tests). Up to six PT grout products commercially-available at the time of the research were tested to determine their propensity to develop soft grout. The raw grout powder was subjected to different levels of temperature and humidity and then mixed and cast with an additional 15% water above the manufacturer’s maximum water recommendations. The test results indicated that the PT grouts performed well if properly handled and applied but the PT grouts can be susceptible to segregation due to the effect of excessive moisture. Some of the grouts developed deficiencies in

non-ideal environmental pre-exposure conditions and improper mixing, and only one of the grout products consistently resulted in the formation of soft grout.

Development of deficient grout in the laboratory tests typically occurred with heat, prehydration and excessive moisture content. Prolonged storage times increased the susceptibility of the prepackaged PT grouts to the formation of soft grout. Another study funded by the FDOT, completed in 2018 entitled, “Evaluation of Shelf Life in Post-Tensioning Grouts” assessed the effect of grout shelf life and pre-exposure of the grout materials on grout segregation [52]. Prolonged exposure of grout materials to elevated temperatures and high relative humidity resulted in significant mass gains, increased particle sizes, and decreased surface areas. The test methods included mass gain, particle size analysis, Blaine fineness, loss on ignition, thermogravimetric analysis, and microwave moisture content. Testing of these parameters would provide a means to monitor the quality of the bagged material. Development by industry stakeholders continues to provide efficient and economical packaging designs as well as clearer markings of product shelf life.

The Florida experience with corrosion associated with the soft grout was different from the general narrative in the industry at the time. Namely, the severe corrosion of PT tendons in the Florida bridges was accommodated by the segregated grout that had low total chloride content. The segregated grout typically also had high free sulfate ion concentrations and high pore water pH. The role of the pore water chemistry of these deficient grouts in the corrosion mechanism was examined by Permeh et al. 2016; 2018 [25,26], in the project entitled “Corrosion of Post-Tensioned Tendons with Deficient Grout.” It was reported that the accumulation of sulfate ions in the deficient grout can form even without external sulfate sources. Steel corrosion in specimens with deficient grout was incurred by the early presence of excessive moisture and the sulfate ion and pH levels. Results of electrochemical testing of steel in alkaline sodium sulfate solution indicated that at pH 12.6, the early presence of sulfate ions (>4,000 ppm sodium sulfate) in solution could be aggressive by impairing the initial passive film development and resulting in the localized corrosion. It was observed that changes in pore water chemistry can affect the initiation of steel corrosion in the presence of sulfate ions, and dissimilar grout conditions lead to adverse macrocell development causing enhanced corrosion rates.

It was of interest to identify procedures that can be implemented to estimate incipient sulfate ion concentrations. In earlier testing, the sulfate levels were initially measured as concentration of sulfate ions in leachate, but units of $g_{sulfate}/g_{powder}$ were reported instead in order to normalize for leachate volume and powder sample mass. A discrepancy in the early testing was the non-standardization of the powder sample mass in terms of drying by the methodologies employed. This discrepancy also remains in field sample testing. The moisture content of grout samples (especially in powder form) may rapidly change due to environmental exposure and time of

exposure. However, drying of the powder may lead to aggregation of sulfate due to the need to maintain consistency in sample mass per leaching method.

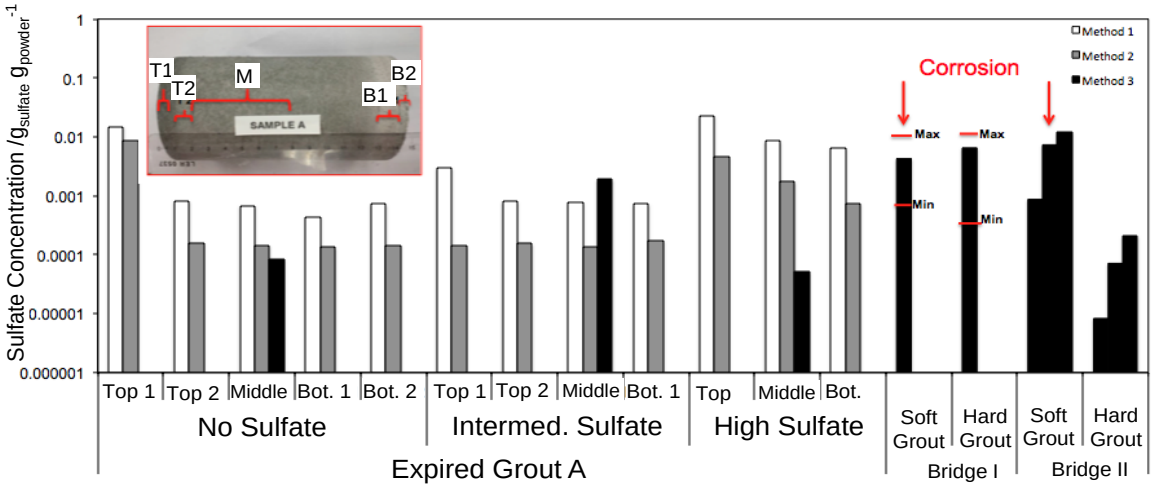

Figure 2.1. Results of grout leaching experiments in lab and field testing.

Results of initial testing of sulfate ion content in grout samples from earlier research are shown in Figure 2.1. Method 1 included procedures to dry the powder samples at 55°C for 24 hours, combine 1g of the dried powder with 1:10 leaching volume at 66°C for 15-18 hours, and filter and dilute the leachate into 100mL solution. Method 2 included procedures to use 1g powder as received with 1:10 leaching volume at room temperature for 1 week, and filter and dilute the leachate into 100mL. Method 3 included procedures to use ~12 g of powder as received, use 1:1 leaching volume at room temperature for 7 days, filter, and collect leachate. Leaching Method 3 (that utilized larger grout powder mass) was only conducted in the central portion of test specimens for the lab-cast grout specimens. Similar leaching methods were used for analysis of field-extracted grout from two Florida bridges that had steel corrosion associated with deficient grout. Results from both bridges were shown for comparison. It was apparent that the reported sulfate content for the lab-cast grout specimens had variability by the leaching methods. Generally, it was observed that for replicate powder samples, higher sulfate content was resolved by leaching Method 1 that employed methodologies to dry the powder sample and to use higher leachate temperature and greater volume. Lower sulfate concentrations were resolved by Methods 2 and 3. It was apparent that there was enhanced sulfate content in the top portions (albeit at relatively thin segments) of the test samples.

Added sodium sulfate contamination also provided greater availability of sulfate ions, but it is seen that separation of grout material cast in lab conditions can allow for accumulation of sulfate ions without external sulfate sources. The resolved sulfate content measured in grout from Bridge I and II are shown for comparison. In the lab-cast grout that contained high level of added sulfate and had lower moisture content, the enhanced leaching procedures caused a significant increase in the

sulfate ion content (presumably due to enhanced dissolution of sulfates that were maintained in cement solid phases or crystalline form such as ettringite). In the grout that contained no added sulfates but had higher moisture content, the enhanced leaching procedures was less pronounced (presumably due to the already incurred dissolution of sulfate caused by the excess moisture content and grout degradation).

Furthermore, in light of the discovered risk of chloride contamination in a commercial grout product production run, the research also assessed the development of corrosion of steel in soft grout in the presence of sulfate ions and low levels of chloride ions. In the work by Permeh et al., [25, 26], additions of 0.08% and 0.2% chloride by cement in itself did not initiate corrosion of steel in the grout, but corrosion developed in deficient grout materials with similar low-level additions of chlorides when combined with as low as 2,000-ppm sodium sulfate in its mix water. The researchers concluded that the assessment of corrosion susceptibility in deficient grout by chloride values alone was insufficient as sulfate ion presence and grout characteristics were also important.

With a large existing bridge inventory with similar grout materials in tendons that exhibited severe corrosion in the two Florida bridges, practical criteria to assess corrosion risk was needed to identify maintenance needs. Efforts to develop test methods to measure the free sulfate ion concentration in deficient grout and the critical sulfate ion concentration associated with the corrosion was made. Permeh et al., 2019 [26] (Figure 2.2) recommended values based on compiled data from associated bridges with soft grout and laboratory test results by differentiating the roles of moisture content, free chloride content, and free sulfate concentrations on corrosion activity. In general, corrosion activity developed in grout with free sulfate concentrations >0.7 $mg_{sulfate}/g_{grout}$. The sulfate ion measurement followed a modified ASTM and Texas methods for soil and was later adapted into Florida specifications FM5-618. PTI M55 specifications draw attention to corrosion in the presence of sulfate ions in deficient grout.

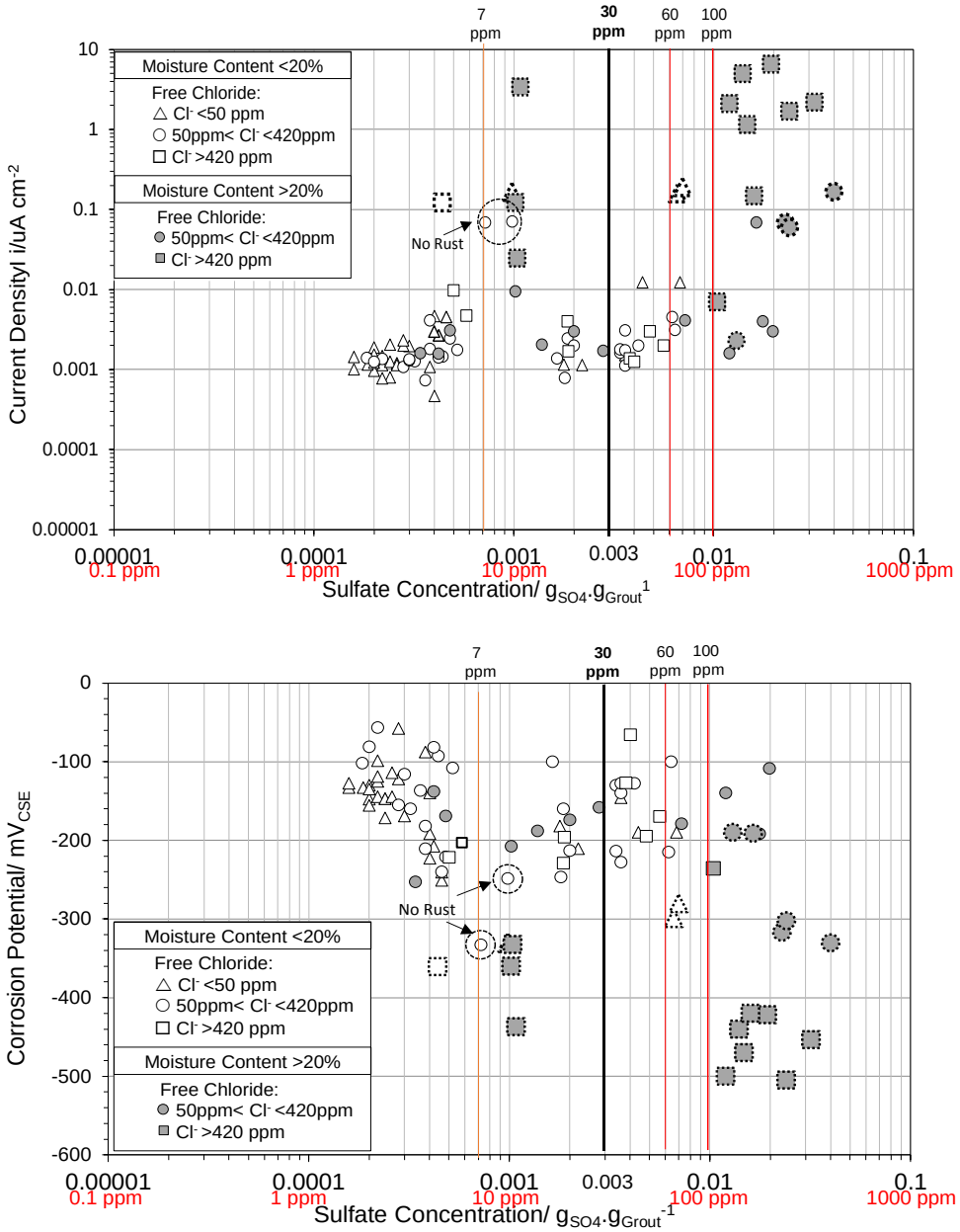

Figure 2.2. Corrosion behavior of steel in deficient grout with elevated sulfate concentration [26]
(0.003 $g_{sulfate}/g_{grout}$, limit following FDOT method FM 5-618-50)

2.5.4 FDOT Sulfate Specifications

Current Florida specifications allow up to a nominal 30 ppm free sulfate ion concentration as defined by FM5-618 (water-soluble sulfate measured by turbidimetry). The sulfate content proposed in the Florida specifications were based on values that were resolved by test methods used as part of the research that was meant to identify mechanisms and risk. The previous research identified that different processing procedures were needed for the various levels of grout physical deficiency and the different procedures yielded different sulfate concentrations.

Since the MIT had been shown to promote some level of grout segregation and is prescribed by FDOT, the setup was used to produce grout samples for further chemical analysis and assessment of sampling procedures.

The FDOT FM 5-618 provides procedures for the sampling of post-tensioned tendon grout. In its current form, the method allows for initial drying of the extracted grout at 60^{o}C for 24 hours and pulverized to pass a No. 100 Mesh. This in part allows for normalization of the tested grout mass for materials with varying initial moisture levels (that may not be controlled during the extraction and transport) as well as practical consideration to minimize the level of gumming of the hardware (with wet cementitious materials) used to render the grout to powder form. The procedure prescribes leaching of 1 gram of the grout in 10 mL (to obtain a 1:10 leaching volume) at ~60^{o}C for 18-24 hours to facilitate dissolution of the sulfate into solution. The leachate is then filtered and diluted with deionized water to reach 100 mL.

The concentration of the sulfate ion is measured by turbidimetric methods although previous research also utilized ion chromatography. Following this testing protocol, the FDOT material specifications section 938 allows up to 30 ppm sulfate ions.

The final sulfate ion concentration normalized for the grout mass can be calculated by the formula:

$$M = \frac{C\ V}{1000\ m}$$

where
M= SO_4^{2-} concentration in g $_{Sulfate}$/g $_{Grout}$
C= SO_4^{2-} concentration of leachate in mg/L
V= Volume of sample in L (0.1 L)
m= dry mass of grout in gr (1 g)

CHAPTER 3. GROUT MATERIAL TESTING

3.1 XRF

X-Ray Fluorescence (XRF) analysis was made for Grout A, B, C, Expired Grout C, Expired Grout D, and a neat grout. This testing was initially made to identify the incipient presence of sulfur-bearing species in the raw material for consideration of the development of the sulfate ions in grout pore water after casting and cement hydration. The raw grout powder was placed on the sample holder. A Jeol SEM with EDS-XRF located in the FCAEM/Dept. of Earth and Env. Sciences at the Florida International University Environmental Science Lab was used (Figure 3.1).

Figure 3.1. Jeol SEM with XRF

In the following section (Figures 3.2- 3.7), SEM images of the grout powder, the sensed counts per second of each element, and table of the powder makeup are given for each material.

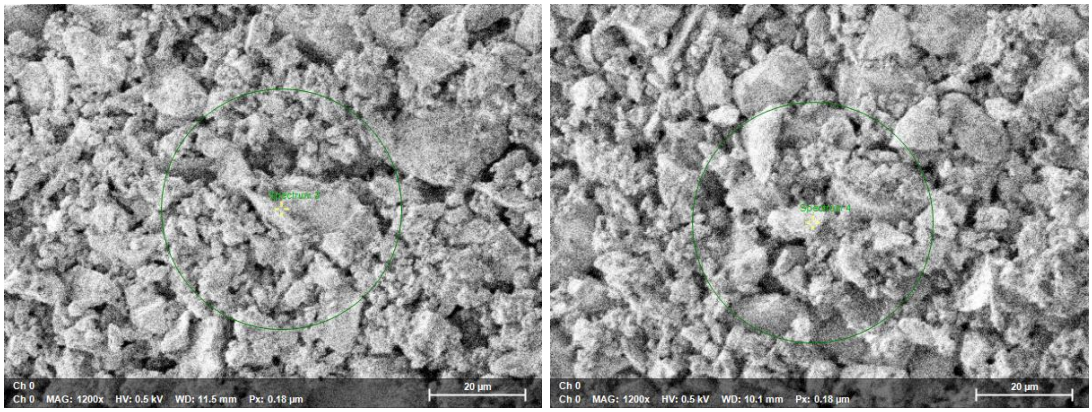

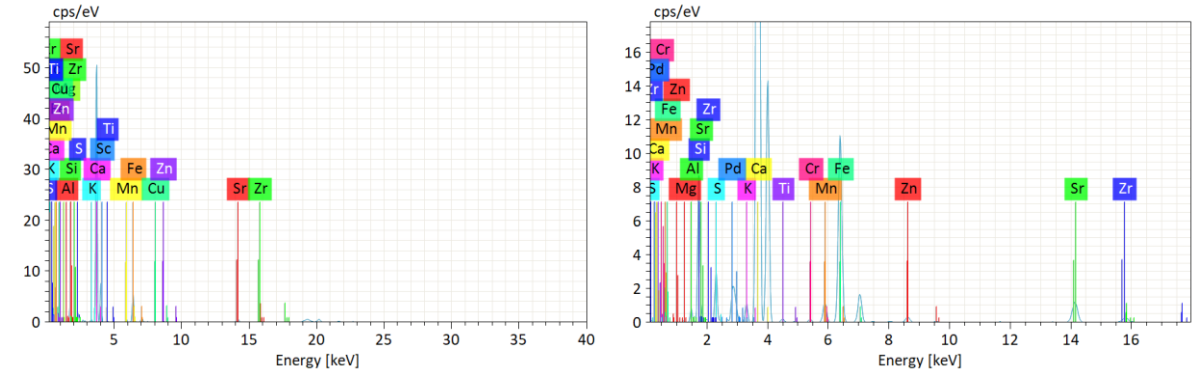

Spectrum 3

Element	At. No.	Netto	Mass [%]	Mass Norm. [%]	Atom [%]	abs. error [%] (1 sigma)	rel. error [%] (1 sigma)
Aluminium	13	7554	0.59	1.86	2.64	0.00	0.00
Silicon	14	103897	3.51	11.13	15.21	0.00	0.00
Sulfur	16	49034	0.58	1.84	2.20	0.00	0.00
Potassium	19	15975	0.28	0.90	0.88	0.00	0.00
Calcium	20	1801971	24.27	76.97	73.72	0.00	0.00
Manganese	25	20448	0.20	0.62	0.43	0.00	0.00
Iron	26	216010	1.69	5.35	3.67	0.00	0.00
Magnesium	12	803	0.15	0.49	0.77	0.00	0.00
Strontium	38	36952	0.14	0.43	0.19	0.00	0.00
Zirconium	40	6194	0.02	0.07	0.03	0.00	0.00
Copper	29	544	0.00	0.01	0.01	0.00	0.00
Zinc	30	6711	0.03	0.10	0.06	0.00	0.00
Titanium	22	3718	0.07	0.23	0.19	0.00	0.00
		Sum	**31.53**	**100.00**	**100.00**		

Spectrum 4

Element	At. No.	Netto	Mass [%]	Mass Norm. [%]	Atom [%]	abs. error [%] (1 sigma)	rel. error [%] (1 sigma)
Magnesium	12	1907	0.37	0.63	1.00	0.00	0.00
Aluminium	13	15273	1.22	2.06	2.94	0.00	0.00
Silicon	14	189749	6.63	11.20	15.31	0.00	0.00
Sulfur	16	69545	0.85	1.43	1.72	0.00	0.00
Potassium	19	32348	0.59	0.99	0.98	0.00	0.00
Calcium	20	3271657	45.08	76.20	73.01	0.00	0.00
Manganese	25	43967	0.43	0.73	0.51	0.00	0.00
Iron	26	430278	3.43	5.80	3.98	0.00	0.00
Zinc	30	14102	0.07	0.12	0.07	0.00	0.00
Strontium	38	70266	0.27	0.45	0.20	0.00	0.00
Zirconium	40	5799	0.02	0.04	0.02	0.00	0.00
Titanium	22	6516	0.13	0.22	0.18	0.00	0.00
Chromium	24	6561	0.08	0.13	0.09	0.00	0.00
		Sum	**59.16**	**100.00**	**100.00**		

Figure 3.2. Grout A Raw Powder Material

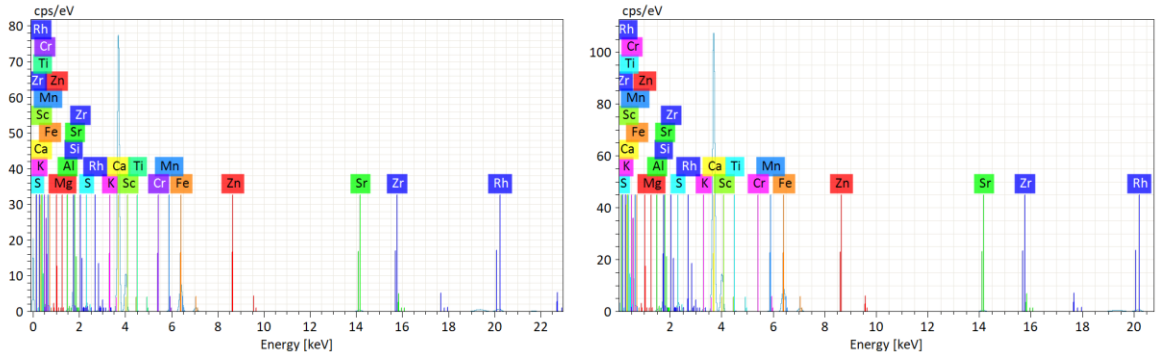

1206-XRF-1.spx

Element	Netto	Mass [%]	Mass Norm. [%]	Atom [%]	abs. error [%] (1 sigma)	rel. error [%] (1 sigma)
Mg	658	0.13	0.32	0.51	0.00	0.00
Al	13019	1.01	2.58	3.67	0.00	0.00
Si	124078	4.25	10.83	14.80	0.00	0.00
S	44990	0.53	1.36	1.62	0.00	0.00
K	459	0.01	0.02	0.02	0.00	0.00
Ca	2311025	30.52	77.76	74.49	0.00	0.00
Fe	298098	2.36	6.00	4.13	0.00	0.00
Sc	0	0.00	0.00	0.00	0.00	0.00
Mn	19875	0.19	0.49	0.34	0.00	0.00
Zn	1503	0.01	0.02	0.01	0.00	0.00
Sr	24148	0.09	0.23	0.10	0.00	0.00
Zr	0	0.00	0.00	0.00	0.00	0.00
Ti	6376	0.13	0.32	0.26	0.00	0.00
Cr	2318	0.03	0.07	0.05	0.00	0.00
	Sum	**39.25**	**100.00**	**100.00**		

1206-XRF-2.spx

Element	Netto	Mass [%]	Mass Norm. [%]	Atom [%]	abs. error [%] (1 sigma)	rel. error [%] (1 sigma)
Mg	1068	0.21	0.39	0.61	0.00	0.00
Al	15761	1.23	2.32	3.31	0.00	0.00
Si	158247	5.42	10.22	13.99	0.00	0.00
S	57121	0.67	1.26	1.51	0.00	0.00
K	0	0.00	0.00	0.00	0.00	0.00
Ca	3179042	42.17	79.52	76.25	0.00	0.00
Fe	356049	2.88	5.43	3.74	0.00	0.00
Sc	0	0.00	0.00	0.00	0.00	0.00
Mn	18558	0.18	0.35	0.24	0.00	0.00
Zn	3610	0.02	0.03	0.02	0.00	0.00
Sr	21210	0.08	0.15	0.07	0.00	0.00
Zr	173	0.00	0.00	0.00	0.00	0.00
Ti	6695	0.14	0.26	0.21	0.00	0.00
Cr	2936	0.03	0.07	0.05	0.00	0.00
	Sum	**53.03**	**100.00**	**100.00**		

Figure 3.3. Grout B Raw Powder Material

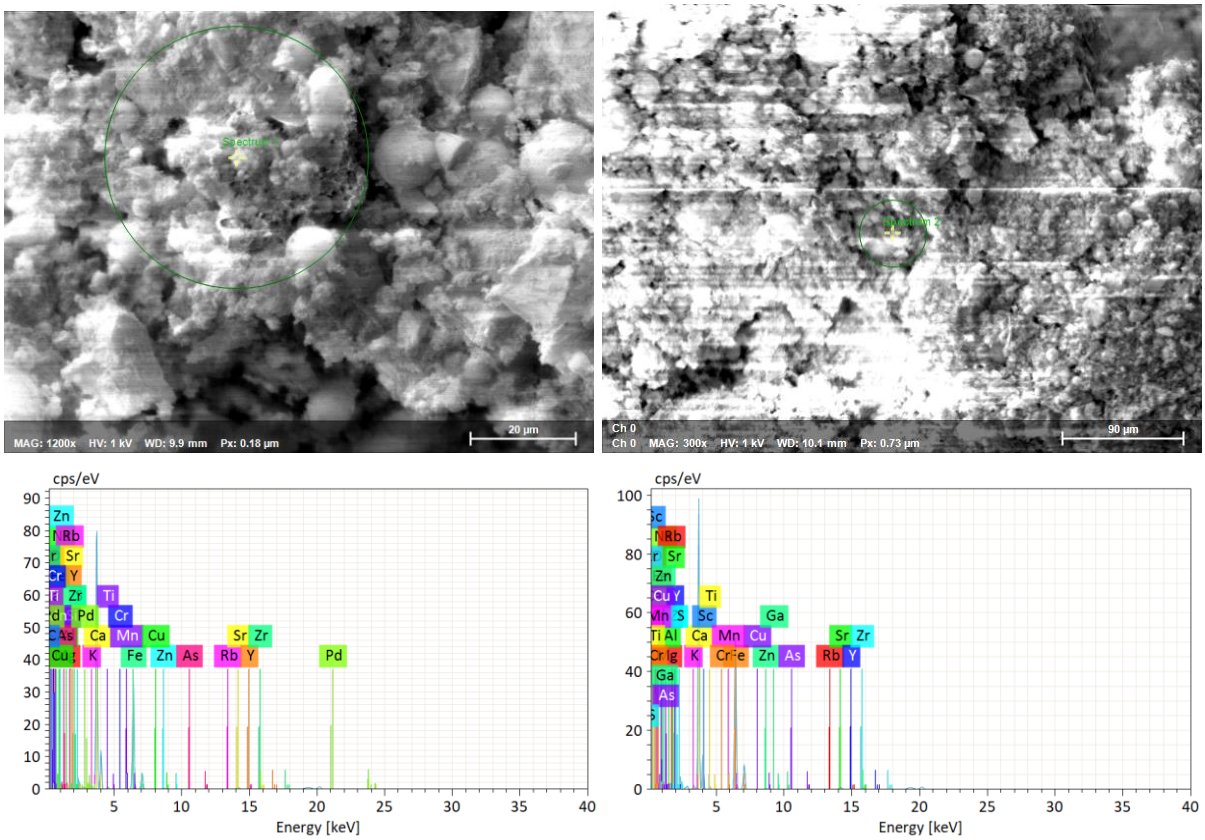

Spectrum 1

Element	At. No.	Netto	Mass [%]	Mass Norm. [%]	Atom [%]	abs. error [%] (1 sigma)	rel. error [%] (1 sigma)
Magnesium	12	8367	1.73	2.30	3.48	0.00	0.00
Aluminium	13	43604	3.81	5.05	6.89	0.00	0.00
Silicon	14	355834	14.37	19.06	24.98	0.00	0.00
Sulfur	16	95408	1.47	1.94	2.23	0.00	0.00
Potassium	19	48019	1.06	1.41	1.32	0.00	0.00
Calcium	20	2839035	42.27	56.07	51.48	0.00	0.00
Iron	26	1350211	9.51	12.61	8.31	0.00	0.00
Sodium	11	460	0.25	0.33	0.54	0.00	0.00
Zinc	30	19891	0.10	0.13	0.07	0.00	0.00
Rubidium	37	2815	0.01	0.01	0.01	0.00	0.00
Strontium	38	45787	0.17	0.23	0.09	0.00	0.00
Yttrium	39	1579	0.01	0.01	0.00	0.00	0.00
Zirconium	40	10732	0.04	0.05	0.02	0.00	0.00
Manganese	25	5647	0.05	0.06	0.04	0.00	0.00
Chromium	24	1637	0.02	0.02	0.02	0.00	0.00
Titanium	22	28480	0.48	0.63	0.49	0.00	0.00
Arsenic	33	2128	0.01	0.01	0.01	0.00	0.00
Copper	29	2882	0.02	0.02	0.01	0.00	0.00
Palladium	46	1364	0.03	0.04	0.02	0.00	0.00
Rhodium	45	56236	0.00	0.00	0.00	0.00	0.00
		Sum	**75.39**	**100.00**	**100.00**		

Spectrum 2

Element	At. No.	Netto	Mass [%]	Mass Norm. [%]	Atom [%]	abs. error [%] (1 sigma)	rel. error [%] (1 sigma)
Magnesium	12	8128	1.79	2.04	3.14	0.00	0.00
Aluminium	13	40304	3.72	4.22	5.87	0.00	0.00
Silicon	14	390492	16.37	18.60	24.85	0.00	0.00
Potassium	19	51103	1.15	1.30	1.25	0.00	0.00
Calcium	20	3124397	46.53	52.88	49.50	0.00	0.00
Iron	26	2166846	15.32	17.41	11.70	0.00	0.00
Sodium	11	489	0.29	0.32	0.53	0.00	0.00
Scandium	21	0	0.00	0.00	0.00	0.00	0.00
Rubidium	37	2498	0.01	0.01	0.00	0.00	0.00
Strontium	38	45989	0.18	0.21	0.09	0.00	0.00
Yttrium	39	1503	0.01	0.01	0.00	0.00	0.00
Zirconium	40	11337	0.05	0.05	0.02	0.00	0.00
Zinc	30	23050	0.12	0.14	0.08	0.00	0.00
Copper	29	3612	0.02	0.02	0.01	0.00	0.00
Manganese	25	4978	0.04	0.05	0.03	0.00	0.00
Titanium	22	37067	0.60	0.68	0.53	0.00	0.00
Chromium	24	2045	0.02	0.02	0.02	0.00	0.00
Gallium	31	672	0.00	0.00	0.00	0.00	0.00
Arsenic	33	2500	0.01	0.01	0.01	0.00	0.00
Sulfur	16	112818	1.78	2.02	2.36	0.00	0.00
Rhodium	45	55569	0.00	0.00	0.00	0.00	0.00
		Sum	**88.00**	**100.00**	**100.00**		

Figure 3.4. Grout C Raw Powder Material

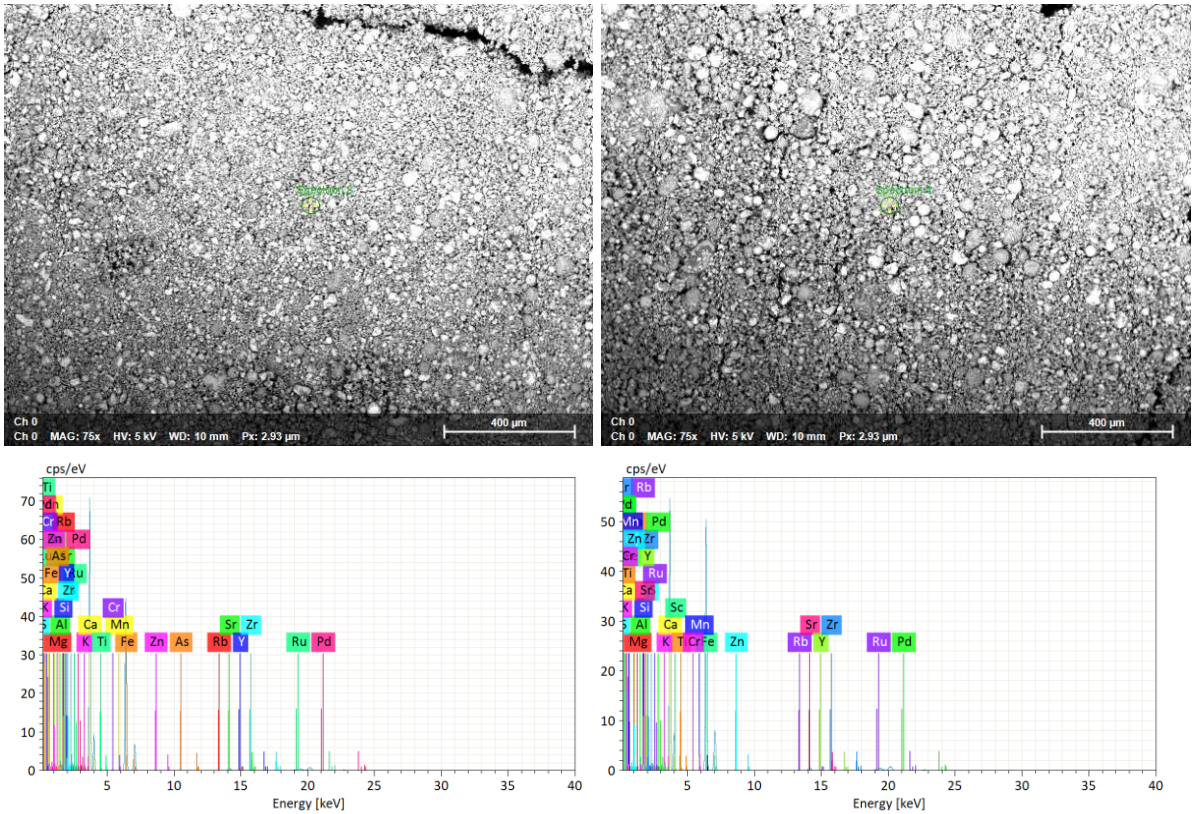

Spectrum 3

Element	Netto	Mass [%]	Mass Norm. [%]	Atom [%]	abs. error [%] (1 sigma)	rel. error [%] (1 sigma)
Mg	1739	0.91	1.41	2.17	0.00	0.00
Al	17885	3.87	6.01	8.37	0.00	0.00
Si	115671	11.67	18.14	24.27	0.00	0.00
S	46876	1.76	2.74	3.21	0.00	0.00
K	17272	0.94	1.47	1.41	0.00	0.00
Ca	896643	31.97	49.68	46.58	0.00	0.00
Fe	724416	11.76	18.28	12.30	0.00	0.00
Ru	14806	0.43	0.67	0.25	0.00	0.00
Na	176	0.24	0.38	0.61	0.00	0.00
Rb	988	0.01	0.01	0.01	0.00	0.00
Sr	15877	0.15	0.23	0.10	0.00	0.00
Y	772	0.01	0.01	0.00	0.00	0.00
Zr	3837	0.04	0.06	0.02	0.00	0.00
Mn	1533	0.03	0.05	0.03	0.00	0.00
Ti	12533	0.46	0.72	0.56	0.00	0.00
Pd	266	0.02	0.03	0.01	0.00	0.00
Cr	1827	0.04	0.06	0.04	0.00	0.00
Zn	3276	0.04	0.06	0.04	0.00	0.00
As	964	0.01	0.02	0.01	0.00	0.00
Rh	23286	0.00	0.00	0.00	0.00	0.00
	Sum	**64.35**	**100.00**	**100.00**		

Spectrum 4

Element	Netto	Mass [%]	Mass Norm. [%]	Atom [%]	abs. error [%] (1 sigma)	rel. error [%] (1 sigma)
Mg	1071	0.55	0.90	1.35	0.00	0.00
Al	19811	4.25	6.88	9.35	0.00	0.00
Si	155838	16.01	25.91	33.84	0.00	0.00
S	17341	0.72	1.17	1.34	0.00	0.00
K	20820	1.20	1.95	1.83	0.00	0.00
Ca	693490	25.26	40.87	37.42	0.00	0.00
Ti	13389	0.45	0.73	0.56	0.00	0.00
Fe	816882	12.35	19.98	13.13	0.00	0.00
Ru	15610	0.44	0.71	0.26	0.00	0.00
Na	201	0.27	0.44	0.70	0.00	0.00
Sc	0	0.00	0.00	0.00	0.00	0.00
Rb	1319	0.01	0.02	0.01	0.00	0.00
Sr	15067	0.13	0.22	0.09	0.00	0.00
Y	727	0.01	0.01	0.00	0.00	0.00
Zr	3487	0.03	0.05	0.02	0.00	0.00
Pd	357	0.02	0.03	0.01	0.00	0.00
Mn	1566	0.03	0.05	0.03	0.00	0.00
Zn	3671	0.04	0.07	0.04	0.00	0.00
Cr	893	0.02	0.03	0.02	0.00	0.00
Rh	23176	0.00	0.00	0.00	0.00	0.00
	Sum	**61.79**	**100.00**	**100.00**		

Figure 3.5. Expired Grout C Raw Powder Material

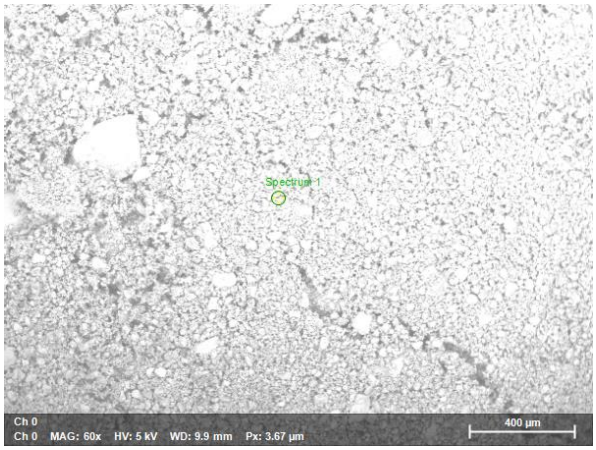

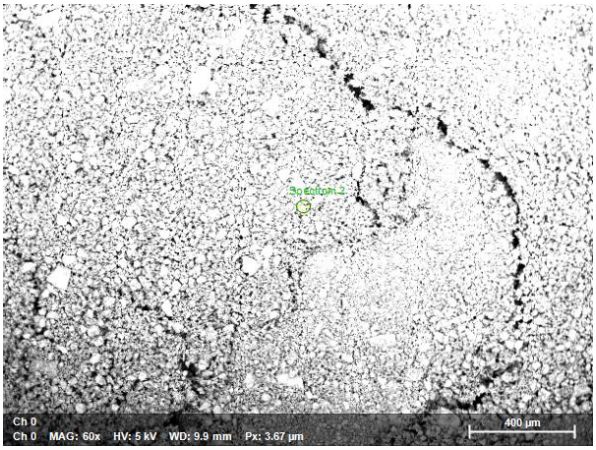

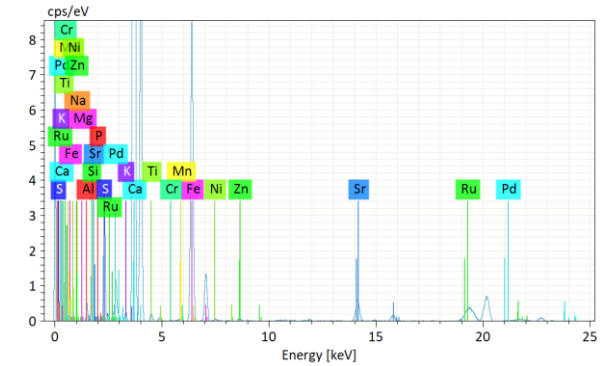

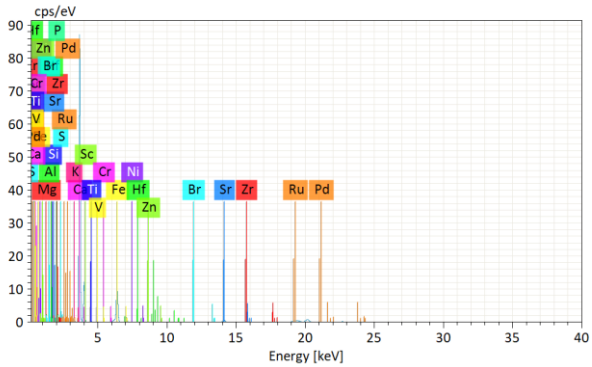

Spectrum 1

Element	Netto	Mass [%]	Mass Norm. [%]	Atom [%]	abs. error [%] (1 sigma)	rel. error [%] (1 sigma)
Al	3783	0.72	1.65	2.36	0.00	0.00
Si	49498	4.07	9.33	12.87	0.00	0.00
S	36610	1.02	2.34	2.83	0.00	0.00
Ca	1039013	33.88	77.59	75.01	0.00	0.00
Fe	140623	2.67	6.11	4.24	0.00	0.00
Sr	15165	0.14	0.31	0.14	0.00	0.00
Ru	12769	0.36	0.82	0.31	0.00	0.00
Mg	736	0.34	0.79	1.25	0.00	0.00
Na	20	0.03	0.06	0.10	0.00	0.00
K	3048	0.13	0.30	0.30	0.00	0.00
Ti	3253	0.15	0.35	0.29	0.00	0.00
P	1046	0.05	0.12	0.15	0.00	0.00
Pd	226	0.01	0.03	0.01	0.00	0.00
Mn	1682	0.04	0.09	0.06	0.00	0.00
Cr	343	0.01	0.02	0.02	0.00	0.00
Ni	917	0.01	0.03	0.02	0.00	0.00
Zn	1351	0.02	0.04	0.02	0.00	0.00
Br	802	0.01	0.02	0.01	0.00	0.00
	Sum	**43.66**	**100.00**	**100.00**		

Spectrum 2

Element	Netto	Mass [%]	Mass Norm. [%]	Atom [%]	abs. error [%] (1 sigma)	rel. error [%] (1 sigma)
Mg	1514	0.71	1.51	2.40	0.00	0.00
Al	4990	0.97	2.04	2.93	0.00	0.00
Si	49374	4.16	8.80	12.13	0.00	0.00
S	37587	1.06	2.25	2.71	0.00	0.00
Ca	1104669	36.18	76.52	73.89	0.00	0.00
Fe	169337	3.20	6.78	4.70	0.00	0.00
Ru	15342	0.43	0.92	0.35	0.00	0.00
K	2817	0.12	0.26	0.26	0.00	0.00
Sc	0	0.00	0.00	0.00	0.00	0.00
Sr	13963	0.13	0.27	0.12	0.00	0.00
Zr	1573	0.01	0.03	0.01	0.00	0.00
Ni	486	0.01	0.01	0.01	0.00	0.00
Hf	433	0.01	0.02	0.00	0.00	0.00
Zn	1039	0.01	0.03	0.02	0.00	0.00
Br	591	0.01	0.01	0.01	0.00	0.00
Cr	312	0.01	0.02	0.01	0.00	0.00
Ti	3067	0.14	0.31	0.25	0.00	0.00
V	973	0.04	0.07	0.06	0.00	0.00
Pd	396	0.02	0.05	0.02	0.00	0.00
P	966	0.05	0.10	0.13	0.00	0.00
	Sum	**47.29**	**100.00**	**100.00**		

Figure 3.6. Expired Grout D Raw Powder Material

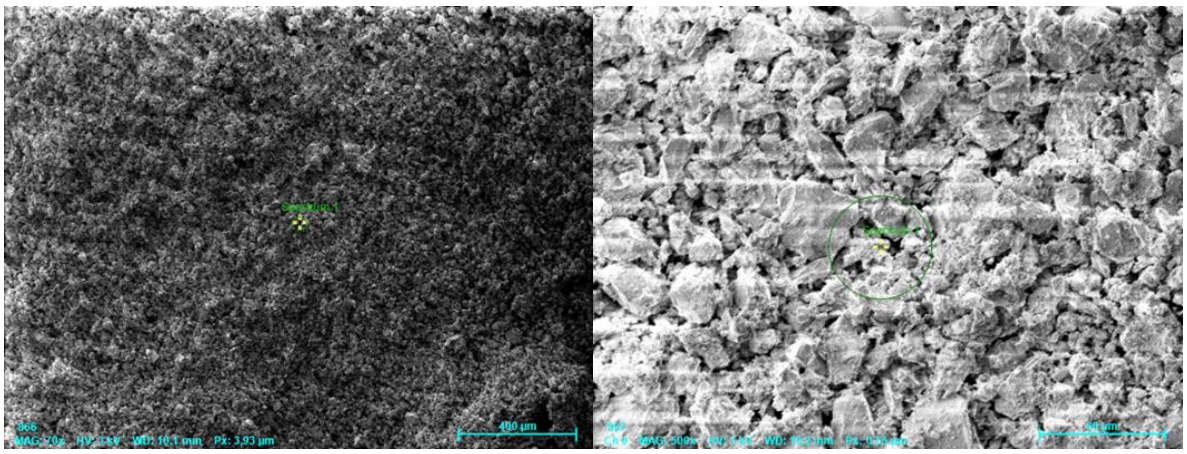

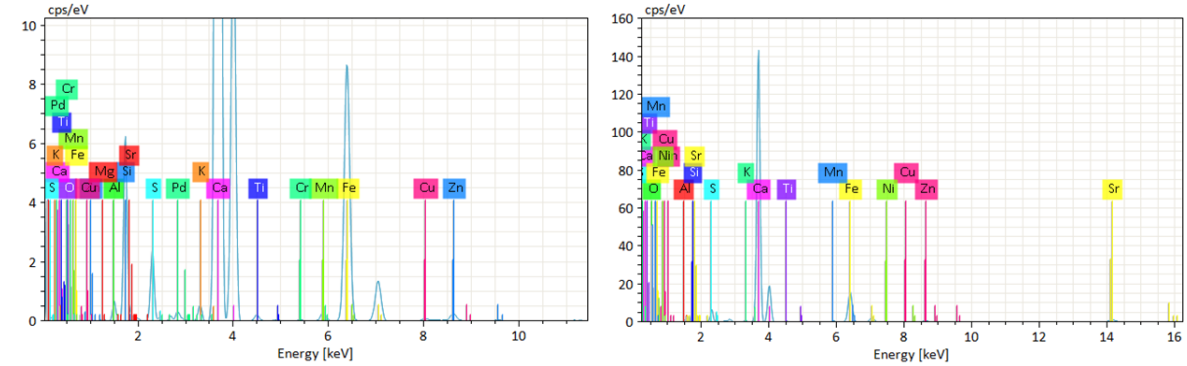

Spectrum 1

Element	At. No.	Netto	Mass [%]	Mass Norm. [%]	Atom [%]	Comp.	Sto. [%]	Sto. Norm. [%]	abs. error [%] (1 sigma)	rel. error [%] (1 sigma)
Aluminium	13	5373	0.96	1.59	1.54	Al2O3	1.81	3.01	0.01	1.36
Oxygen	8	0	20.15	33.50	54.63		0.00	0.00	0.09	0.43
Silicon	14	53866	4.10	6.81	6.33	SiO2	8.76	14.57	0.02	0.43
Calcium	20	1276956	31.70	52.71	34.31	CaO	44.35	73.75	0.03	0.09
Iron	26	141902	1.88	3.13	1.46	Fe2O3	2.69	4.47	0.00	0.27
Strontium	38	10646	0.06	0.11	0.03	SrO	0.08	0.13	0.00	0.93
Zinc	30	4551	0.04	0.06	0.02	ZnO	0.05	0.08	0.00	1.48
Manganese	25	4293	0.07	0.12	0.06	MnO	0.09	0.15	0.00	1.53
Titanium	22	2871	0.10	0.16	0.09	TiO2	0.16	0.27	0.00	1.87
Potassium	19	6257	0.22	0.36	0.24	K2O	0.26	0.43	0.00	1.26
Sulfur	16	22462	0.55	0.91	0.74	SO3	1.36	2.27	0.00	0.67
Magnesium	12	661	0.29	0.49	0.52	MgO	0.49	0.81	0.01	3.89
Palladium	46	317	0.01	0.02	0.01		0.01	0.02	0.00	1.51
Chromium	24	415	0.01	0.01	0.01	Cr2O3	0.01	0.02	0.00	4.91
Copper	29	1047	0.01	0.02	0.01		0.01	0.02	0.00	3.09
		Sum	**60.14**	**100.00**	**100.00**		**60.14**	**100.00**		

Spectrum 1

Element	At. No.	Netto	Mass [%]	Mass Norm. [%]	Atom [%]	Comp.	Sto. [%]	Sto. Norm. [%]	abs. error [%] (1 sigma)	rel. error [%] (1 sigma)
Aluminium	13	9086	1.67	1.81	1.75	Al2O3	3.15	3.41	0.02	1.05
Oxygen	8	0	31.31	33.86	55.19		0.00	0.00	0.12	0.37
Silicon	14	73673	5.80	6.27	5.82	SiO2	12.41	13.42	0.02	0.37
Sulfur	16	64534	1.62	1.75	1.42	SO3	4.04	4.37	0.01	0.39
Calcium	20	1853589	47.60	51.48	33.50	CaO	66.60	72.03	0.03	0.07
Iron	26	259496	3.50	3.79	1.77	Fe2O3	5.01	5.41	0.01	0.20
Potassium	19	9950	0.36	0.39	0.26	K2O	0.43	0.47	0.00	1.00
Titanium	22	5021	0.17	0.19	0.10	TiO2	0.29	0.31	0.00	1.41
Strontium	38	28980	0.18	0.20	0.06	SrO	0.22	0.23	0.00	0.57
Zinc	30	9640	0.08	0.09	0.04	ZnO	0.10	0.11	0.00	1.01
Copper	29	4024	0.04	0.04	0.02		0.04	0.04	0.00	1.58
Nickel	28	644	0.01	0.01	0.00	NiO	0.01	0.01	0.00	3.94
Manganese	25	7262	0.12	0.13	0.06	MnO	0.16	0.17	0.00	1.17
Chromium	24	815	0.02	0.02	0.01	Cr2O3	0.02	0.03	0.00	3.50
		Sum	**92.47**	**100.00**	**100.00**		**92.47**	**100.00**		

Figure 3.7. Neat Grout Raw Powder Material

Tables 3.1 and 3. 2 list the chemical makeup for relevant elements in the grouts. Figure 3.7 shows the comparison graphically. In previous research on the soft grout from a Florida bridge, the deficient grout had high alkali and sulfate content and low chloride content. Also, commercial grouts have used crushed calcium carbonate and crushed silicates as part of the mix design. Identification of these elements in the raw grout and comparisons to deficient grout created in the lab will be important to address procedures for chemical analysis of the deficient grout.

Table 3.1. Grout chemical makeup (mass %)

Mass (%)	Grout A	Grout B	Grout C	Expired Grout C	Expired Grout D	Neat Grout
Sodium (Na)	-	-	0.25, 0.29	0.24, 0.27	0.03, -	- ,-
Potassium(K)	0.28,0.59	0, 0.01	1.06, 1.15	0.94, 1.20	0.12, 0.13	0.22, 0.36
Calcium (Ca)	24.27, 45.08	30.52, 42.17	42.27, 46.53	25.26, 31.97	33.88, 36.18	31.7, 47.6
Silicon (Si)	3.51, 6.63	4.25, 5.42	14.37,16.37	11.67, 16.01	4.07, 4.16	4.1, 5.8
Sulfur (S)	0.58, 0.85	0.53, 0.67	1.47, 1.78	0.72,1.76	1.02, 1.06	0.55, 1.62
Chloride (Cl)	-	-	-	-	-	-

Table 3.2. Grout chemical makeup (atomic %)

Atom (%)	Grout A	Grout B	Grout C	Expired Grout C	Expired Grout D	Neat Grout
Sodium (Na)	-		0.53, 0.54	0.61, 0.70	0.1, -	-, -
Potassium(K)	0.88, 0.98	0, 0.02	1.32, 1.25	1.41, 1.83	0.26, 0.3,	0.24, 0.26
Calcium (Ca)	73.01-73.72	74.49, 76.25	49.50, 51.48	37.42, 46.58	73.89, 75.01	34.31, 33.50
Silicon (Si)	15.21, 15.31	13.99, 14.80	24.85, 24.98	24.27, 33.84	12.13, 12.87	6.33, 5.82
Sulfur (S)	1.72, 2.20	1.51, 1.62	2.23,2.36	1.34, 3.21	2.71, 2.83	0.74, 1.42
Chloride (Cl)	-	-	-	-	-	-

In the past research, the soft grout was found to have an accumulation of alkalis and sulfate in the pore water. Grout C did not develop the soft grout deficiency as observed in the tendons that exhibited strand corrosion. It was noted that the raw powder had higher concentrations of alkalis and sulfur. Grout D that did segregate had lower concentrations of alkalis and sulfur in the raw powder. Grout A and B showed low alkali and sulfur levels in the raw grout. Analysis made for the lab specimens subjected to adverse conditions to promote segregation (discussed later) will provide clarification on how these compounds in the raw form are related to pore water concentrations after grout hydration and the possible adverse transport processes.

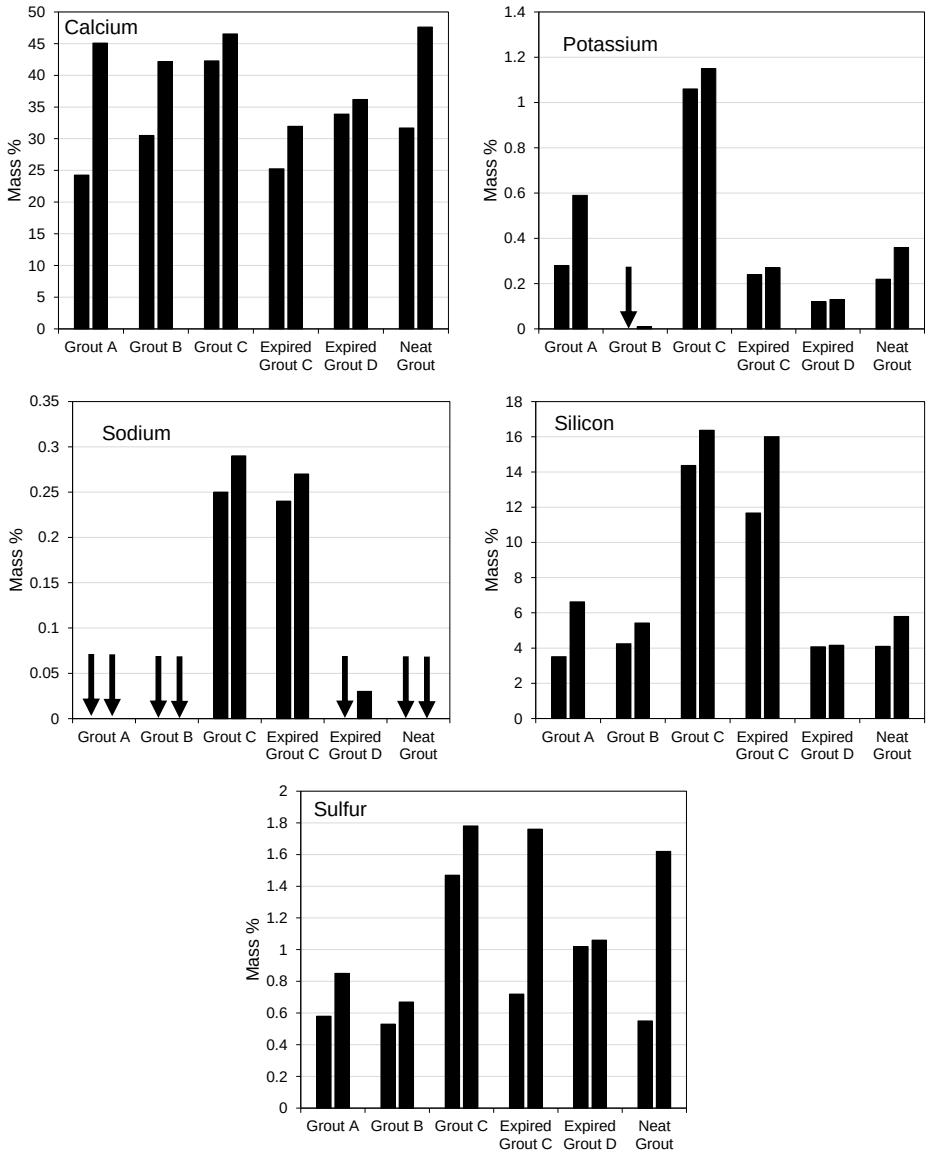

Figure 3.7. Comparison of grout chemical makeup.

3.2 Schupak Bleed Test

Schupak bleed tests (Figure 3.8) were performed for Grouts A, B, C and the neat grout during the time of grout mixing and casting as listed in Table 3.3. The Shupak test was conducted at either 50 or 100 psi typically for 5 minutes. The results are listed in the table and presented graphically in Figure 3.9.

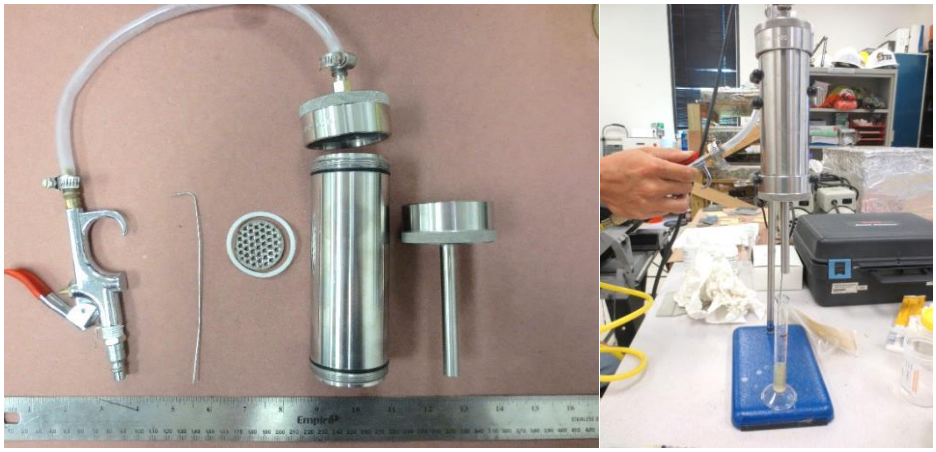

Figure 3.8. Schupak bleed test apparatus.

Attesting to the enhanced anti-bleed performance of the thixotropic grouts, the amount of developed bleed water was significantly lower than that of the 0.45 w/c neat grout where up to 50 mL of bleed water formed in the latter. Grout C showed good anti-bleed performance. Indeed the test was difficult to conduct for that material and resulted in premature degradation of the Gelman filter. The other grouts yielded up to 2.5 mL of collected water without excess mix water (but this was in some cases attributed to blowout of the Gelman filter). Grout A (not specified for vertical applications) sometimes yielded more bleed water when mixed with excess water.

The bleed water was collected, and the sulfate concentration was measured using a Hach portable turbidimeter, following FM 5-553. The bleed water contained a high concentration of sulfates, so the sample was diluted by 100 times. The results of the sulfate testing is shown in Figure 3.9. The solutions from Grout A, B, and C all had higher sulfate ion concentrations (that exceeded the 7,000 ppm limit for the test method) than the neat grout.

Table 3.3. Results of Schupak bleed test

Name	Water	Casting Date	Details of testing	Volume (mL)	Sulfate (ppm)
Grout A	Control[1]	08/06/2019	50psi, 5min	2	7400
			50psi, 5min	2	7400
		08/16/2019	100psi, 5min	2.2	-
			100psi, 5min	2.1	-
		10/07/2019	50psi, 5min	1.2	>7000
		12/18/2019	50psi, 5min	2.2	>7000
		06/08/2020	50psi, 5min	0	NA
	10%[2]	07/16/2019	50psi, 5min	2.2	7542
			50psi, 5min	3	5188
			100psi, 5min	6	2071
			50psi, 10min	2.2	4592
		08/05/2019	50psi, 5min	1	4800
		10/07/2019	50psi, 5min	2	5392
		11/21/2019	50psi, 5min	2	4187
			50psi, 5min	2	>7000
			50psi, 5min	1	7576
		06/08/2020	50psi, 5min	2	3400
		06/09/2020	50psi, 5min	2	4800
Grout B	Control[1]	08/16/2019	100psi, 5min	2.5	>7000, 4800*
			100psi, 5min	2	>7000, 4000*
		06/08/2020	50psi, 5min	1	-
	10%[2]	12/04/2019	50psi, 5min	1	>7000
			50psi, 5min	2	5500
			50psi, 5min	1	>7000, 1400*
			50psi, 5min	1	>7000, 3232*
		06/09/2020	50psi, 5min	2	>7000
Grout C	Control[1]	08/02/2019	50psi, 5min	<1	>7000
		08/15/2019	100psi, 5min	0	NA
		10/07/2019	50psi, 5min	1	-
	10%[2]	08/15/2019	100psi, 5min	0	NA
		10/07/2019	50psi, 5min	0	NA
Neat Grout	0.45 w/c	08/02/2019	50psi, 5min	50	4836
		08/05/2019	50psi, 5min	50	4843
		10/07/2019	50psi, 5min	40	4009

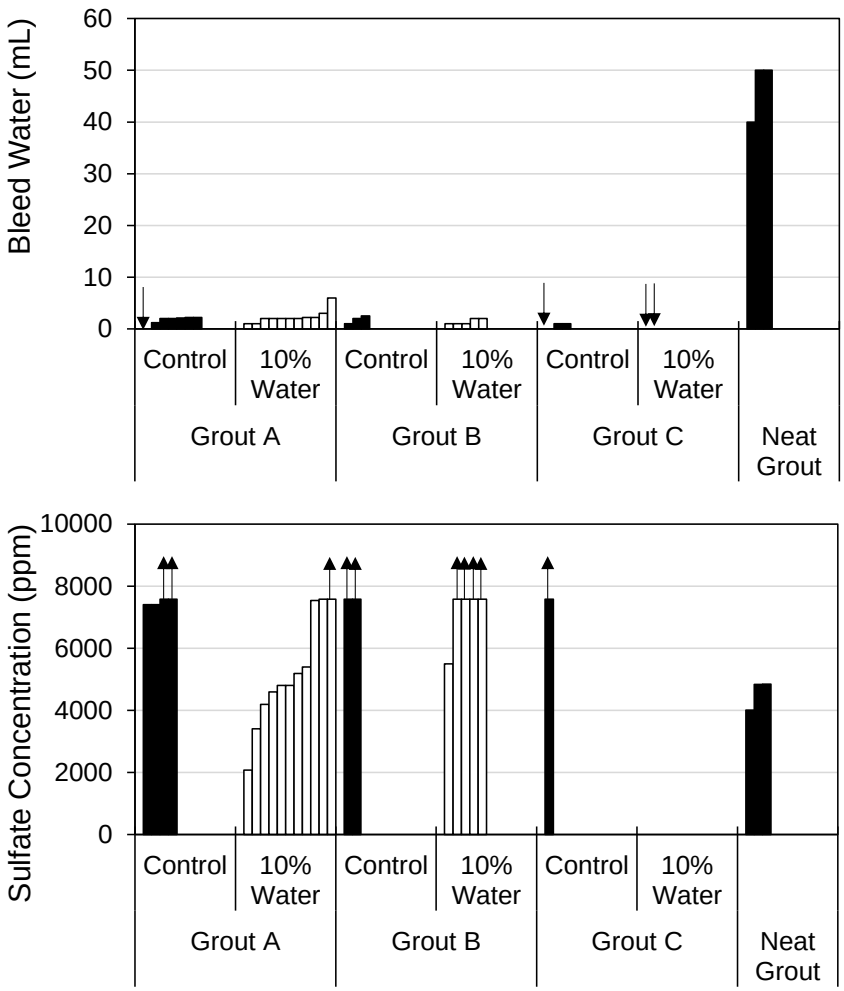

Figure 3.9. Results of Schupak bleed test and sulfate concentration

Comparisons of the sulfate concentration measured in the bleed water and the sulfur content of the unreacted grout from the XRF analysis are shown in Figure 3.10. No distinct correlation between the grout sulfur content and the sulfate ion concentration in the bleed water was observed, and relatively high levels of sulfate ions can develop in the bleed water for the grouts. Indeed, as detailed earlier, the grout product in the Florida bridge with segregated grout that had high sulfate content in the pore water did not have sulfur content in the raw powder. Grout C had higher sulfur content in the raw grout but did not readily produce bleed even with the excess mix water.

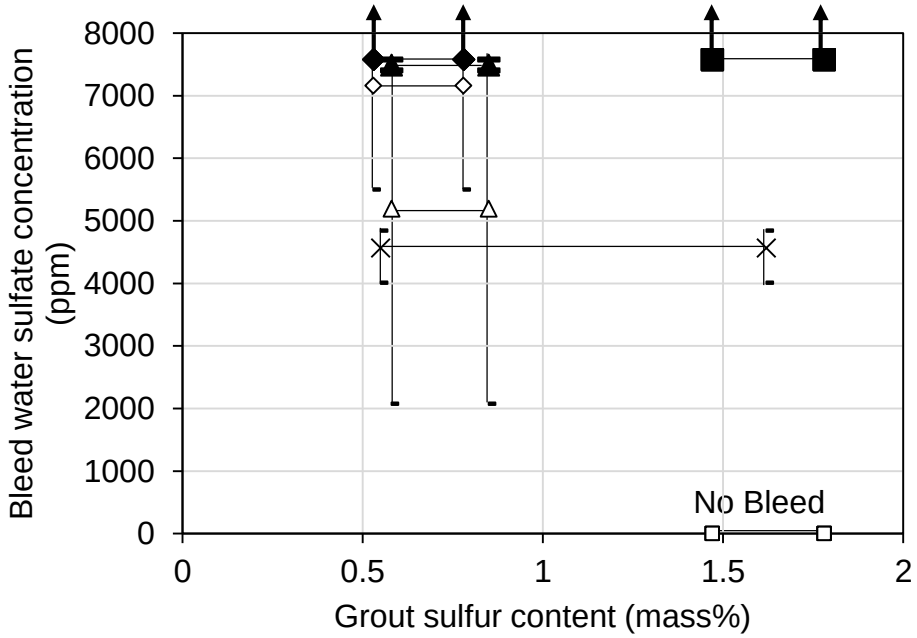

Figure 3.10. Correlation of sulfate concentration in bleed water and sulfur content in grout powder.
Triangle: Grout A. Diamond: Grout B. Square: Grout C. Cross: Neat grout
Black:Control. White: 10%Excess mix water.

CHAPTER 4. INVERTED TEE TEST

4.1 METHODOLOGY

Grout specimens cast following the inverted-tee test were prepared to be used as stock for lab sulfate analysis. From previous research, it was identified that deficient grout can form due to the displacement of water during the pumping stage of the grout installation. For example, deficient grout was observed to form at the top-most elevation of the relatively large-scaled modified incline-tube test when excess mix water was added but was not well manifested for small cylinder tests. An inverted T-test (INT) was proposed where a dramatic change in the vertical axial cross-section of the test specimen was introduced. A schematic of the INT is shown in Figure 4.1. INT specimens were cast without steel (as a complement to instrumented specimens used for the sister project (BDV29 977-44) to develop an accelerated corrosion test) for grout material testing. The grout material was partitioned as shown in Figure 10. Details on the grout material characteristics are reported in the BDV29-977-44 report. Table 4.1 details the conditions for grout material specimens.

Table 4.1. INT grout material specimen

Material	Test Condition	Grout Condition	Name	Date Cast	No. of Specimen[3]	
					header	body
Grout A	Control	AR[1], 10%[2]	IM55	06/10/2020	10	2
			IM56	06/10/2020	10	2
		AR, 10%, S[4]	IM57s	06/12/2020	10	2
		AR, 10%, C[5]	IM58c	06/12/2020	10	2
		AR, 10%, S+C[6]	IM59s+c	06/12/2020	10	2
Grout B	Control	AR	IM63[7]	06/08/2020	10	2
			IM64[7]	06/08/2020	10	2
		AR, 10%	IM65	06/10/2020	10	2
			IM66	06/10/2020	10	2
		AR, 10%, S	IM67s	06/12/2020	10	2
		AR, 10%, C	IM68c	06/12/2020	10	2
		AR, 10%, S+C	IM69s+c	06/12/2020	10	2
	High-level Constriction	AR	IM610S	06/22/2020	4	2
			IM611S	06/22/2020	5	2
		AR, 10%	IM614S	06/22/2020	6	2
			IM615S	06/22/2020	5	2
	Low-level Constriction	AR	IM612L	06/22/2020	12	2
			IM613L	06/22/2020	12	2
		AR, 10%	IM616L	06/22/2020	12	2
			IM617L	06/22/2020	12	2
Grout C	Control	AR, 10%	IE5	06/10/2020	10	2
			IE6	06/10/2020	10	2
		Expired, 10%	IOE5	06/10/2020	10	2
			IOE6	06/10/2020	10	2

Grout D	Control	Expired, 10%	IS5	06/10/2020	10	2
			IS6	06/10/2020	10	2
Neat Grout	Control	0.45 w/c	IC5	06/10/2020	10	2
			IC6	06/10/2020	10	2
		AR, 10%, S	IC7s	06/12/2020	10	2
		AR, 10%, C	IC8c	06/12/2020	10	2
		AR, 10%, S+C	IC9s+c	06/12/2020	10	2
	High Constriction	0.45 w/c	IC10S	06/22/2020	12	2
			IC11S	06/22/2020	12	2
	Low Constriction	0.45 w/c	IC12L	06/22/2020	12	2
			IC13L	06/22/2020	12	2
	Vertical Deviation 1’	0.45 w/c	ICV1	05/26/2020	3	2
	Vertical Deviation 2’	0.45 w/c	ICV2	05/18/2020	5	3
	Vertical Deviation 5’	0.45 w/c	ICV3	05/26/2020	14	2
	Vert. Dev. + Constriction	0.45 w/c	ICV4	05/18/2020	6	5

1. As-Received. 2. 10% extra mix water. 3. No. of cut specimens. 4. 2,000 ppm sulfate. 5. 832 ppm chloride. 6. Combined 2,000 ppm sulfate and 832 ppm chloride. 7. Cast with steel bar.

An excess of mix water, 10% above the manufacturers’ recommended limit was added. For the INT test, the test grouts were installed by a manual pump. Test conditions included the grout product, tee-stem height (1 ft to 5 ft), space constriction (with filters), grout pre-hydration (using expired grouts), and influence of external ion contamination (sulfate and chloride ions). Figure 4.1 shows how filters were placed to create a flow constriction between the tee body and tee stem. Figure 4.2 shows INT grout specimen partition plan for physical and chemical testing.

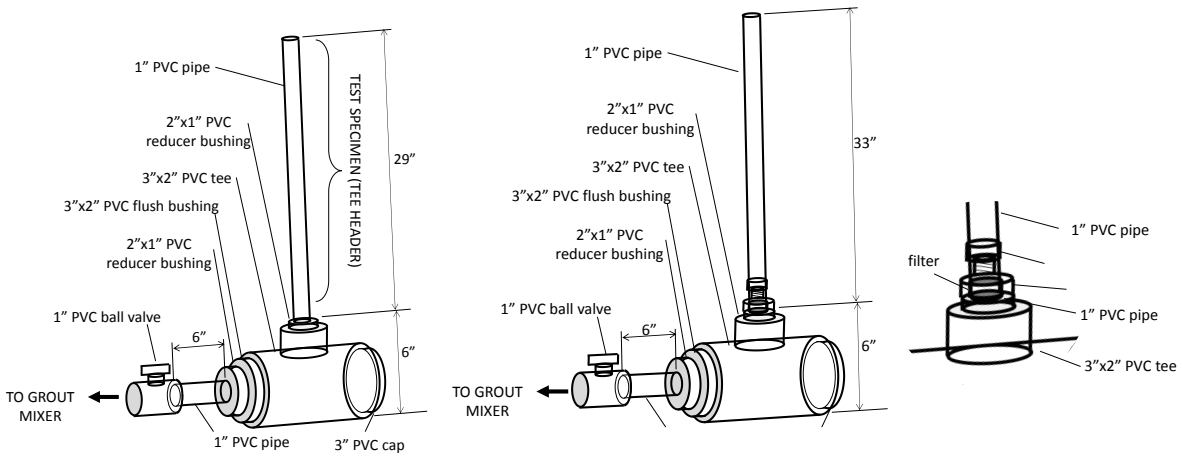

Figure 4.1. Schematic of typical inverted-tee specimens.
(Right: In some test cases, different tee header lengths and filters were used).

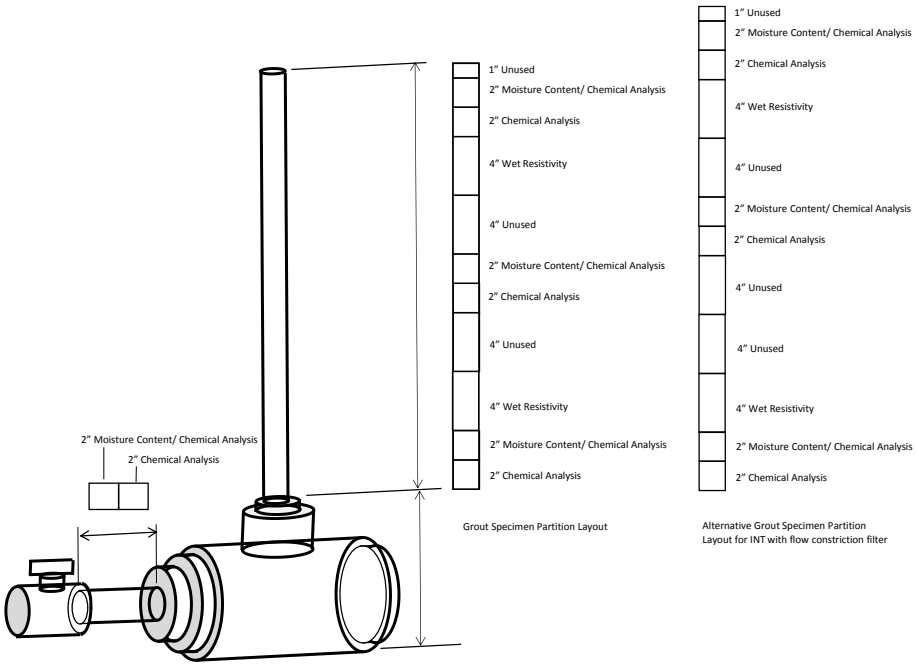

Figure 4.2. INT Grout specimen partition plan.

In some cases, flow constriction through the filter prevented complete filling of the tee stem and an alternative partition plan following the top 13" as shown was used. Figure 4.3 shows INT test assembly and component.

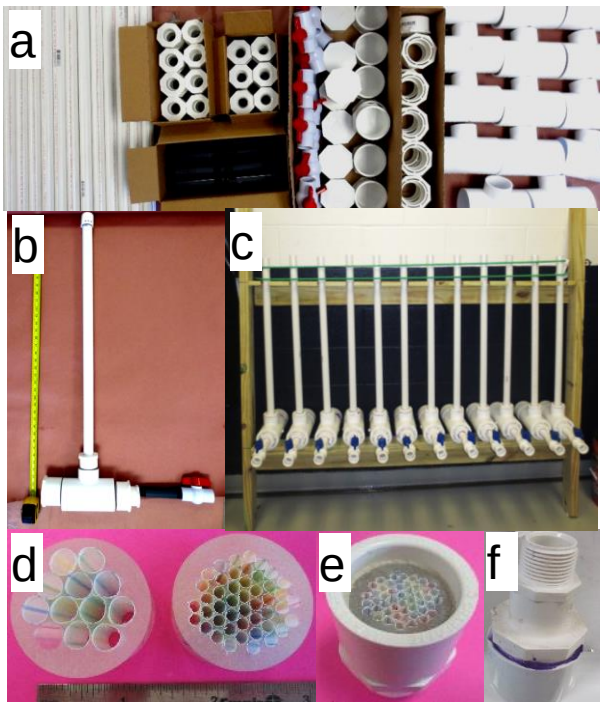

Figure 4.3. INT Assembly.
a. INT PVC components. b. Completed INT assembly. c. INT assembly setup for grouting. d. Filters to introduce flow constriction. e. Internal view of filter assembly. f. External view of filter assembly

The PVC components of the INT as shown in Figures 4.1- 4.2 were collected and assembled as shown in Figure 4.3a, b, and c. The filters to provide grout flow constrictions were made by casting plastic straws of different diameters in epoxy within a 1.25-inch diameter mold such that a ratio of open space to close space on the transverse area was approximately 2.5 following PTI specifications. The bottom end of the straws were initially plugged with silicone prior to being cast in the epoxy to prevent the epoxy from seeping into the cylindrical spaces within the straws. The silicone could easily be removed after hardening of the epoxy. Two filter sizes were made including using twelve 0.25-inch diameter straws or forty-six 0.12-inch diameter straws. The filters and PVC filter assembly for the flow constriction experiments are shown in Figure 4.3 d, e, and f.

The completed INT specimen assemblies were placed on wooden racks to ensure vertical stability during the grout pumping process. The grout was mixed using an electric mixer. After mixing, the grout was poured into a manual grout pump (Figure 4.5) and the grout was pumped into each INT assembly allowing for grout to fill the mold and flow out of the stem prior to closing the inlet PVC ball valve at the tee body.

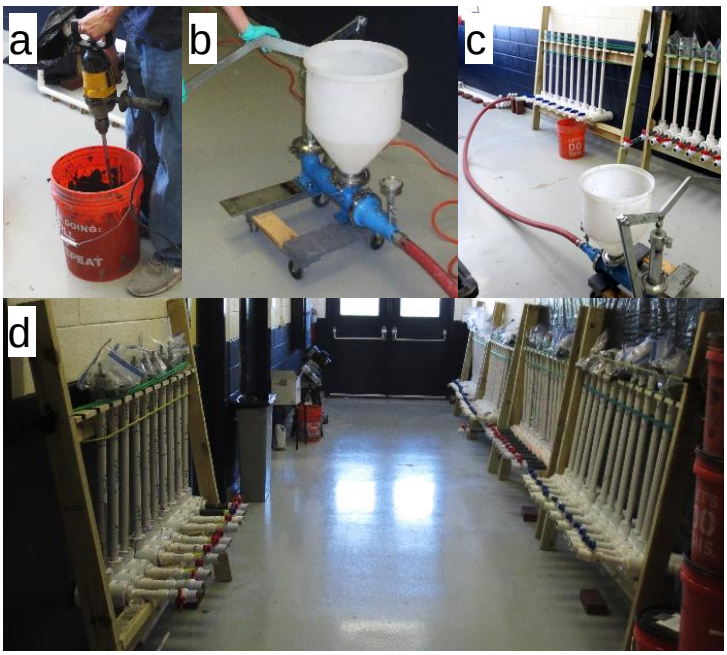

Figure 4.5. Grout Mixing and Pumping for INT.
a. Grout mixing. b. Manual grout pump. c. Setup for INT grout injection. d. Grouted INT specimens.

After 28 days curing within the INT mold, the PVC was cut at each partition mark for each specimen with an electric chop saw. The PVC pipe mold was removed by making two circumferential cuts at the top and bottom of the specimen (~1 cm distance from each end) and two longitudinal slits. An example of a set of INT test specimens is shown in Figure 4.6.

Figure 4.6. INT Test specimen fabrication.

The INT grout testing specimens were cut into segments as shown in Figure 4.2 and Figure 4.6. Following Figure 4.2, specimens from the tee header were sorted for chemical analysis.

For the specimens selected for chemical analysis (including grout specimens from the tee stem and from the tee-body inlet pipe), the grout segments were ground to a powder and collected after sieving through a no. 100 sieve (Figure 4.7c-f). The grinding process included pre-drying the grout fragments at 110^{o}C or 60^{o}C. Pre-drying the grout fragments are important practical consideration as the moisture in the grout will create residue on the grinding device. Furthermore, the pre-drying can normalize grout specimens with different moisture content.

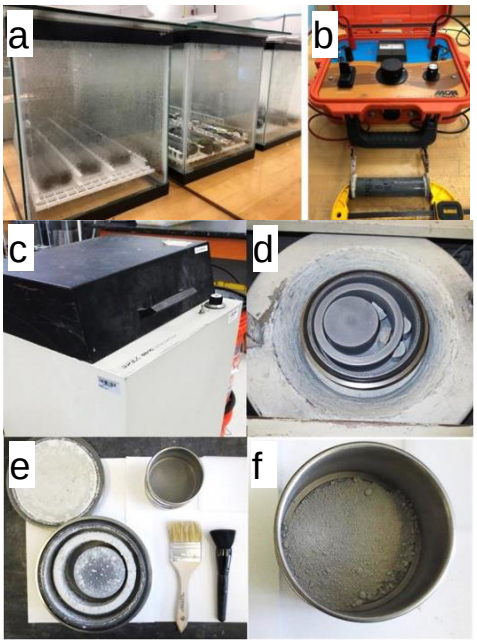

Figure 4.7. INT Grout material testing.
a. 100%RH exposure. b. Electrical resistance measurement. c. External view of Shatterbox. d. Grinding grout fragments. e. Collection of ground grout powder. f. Sieving grout powder.

4.2. LEACHING TEST METHODS

The laboratory testing involving the ex-situ leaching of the grout materials from the INT specimens, including those specimens cast to assess construction practices and to develop alternative accelerated corrosion test methods. Table 4 lists the six leaching test methods employed to assess the effect of leaching heating, heating time, leaching volume, grout sample mass, and drying temperature. For this set of experiments, grout from the top most portion (typically section 9) of the tee header was used as it was anticipated that this location would have the highest sulfate accumulation.

Test method 1 conforms to the current FDOT method. During the early investigative study on the presence of sulfates in deficient grout, field sampling of the segregated soft grout was relatively limited. Likewise, laboratory testing to simulate the grout segregation generally resulted in poor yields of physically deficient grout. Therefore, methodologies to test 1 gram of grout material were utilized. However, larger grout test masses may provide a better representation of the accumulated sulfate concentrations particularly if the sulfate levels are well stratified in the grout. Comparisons of test method 1 and 5 would ideally identify differentiation in sulfate concentration with different initial grout test masses. Subsequent test methods used the greater initial grout mass.

Comparison of test method 5 and 6 would ideally identify differentiation due to the effect of higher temperature drying. As mentioned earlier, the drying is beneficial as a practical matter to minimize the level of gumming of the hardware used to pulverize the grout material and reduce the labor involved in test preparation.

Comparison of test method 5 and 3 would ideally identify differentiation due to the leaching volume. Larger leaching volumes would facilitate the dissolution of sulfate into solution especially if the sulfate concentration was initially high. Likewise, comparison of test method 5 with test methods 2 and 4 would ideally identify differentiation due to the heating and heating time. Leaching at higher temperatures would ideally facilitate faster sulfate dissolution.

Table 4.2. Leaching test parameters

Method	Effect of Major Parameter	Drying Before Crush	Particle Size After Crush	Mass	Solid to water ratio (Leaching Volume)	Volume of DI Water	Heating Solution at 55°C-60°C
1	Current Method (FDOT)	at 60°C	100 mesh	1 gr	1:10 Volume	10 mL	18 hrs.
2	Heating time	at 60°C	100 mesh	5 gr	1:10 Volume	50 mL	4 hrs.
3	Leaching Volume	at 60°C	100 mesh	5 gr	1:40 Volume	200 mL	18 hrs.
4	No Heat	at 60°C	100 mesh	5 gr	1:10 Volume	50 mL	No Heat
5	Mass	at 60°C	100 mesh	5 gr	1:10 Volume	50 mL	18 hrs.
6	Drying	at 100°C	100 mesh	5 gr	1:10 Volume	50 mL	18 hrs.

All leachate topped-off to 100 mL except for Method 3 that was topped off to 250 mL

4.3. RESULTS

The results of the leaching experiments are shown in Table 4.3 and generalized in Figure 4.8.

Table 4.3. Results of Leaching Experiments

Grout	Test Condition	Grout Condition	Name	Leaching Method	pH	Sulfate Concentration	
						Leachate (ppm)	Grout (mg/g)
Grout A	Control	AR[1], 10%[2]	IM55	1	12.49	8.9	0.89
				2	12.48	50	1
				3	12.51	28	1.4
				4	12.8	83	1.66
				5	12.69	17	0.34
				6	12.69	6.7	0.13
			IM56	1	12.13	8.9	0.89
				2	12.47	48	0.96
				3	12.43	28	1.4
				4	12.84	82	1.64
				5	12.6	19	0.38
				6	12.63	5	0.1
Grout B	Control	AR, 10%	IM65	1	12.49	7.1	0.71
				2	12.09	21	0.42
				3	12.47	23	1.15
				4	12.52	27	0.54
				5	12.49	19	0.38
				6	12.64	5	0.1
			IM66	1	12.47	7.2	0.72
				2	12.5	23	0.46
				3	12.5	21	1.05
				4	12.58	46	0.92
				5	12.58	20	0.4
				6	12.64	5	0.1
Grout D	Control	Expired, 10%	IS5	1	12.53	17	1.7
				2	12.51	57	1.14
				3	12.48	45	2.25
				4	12.71	99	1.98
				5	12.47	41	0.82
				6	12.59	34	0.68
			IS6	1		24	2.4
				2	12.67	120	2.4
				3	12.51	69	3.45
				4	12.67	150	3
				5	12.51	71	1.42
				6	12.64	80	1.79
Neat Grout	Control	0.45 w/c	IC5	1	12.7	6.9	0.69
				2	12.4	35	0.7
				3	12.5	22	1.1
				4	12.7	54	1.08
				5	12.7	18	0.36
				6	12.7	5	0.10
			IC6	1	12.64	3.9	0.39
				2	12.64	45	0.9
				3	12.54	34	1.7
				4	12.7	65	1.3
				5	12.69	24	0.48
				6	12.64	5	0.1

1. As-Received. 2. 10% extra mix water. 3. No. of cut specimens. 4. 2,000 ppm sulfate. 5. 832 ppm chloride. 6. Combined 2,000 ppm sulfate and 832 ppm chloride. 7. Cast with steel bar.

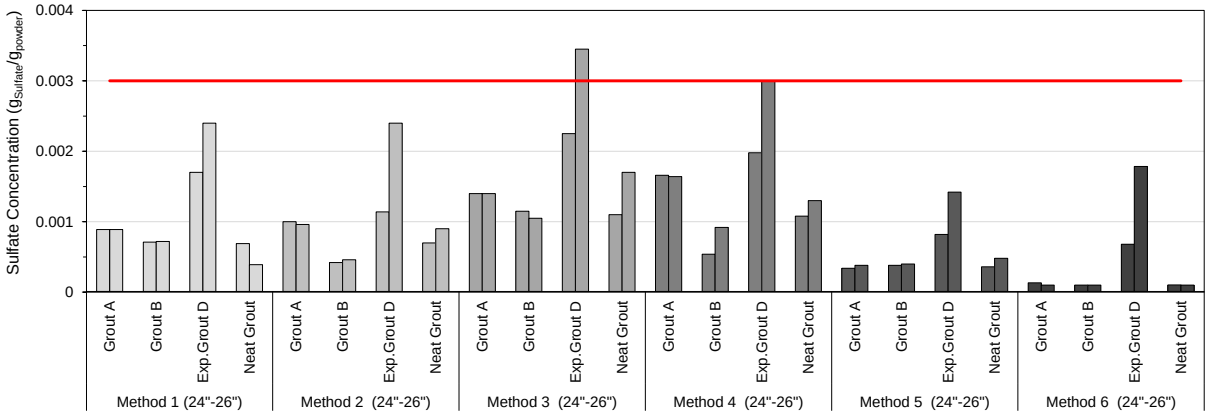

Figure 4.8. Results of sulfate ion leaching experiments.

It was apparent that the various grout products can yield different levels of sulfate ions. Grout product D, which was the grout product used in the Florida bridge that had developed soft grout and steel strand corrosion, yielded higher sulfate concentrations than the other grouts tested.

In comparison of leaching methods 1 and 5, the larger sample mass (as expected) yielded higher sulfate concentrations in the leachate (Figure 4.9). However, the increase in sulfate concentration was not commensurate to the larger sample mass. Indeed, on a mass-per-mass basis, leaching of the larger grout mass yielded lower concentrations. Increasing the leaching volume from 1:10 to 1:40 as tested in methods 5 and 3, showed further increase in the leachate sulfate concentration and also yielded higher sulfate concentrations on a mass-per-mass basis. Comparisons of leaching methods 5, 2, and 4 did not show a strong effect of heating to enhance the leaching of the sulfates and indeed, the cases where no heating was employed yielded greater sulfate ion concentrations in the leachate (Figure 4.9). Comparison of drying methodologies for the extracted grout showed a significant decrease in the leaching of sulfate ions at the 100^{o}C temperature in comparison to the 60^{o}C drying temperature with the exception of Grout D (Figure 4.9).

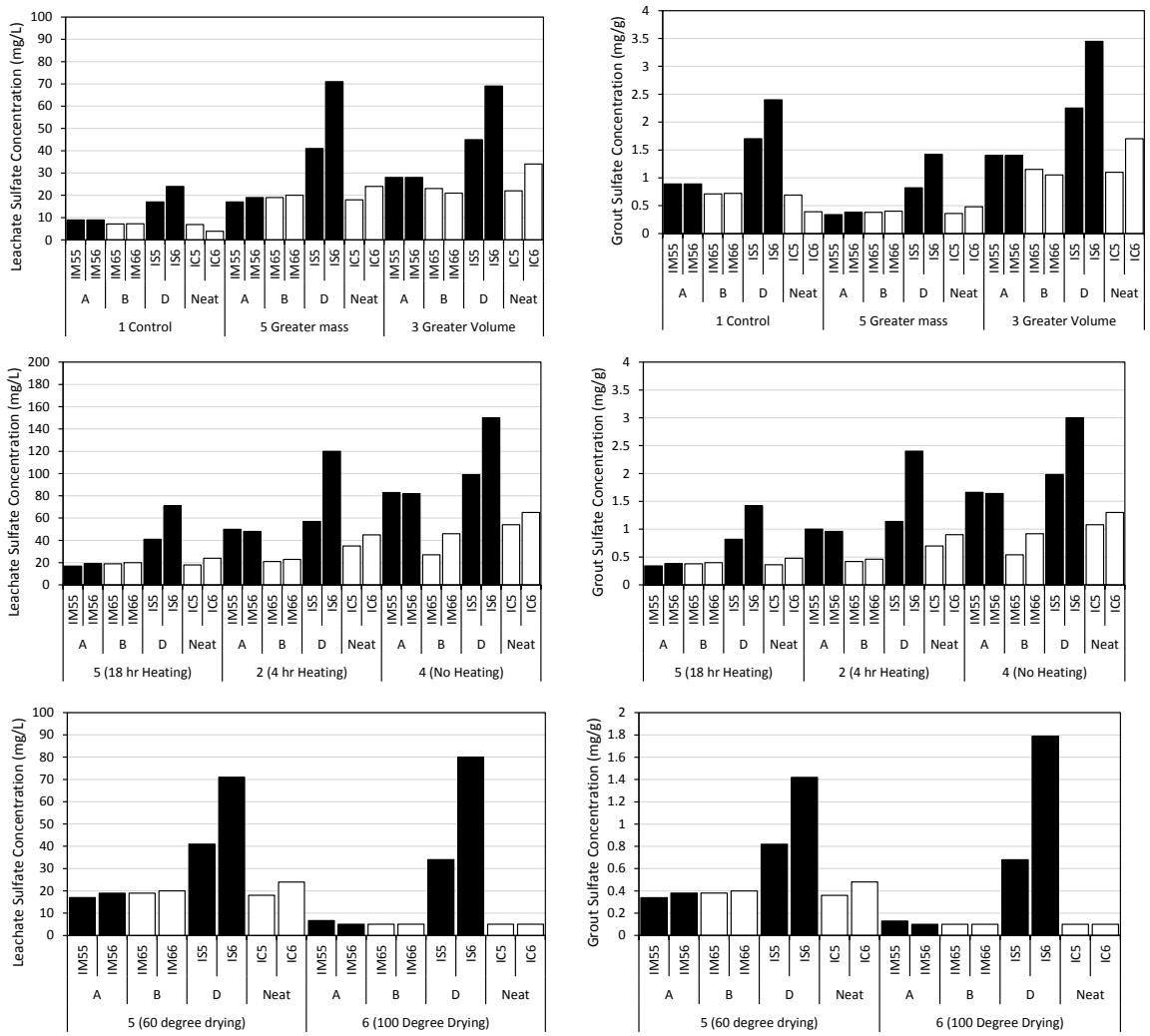

Figure 4.9. Results of leaching experiments

The sulfate ion concentrations in the leachate was correlated to the sulfate concentration normalized by the grout sample mass (Figure 4.10). As expected, there was a linear relationship between the leachate and grout sulfate content conforming to the equation

$$M = \frac{C\,V}{1000\,m}$$

where

M= SO_4^{2-} concentration in g $_{Sulfate}$/g $_{Grout}$

C= SO_4^{2-} concentration of leachate in mg/L

V= Volume of sample in L (L)

m= dry mass of grout in gr (g).

The grout sulfate concentration ($g_{sulfate}/g_{grout}$) would be a function of the leachate concentration by a factor 0.1 (0.1L/1g) for leaching method 1, 0.02 (0.1L/5g) for leaching method 2-6, and 0.05 (0.25L/5g) for leaching method 3.

For example, utilizing the current FDOT methodologies, the maximum allowable leachate sulfate concentration of 30 ppm would be 3 mg/g. Adoption of leaching methods 3 or 5 would require a different maximum leachate sulfate concentration value, such as 60 ppm or 150 ppm; respectively, if 3 mg/g represented a conservative limit value.

Examination of Figures 4.9 and 4.10 revealed that larger grout mass size and greater leaching volume would allow for elevated dissolution of sulfates. Although the different grout products tested can vary in terms of its robustness to segregation and sulfate accumulation, the general material set used for the testing of the leaching methods were the same. It was evident from Figure 4.10 that the leaching volume is an important factor. Leaching methods 1 and 5 both used a 1:10 leaching volume ratio; but (as can be seen in Figure 2) even though the leachate concentration was higher in the latter, the normalized concentration by grout mass was much lower. It was apparent that the 1:10 leaching volume ratio for the larger grout sample mass was not as efficient in leaching the sulfate from the grout particles. Furthermore, when the leaching volume was increased to 1:40, the leaching efficiency was much higher.

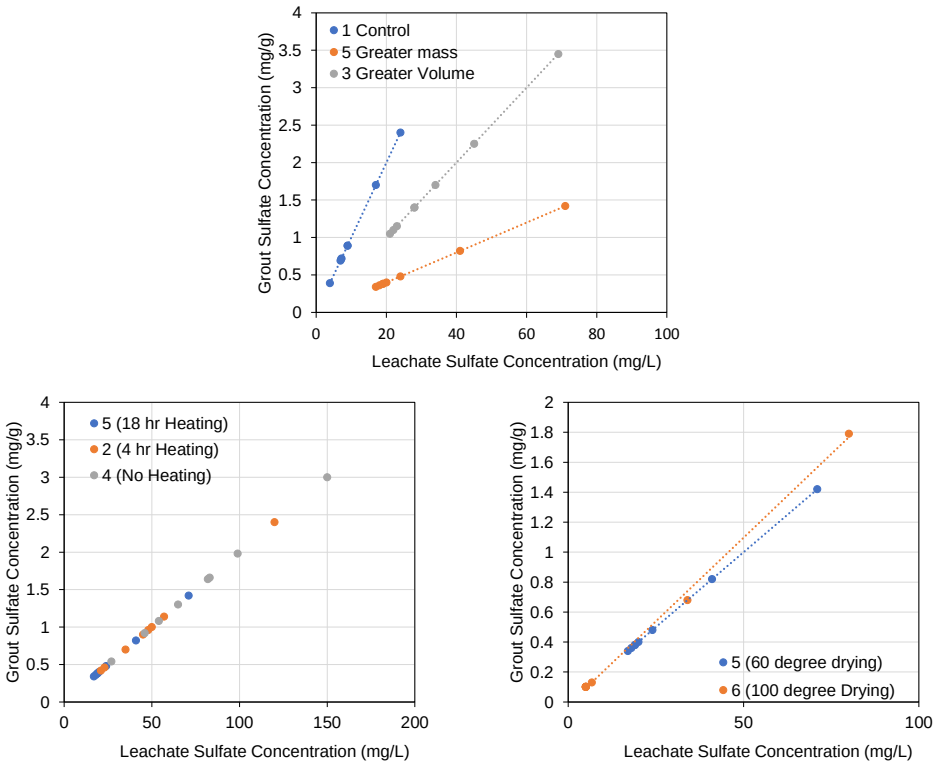

Figure 4.10. Correlation of leachate and grout sulfate concentration

Heating of the leaching solution to ~60ºC at both 4 hours and 18 hours unexpected showed lower sulfate ion concentrations than the non-heated samples. The relatively low heating temperature did not allow for spillage and watch glasses

were used to cover the beakers. The heating is expected to facilitate the dissolution of sulfates especially at higher concentrations. This discrepancy was not resolved.

Drying the grout samples is necessary for practicality to reduce the level of test preparation (to minimize the gumming of the pulverizing equipment) and to normalize the mass of test specimens (such as samples with high moisture content that can quickly dry in test preparation and transport). Drying of the grout samples to 100^{o}C yielded low sulfate content likely due to evaporative processes and is not recommended.

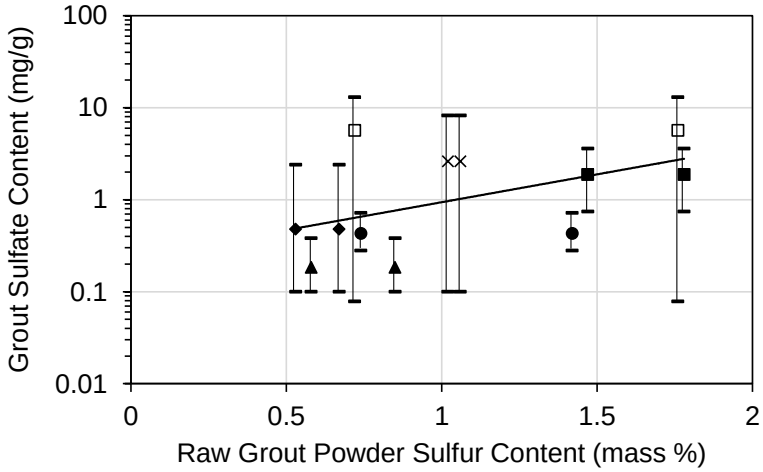

Figure 4.11. Correlation of sulfate content in hardened grout and grout powder. Triangle: Grout A. Diamond: Grout B. Square: Grout C. Cross: Grout D. Circle: Neat grout

Figure 4.11 shows the correlation of sulfate content in hardened grout and grout powder. Cementitious materials such as grout inherently contain some level of sulfur-bearing compounds such as SO_3 or in components such as gypsum and kiln dust. However, the presence of these sulfur-bearing components does not necessarily relate to its ability to accumulate in the deficient grout by some transport mechanism and dissolution into the grout pore water. The grout sulfate content resolved by leaching method 5 and the mass percent of sulfur identified by XRF of the raw grout powder were compared. As shown in Figure 4.11, there is a general trend in the resolved grout sulfate content and the raw powder sulfur content but was not strongly correlated.

The sulfate content associated with severe corrosion was associated with deficient grout materials with high moisture content. As such, it is recommended that the sulfate testing be incorporated into material testing to assess the susceptibility of grout materials to segregate. Test methods such as the modified incline tube test incorporating overwatering in the grout mixing or alternative testing to facilitate the capturing of displaced water such as the inverted-tee test should be considered for

grout material sampling. In the field, extraction of grout materials from locations typically associated with moisture and/or bleedwater such as at high points, points of deviation, and at joints should be considered. The grout from the INT specimens were further tested to assess the effects of poor construction on the extent to which sulfate ions can accumulate including overwatering, prehydration, external contamination, and flow constriction. Leaching was made following method 5. Results are shown in Table 4.4-4.6 and Figures 16-19.

Table 4.4. Results of Leaching Experiments (Grout A)

Grout	Test Condition	Grout Condition	Name	INT Segment	pH	Sulfate Concentration	
						Leachate (ppm)	Grout (mg/g)
Grout A	Control	AR[1], 10%[2]	IM55	1	12.64	5	0.1
				5	11.81	5.6	0.112
				B	12.69	5	0.1
				10	12.67	35	0.7
			IM56	1	12.7	5	0.1
				5	12.66	12	0.24
				A	12.7	5	0.1
				10	12.7	34	0.68
		AR, 10%, S[3]	IM57s	1	12.72	5	0.1
				6	12.7	5.4	0.108
				9	12.66	5	0.1
				A	12.7	5	0.1
		AR, 10%, C[4]	IM58c	1	12.6	5	0.1
				5	12.63	5	0.1
				9	12.6	5	0.1
				A	12.65	5	0.1
		AR, 10%, S+C[5]	IM59s+c	1	12.63	5	0.1
				5	12.62	5	0.1
				9	12.64	5	0.1
				A	12.61	5	0.1

1. As-Received. 2. 10% extra mix water. 3. 2,000 ppm sulfate. 4. 832 ppm chloride. 5. Combined 2,000 ppm sulfate and 832 ppm chloride.

Table 4.5. Results of Leaching Experiments (Grout B)

Grout	Test Condition	Grout Condition	Name	INT Segment	pH	Sulfate Concentration	
						Leachate (ppm)	Grout (mg/g)
Grout B	Control	AR[1]	IM63	1	12.53	5	0.1
				9	12.55	5.3	0.106
				B	12.59	5	0.1
			IM64	1	12.57	5	0.1
				9	12.6	5	0.1
				B	12.62	5	0.1
		AR, 10%[2]	IM65	1	12.52	120	2.4
				5	12.52	5	0.1
				A	12.54	10	0.2
				10	12.73	66	1.32
			IM66	1	12.56	5	0.1
				5	12.54	6.7	0.134
				A	12.45	5	0.1
				10	12.64	56	1.12
		AR, 10%, S[3]	IM67s	1	12.58	5	0.1
				5	12.61	9.8	0.196
				9	12.64	6.3	0.126
				A	12.65	9.6	0.192
		AR, 10%, C[4]	IM68c	1	12.63	12	0.24
				5	12.66	7.9	0.158
				9	12.67	5	0.1
				A	12.67	6.7	0.134
		AR, 10%, S+C[5]	IM69s+c	1	12.65	5	0.1
				5	12.63	7.1	0.142
				9	12.65	5	0.1
				A	12.58	9	0.18
	High Constriction	AR	IM610S	3	12.57	5	0.1
				A	12.57	5	0.1
			IM611S	3	12.58	5	0.1
				A	12.57	5.8	0.116
		AR, 10%	IM614S	1	12.51	5	0.1
				5	12.44	8.2	0.164
				A	12.5	5	0.1
			IM615S	2	12.48	6.5	0.13
				A	12.47	14	0.28
	Low Constriction	AR	IM612L	1	12.61	6.9	0.138
				10	12.55	5	0.1
				A	12.6	5	0.1
			IM613L	1	12.63	5	0.1
				10	12.65	5	0.1
				A	12.64	5.2	0.104
		AR, 10%	IM616L	1	12.5	8.5	0.17
				10	12.47	9.7	0.194
				A	12.49	8.8	0.176
			IM617L	1	12.54	5	0.1
				10	12.53	5	0.1
				A	12.57	5	0.1

1. As-Received. 2. 10% extra mix water. 3. 2,000 ppm sulfate. 4. 832 ppm chloride. 5. Combined 2,000 ppm sulfate and 832 ppm chloride.

Table 4.6. Results of Leaching Experiments (Grout C, D, and neat grout)

Grout	Test Condition	Grout Condition	Name	INT Segment	pH	Sulfate Concentration	
						Leachate (ppm)	Grout (mg/g)
Grout C	Control	AR[1], 10%[2]	IE5	9	12.39	38	0.76
				B	12.17	180	3.6
			IE6	9	12.4	37	0.74
				B	12.21	120	2.4
		Expired, 10%	IOE5	9	11.92	470	9.4
				A	12.35	8	0.16
			IOE6	9	11.73	3.9	0.078
				A	12.15	650	13
Grout D	Control	Expired, 10%	IS5	A	12.68	5	0.1
				10	12.69	250	5
			IS6	A	12.66	5	0.1
				10	12.16	410	8.2
Neat Grout	Control	0.45 w/c	IC5	1	12.6	19	0.38
				5	12.65	18	0.36
				10	12.74	21	0.42
				A	12.64	19	0.38
			IC6	1	12.65	14	14
				5	12.6	17	17
				10	12.73	36	36
				A	12.52	19	19
		AR, 10%, S[3]	IC7s	1	12.67	8.9	0.178
				5	12.68	5.2	0.104
				9	12.55	12	0.24
				A	12.57	7	0.14
		AR, 10%, C[4]	IC8c	1	12.53	5	0.1
				5	12.68	5	0.1
				9	12.65	5	0.1
				A	12.68	5	0.1
		AR, 10%, S+C[5]	IC9s+c	1	12.64	8.7	0.174
				5	12.62	6.5	0.13
				9	12.68	5	0.1
				A	12.67	5	0.1
	High Constriction	0.45 w/c	IC10S	1	12.55	21	0.42
				11	12.61	18	0.36
				A	12.62	19	0.38
			IC11S	1	12.26	20	0.4
				10	12.58	19	0.38
				A	12.6	20	0.4
	Low Constriction	0.45 w/c	IC12L	1	12.58	30	0.6
				10	12.6	27	0.54
				A	12.53	28	0.56
			IC13L	1	12.64	5	0.1
				10	12.67	10	0.2
				A	12.48	7.2	0.144

1. As-Received. 2. 10% extra mix water. 3. 2,000 ppm sulfate. 4. 832 ppm chloride. 5. Combined 2,000 ppm sulfate and 832 ppm chloride.

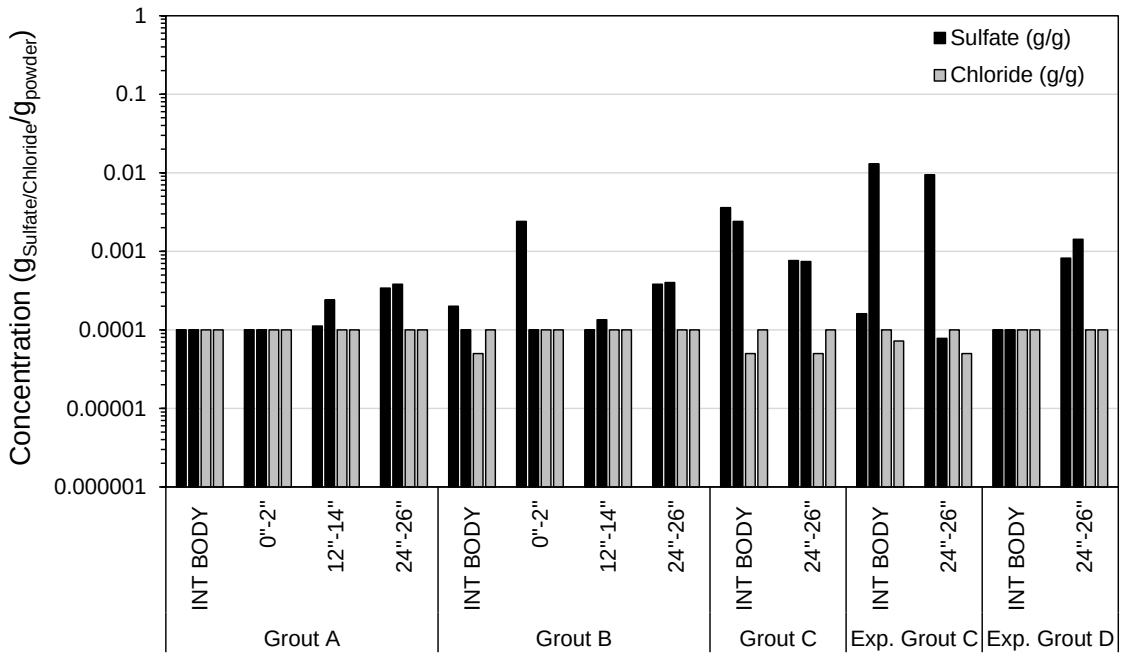

Figure 4.12. Comparison of sulfate ion concentrations in grout from INT tee header and tee body.

As discussed earlier, the different grout products had different yields of leached sulfate ions in the INT header. As shown in Figure 4.12, higher sulfate levels were generally observed in the tee header than the tee body likely relating to the displacement of water to the top of the specimen. As leaching method 5 was used here, it would be presumed that these concentrations can be higher (such as by using greater leaching volume).

Figures 4.13 and 4.14 show the resolved sulfate concentrations in grouts subjected to sulfate contamination. Consistent with previous research, it was shown that the sulfate ion accumulation in the deficient grout (here in the tee header) can develop without external contamination. In the test conditions with an additional 2,000 ppm sulfate, the resolved sulfate concentrations were lower than the control mix. It was observed that when the additional sodium sulfate was added to the mix water, the grout mix was thicker where less water per solids was present. This would create a lower water-to-cement ratio and overall less water availability to be involved in the material segregation.

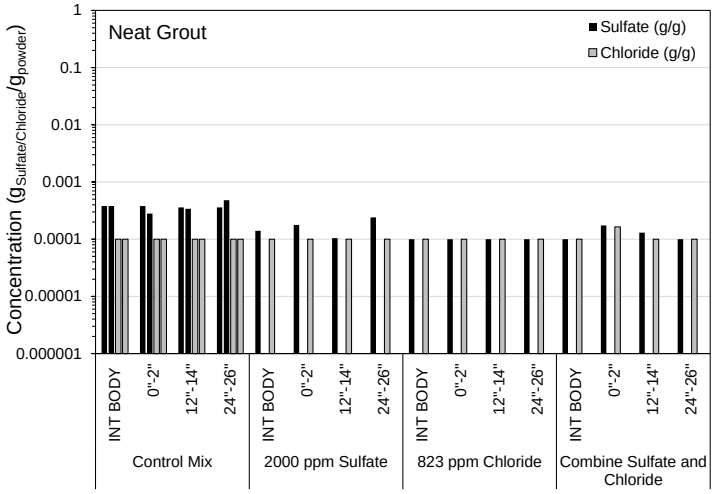

Figure 4.13. Sulfate ion concentration in neat grout subjected to external contamination.

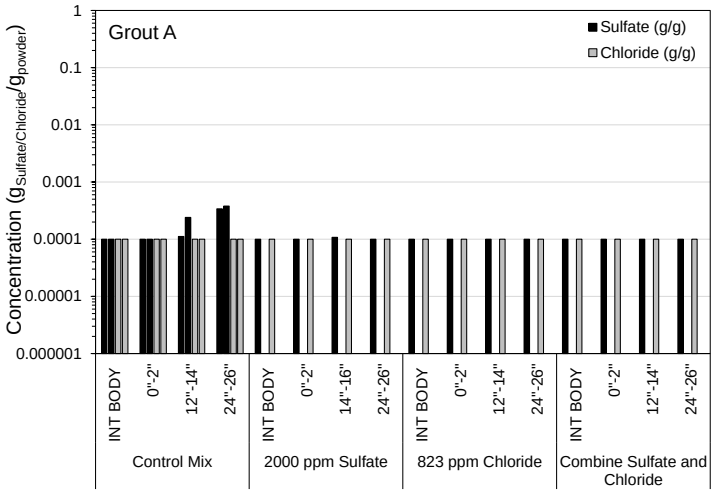

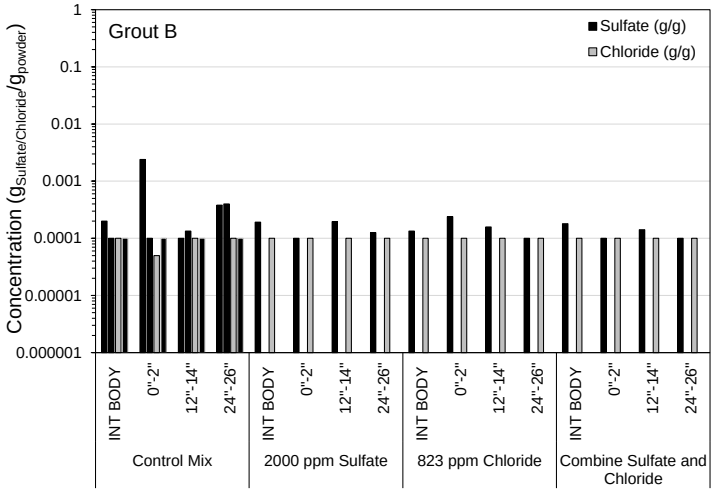

Figure 4.14. Sulfate ion concentration in grouts A and B subjected to external contamination.

As shown in Figure 4.15, the addition of excess mix water in the INT setup for the grouts allowed for moisture displacement and accumulation of sulfate ions relative to the conditions with no excess mix water. However, the experiments did not show appreciable effects due to the grout flow constriction. Further discussion on these experiment can be found in the sister project final report BDV29 977-44.

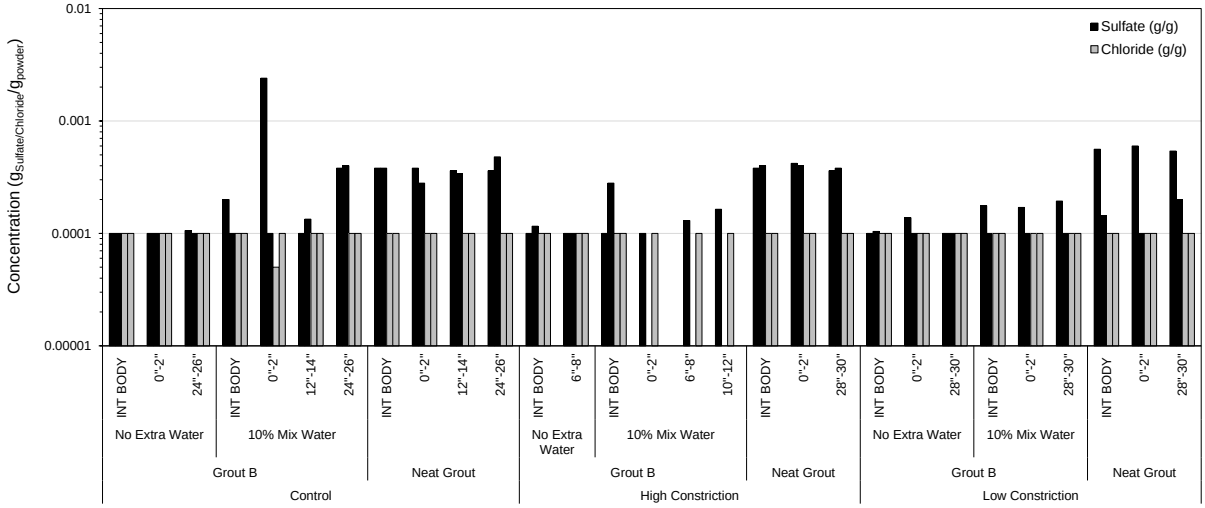

Figure 4.15. Sulfate ion concentration in grout subjected to flow constriction

CHAPTER 5. MODIFIED INCLINE TUBE TEST

5.1 METHODOLOGY

The MIT test generally consists of pumping grout in a 3-inch diameter pipe, along a 15-foot length at a 30 degree incline. A schematic of the specimen assembly used in this research is shown in Figure 5.1. The relatively high grout volume and the vertical deviation could promote transport of moisture if the grout material is susceptible to bleed or segregate. The MIT test also included excess mix water to promote the moisture transport.

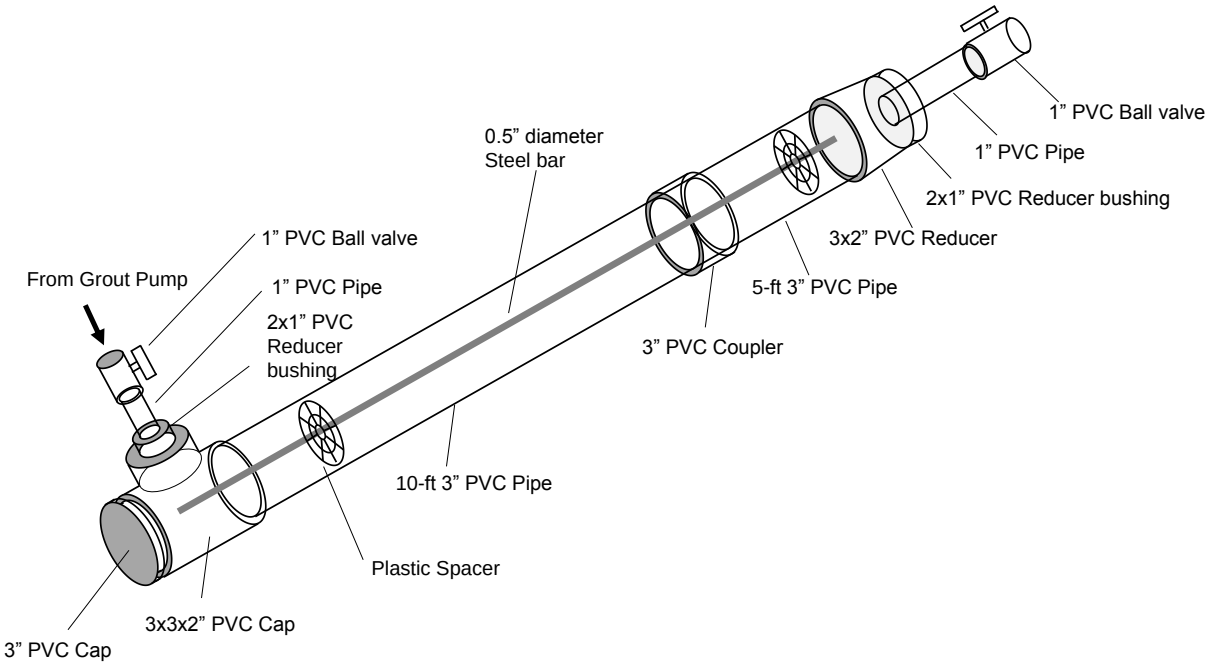

Figure 5.1. MIT test assembly

A 15-foot 0.5-inch diameter steel bar was placed in the MIT for additional corrosion testing as part of the sister project, "Accelerated Corrosion Testing of Grouts for PT Steel Strand." The steel bar was cut to length and cleaned with acetone (Figure 2A). The PVC components were assembled according to Figure 5.1 and the steel bar was placed within the pipe, centered with rebar spacers. The specimens were placed on a steel frame with a 30 degree incline, as shown in Figure 5.2B-D.

Figure 5.2. MIT assembly.
A. Steel bar. B. Front view of assembly. C. Side view of assembly. D. View of steel bar near MIT outlet.

Figure 5.3. MIT grout mixing and injection

Grout A had been used for horizontal PT applications and Grout B had been used for vertical applications. The grout mixes for both products incorporated 10% excess mix water from the manufacturer's recommendation. It was thought that the two products designed for different applications (horizontal and vertical) can be used as a foil, and the two products with non-ideal excess mix water and subject to the vertical deviation in the MIT testing would ideally create differentiation in the grout within the assembly to provide test material for subsequent laboratory testing of deficient grout.

For each specimen, four 25-pount batches were weighed and mixed on site (Figure 3A-B) and pumped into the PVC assembly. A manual grout pump was used to inject the grout into the MIT assemble (Figure 5.3C-D). Grout was allowed to freely flow out of the PVC outlet. The outlet valve was first closed followed by the inlet valve.

Details of the MIT specimens are shown in Table 5.1.

Table 5.1. MIT specimens

Name	Condition	Casting Date	Number of Samples Cast	Specimen Name
Grout A	As-received grout with 10% ext water	11/20/2019	1	MIT-1
		11/21/2019	3	MIT-2
				MIT-3
				MIT-4
		12/03/2019	2	MIT-6
				MIT-8
Grout B	As-received grout with 10% ext water	12/04/2019	3	MIT-9
				MIT-10
				MIT11
		12/17/2019	3	MIT-13
				MIT-14
				MIT16

5.2 SULFATE TESTING

Grout was sampled from each of the MIT specimens within the top and bottom 6 inches of the duct. A 1.25-inch diameter core was extracted, and the grout was prepared following leaching method 1 and 3. The sulfate concentration of the leachate was measured using a Hach portable turbidimeter, following FM 5-553. The leachate has a diluted concentration of sulfate; 10-mL of the leachate was directly tested. The results of testing are listed in Tables 5.2 and 5.3.

Table 5.2. Results of leaching experiments (method 3)

Name	Condition	Casting Date	Specimen Name	Leachate pH		Sulfate Content ppm (mg/g)	
				Top	Bottom	Top	Bottom
Grout A	As-received grout with 10% extra water	11/20/2019	MIT-1	12.6	12.6	11 (0.55)	11 (0.55)
		11/21/2019	MIT-2	12.6	12.6	9 (0.45)	8 (0.4)
			MIT-3	12.7	12.6	10 (0.5)	4 (0.2)
			MIT-4	12.7	12.6	10 (0.5)	7 (0.35)
		12/03/2019	MIT-6	12.6	12.7	9 (0.45)	12 (0.6)
			MIT-8	12.6	12.5	5 (0.25)	7 (0.35)
Grout B	As-received grout with 10% extra water	12/04/2019	MIT-9	12.6	12.6	8 (0.4)	6 (0.3)
			MIT-10	12.6	12.6	9 (0.45)	13 (0.65)
			MIT11	12.6	12.6	8 (0.4)	10 (0.5)
		12/17/2019	MIT-13	12.7	12.4	7 (0.35)	3 (0.15)
			MIT-14	12.7	-	12 (0.6)	- (-)
			MIT16	12.6	12.7	13 (0.65)	2 (0.1)

Table 5.3. Results of leaching experiments (method 1)

Name	Condition	Casting Date	Specimen Name	Leachate pH		Sulfate Content ppm (mg/g)	
				Top	Bottom	Top	Bottom
Grout A	As-received grout with 10% extra water	11/20/2019	MIT-1	12.14	12.32	X	X
		11/21/2019	MIT-2	12.16	12.29	X	X
			MIT-3	11.7	12.33	X	X
			MIT-4	12	12.11	X	X
		12/03/2019	MIT-6	11.99	12.35	X	6 (0.6)
			MIT-8	11.8	12.03	X	X
Grout B	As-received grout with 10% extra water	12/04/2019	MIT-9	12.08	11.87	X	X
			MIT-10	12.15	11.91	X	X
			MIT11	11.92	12.04	X	X
		12/17/2019	MIT-13	12.14	12.32	X	X
			MIT-14	11.96	-	X	-
			MIT16	11.92	12.2	X	X

X- below detection limit

Relatively low sulfate ion concentrations were measured in the leachate solution following leaching method 3, and there was experimental scatter for the replicate MIT specimens. However, comparisons of the average sulfate concentrations (as shown in Figure 5.4) do indicate differentiation of the sulfate content in the grout from the upper and lower elevations of the MIT specimens. For both Grout A and B, the average sulfate content in the grout from the top of the specimen was higher than the average sulfate content from the bottom of the specimen.

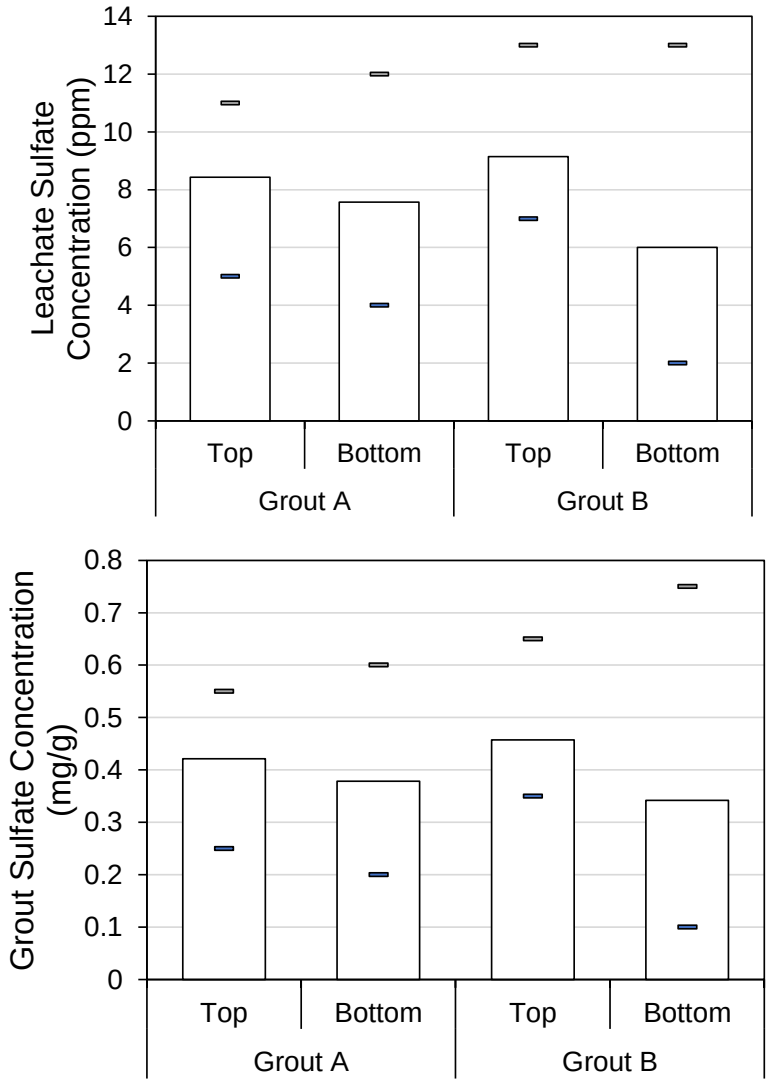

Figure 5.4. Comparison of sulfate content in grout from upper and lower elevations of MIT

Leaching of the same grout materials from the MIT following leaching method 1 typically resulted in values below the detection limit of the colorimeter. It was apparent that leaching following method 3 was more efficient with respect to the level of dilution as part of the test protocol and within the detection limit following turbidimetric methods.

5.3 CORROSION TESTING

The corrosion activity of the embedded steel bar was assessed by measurement of the open-circuit potential, polarization resistance (Rp) by the linear polarization resistance method (LPR), and solution resistance by electrochemical impedance spectroscopy (EIS). At the base of each tendon, the embedded steel bar was exposed so that electrical contact can be made for the electrochemical testing. Six portals along the length of the MIT specimen were made to expose the grout

within the duct by cutting and removing the PVC cover. A counter electrode made out of activated titanium mesh (4 x 3 inch) was inserted between two wet sponges was affixed to exposed grout surface. A pen copper/copper-sulfate reference electrode was placed at the center of the fixture.

The LPR measurements were made from the open-circuit condition (OCP) and cathodically polarized 25 mV at a 0.1 mV/s scan rate. The Rp was corrected for the solution resistance resolved as the high frequency limit from EIS. EIS was measured at the OCP with a 10 mV a.c. excitation voltage from 100 kHz to 1 kHz.

The OCP for the steel in the MIT specimens are shown in Figure 5.5. The OCP of the steel showed a modest decrease to more electronegative potentials at the upper 5 feet of the tendons. However, the potentials overall were generally indicative of passive conditions. Indeed the resolved Rp shown in Figure 5.6 did not show strong indication for elevated corrosion rates for the steel at the upper elevations.

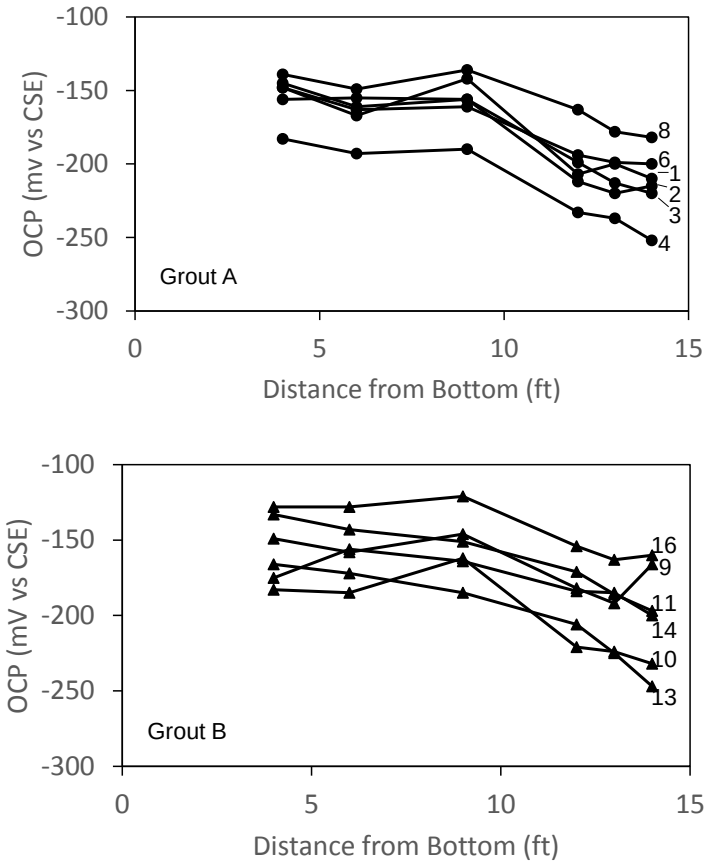

Figure 5.5. Open-circuit potential of steel in MIT specimens

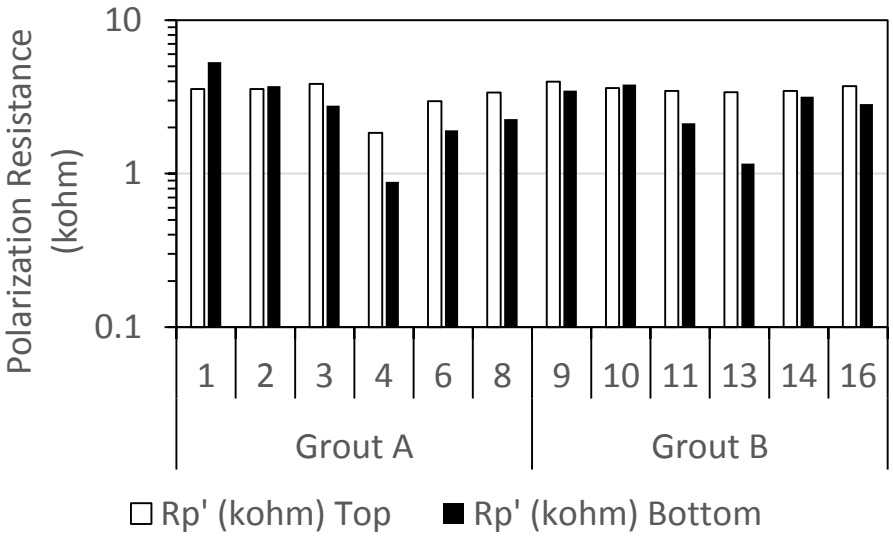

Figure 5.6. Polarization resistance of steel in MIT specimens

The resolved solution resistance of the grout however was strongly differentiated between locations from the top and bottom of the tendon, indicating differentiation in the grout and moisture content (Figure 5.7). Lower solution resistance was resolved for grout at the top of the tendon than at the lower elevations, further supporting the use of the MIT as means to test grout performance. It was noted that greater differentiation in solution resistance between tendon elevations as well as lower values were obtained for Grout A compared to Grout B. Indeed Grout B had better performance as it was designed for vertical PT applications and Grout A has been accepted for only horizontal PT applications. The sulfate content in Grout B was much greater differentiated between the high point elevation (~0.48 mg/g) and the low point elevation (~0.13 mg/g) than for Grout A, but Grout A showed as much as ~0.6 mg/g sulfate at high and low point elevations.

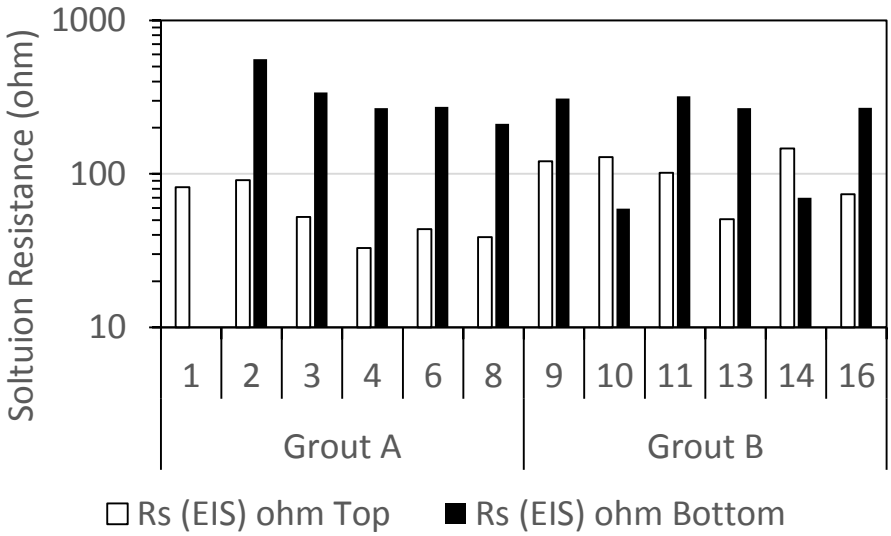

Figure 5.7. Solution resistance of grout from MIT specimens

The corrosion potentials and corrosion current densities for the steel embedded in the MIT specimens and the INT specimens were correlated to the grout sulfate content. Figure 5.8 and 5.9 show correlation of steel corrosion potential and corrosion current density with grout sulfate content. As shown in Figure 5.8, the corrosion potential decreases to more electronegative values at the higher sulfate concentrations. Likewise, the corrosion current density showed a general increasing trend with the higher sulfate levels (Figure 5.9). The values produced from the test program here were consistent with historical data from earlier research, further verifying the adverse effects of elevated sulfate ion concentrations in the segregate grout. The expired grouts developed the highest sulfate ion concentrations and showed the greatest susceptibility for corrosion development.

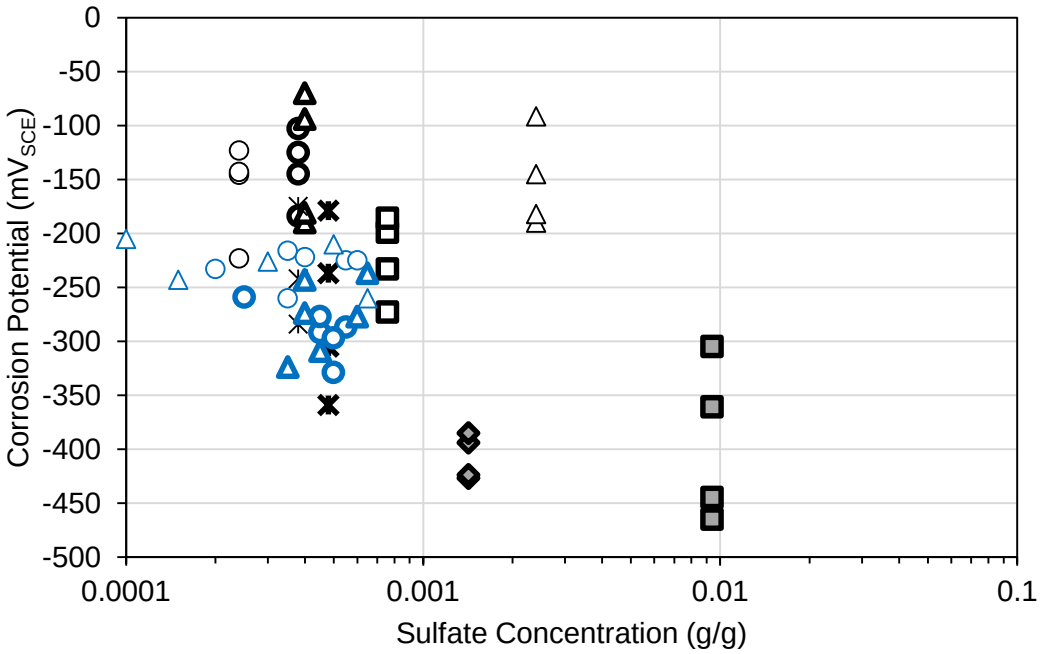

Figure 5.8. Correlation of steel corrosion potential and grout sulfate content. Circle: Grout A. Triangle: Grout B. Square: Grout C. Diamond: Grout D. Cross: Neat Grout. Filled: Expired Grout. Blue: MIT. Black: INT.

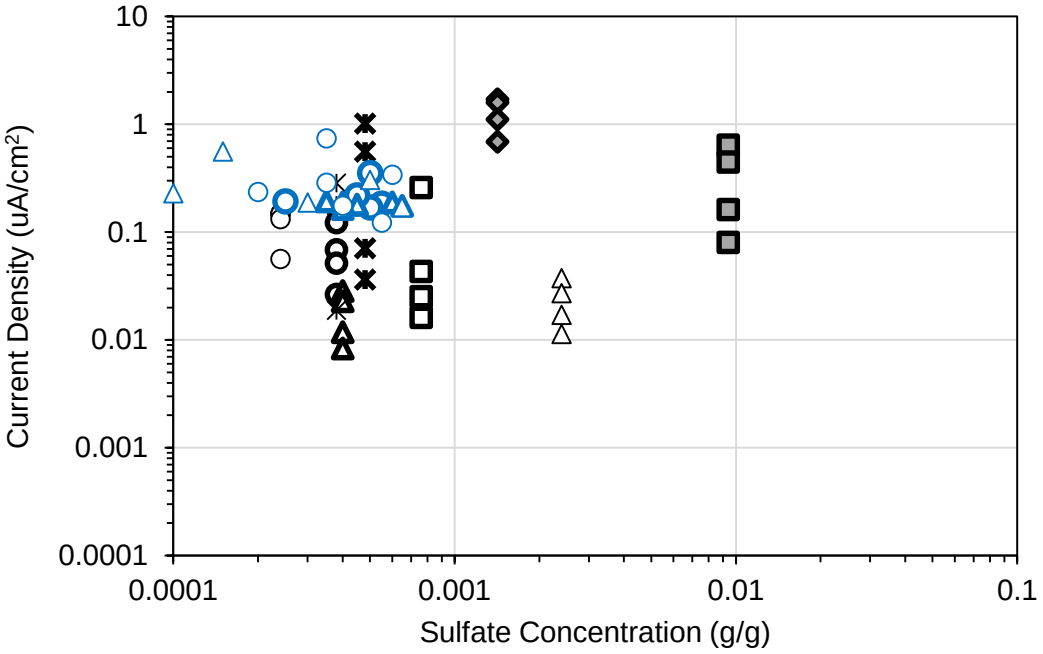

Figure 5.9. Correlation of steel corrosion current density and grout sulfate content. Circle: Grout A. Triangle: Grout B. Square: Grout C. Diamond: Grout D. Cross: Neat Grout. Filled: Expired Grout. Blue: MIT. Black: INT.

CHAPTER 6 SULFATE ION MOBILITY

Test results from MIT specimens cast as part of an earlier study were evaluated to identify the mobility and stratification characteristics of sulfate and chloride ions, and moisture during grout hydration in tendons. Experiments were conducted with 15-foot tendons which were cast in clear PVC pipes with 3-inch diameter.

6.1. MATERIALS AND METHODS

Test tendons were prepared using 15-foot long, 3-inch diameter clear PVC pipes and were positioned at 30^o incline as shown in Figure 6.1. Two 7-wire pre-stressed strands (270 7W low relaxation, 0.6-inch diameter) were placed within each tendon. All grout materials used were past the expiration dates indicated by the manufacturer. The grout mixtures were prepared with 15% excess mix water over the manufacturer's recommendation. Sulfate and chloride ion concentrations in the mix water were adjusted using Na_2SO_4 and NaCl, respectively. The test samples were prepared to contain ~0.09%, ~0.9%, ~5.5% sulfate levels (2,000 ppm, 20,000 ppm, 150,000 ppm Na_2SO_4, referred as low, medium, and high sulfate samples) and ~0.08% and ~0.2% chloride levels (2,800 ppm, 7,000 ppm NaCl, referred as low and high chloride samples) by cement mass. One pair of tendons was considered as the control with no chemical addition in the mix water. Duplicate tendons were prepared for each test condition.

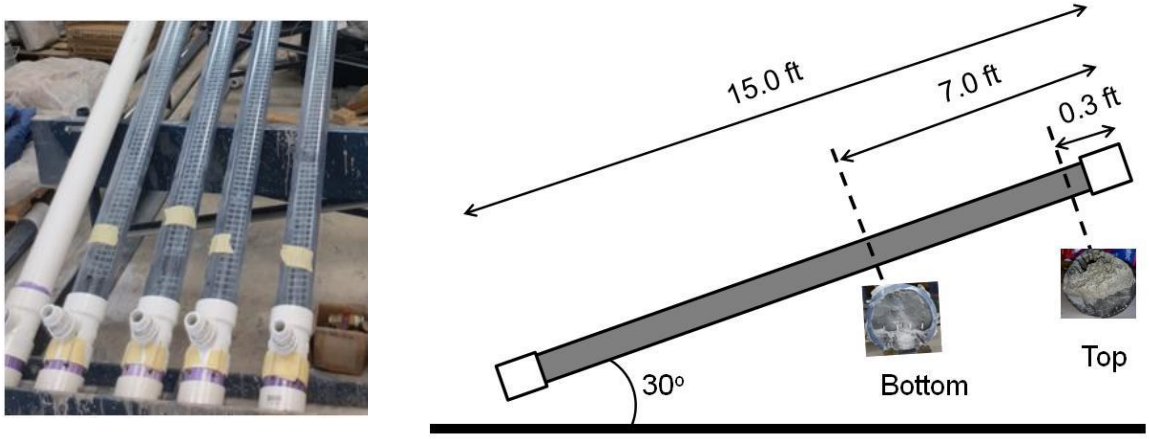

(a) (b)

Figure 6.1**.** Modified Incline Tube Test (MIT) tendons.
(a) 15-ft test tendons, (b) Schematic of the orientation and sampling locations

After one year, the test tendons were cut and evaluated by visual examination and chemical analyses. The chemical analyses for sulfate and chloride ions were conducted for the grout samples collected from the top (~0.3 ft from top) and bottom

(~7 ft from top) sections of the tendons. The moisture content of the grout samples was determined by ASTM C642.

The collected grout samples were crushed to pass a No. 100 sieve. An ex-situ leaching procedure following a FM 5-618 method was adopted for determination of sulfate and chloride. This method included drying the powder samples at 55°C for 24 hours, combining 1g dried powder with 1:10 leaching volume at 66°C for 15-18 hours, followed by filtering and diluting the leachate into 100 mL solution. Sulfate and free chloride ion analyses were conducted by ion chromatography. The results were reported as mg ion as SO_4^{2-} or Cl^- per kilogram of dry powder mass.

6.2. RESULTS AND DISCUSSION

The visual examination of the tendon cut after one year showed noticeable differences in the appearances of the grout samples that were prepared with different conditions. Moisture content analyses of the grout samples from the top sections showed significantly higher levels than the bottom samples as shown in Fig. 2. Severe grout segregation was observed at top section of the tendons with zero and medium added sulfate concentrations. These samples also had the highest moisture content (near 70%) in comparison to the other test tendons (Figure 6.2).

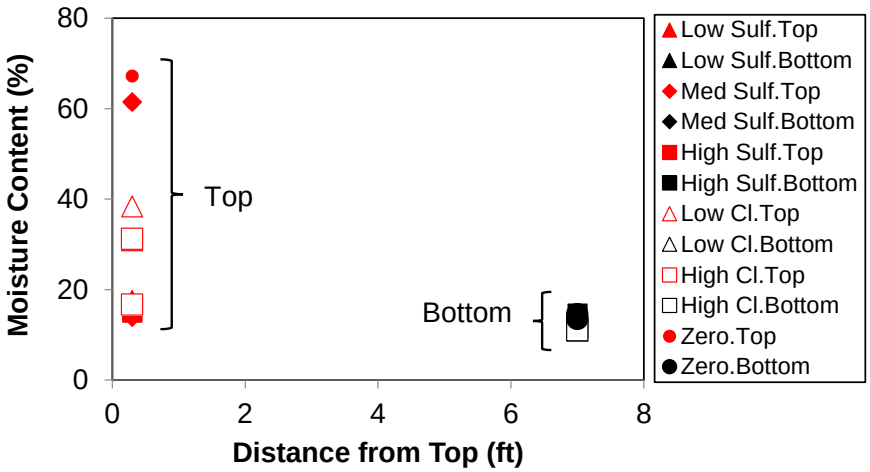

Figure 6.2. Variation in the moisture content of the grout samples from top and bottom segments of the tendons.

Significantly higher levels of both sulfate and chloride ions were detected in the grout samples collected from the top of the tendons in comparison to those collected 7-feet from the top (bottom) (Figure 6.3). One sample with medium sulfate concentration (20,000 ppm) exhibited very high concentrations. This anomaly may be caused by mixing inefficiencies during grout preparation which may have resulted in formation of pockets with high sulfate concentration that did not blend with the rest of the mixture. It is likely that presence of the salts reduced the water availability in the pore structure. Although very low levels of chloride ions were added to the mix,

the moisture content in the samples from the top of tendons with added NaCl was half of those from the control tendons with no added ions.

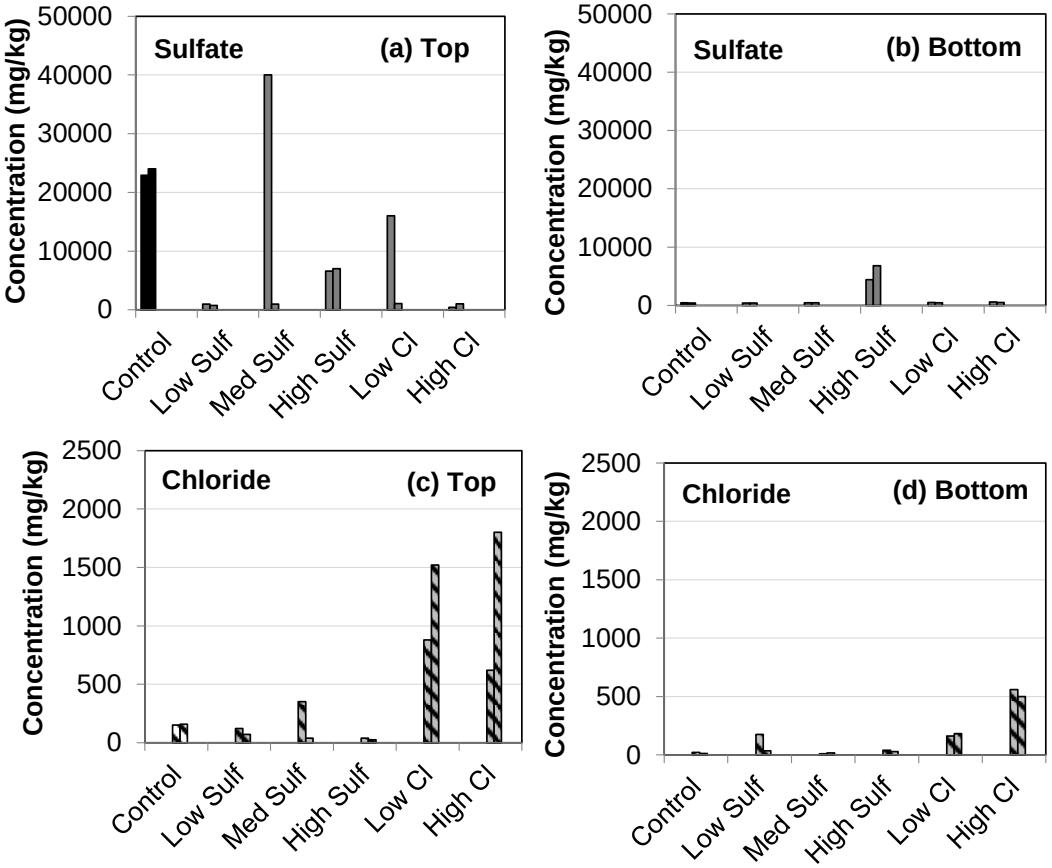

Figure 6.3. Sulfate and chloride levels in the samples taken from the top and bottom segments of the test tendons after one year.
The samples with 2,000 ppm, 20,000 ppm, 150,000 ppm Na_2SO_4 in mix water are referred as low, medium, and high sulfate samples; and those with 2,800 ppm, 7,000 ppm NaCl in mix water are referred as low and high chloride samples. (a) and (b) sulfate levels in grout samples from top and 7-feet from top, respectively; (c) and (d) chloride levels in grout samples from top and 7-feet from top, respectively.

Figure 6.4 presents the variation of ion concentrations with moisture content in the grout samples collected from top and 7-feet from the top (bottom). Tendons with segregated grout conditions in the top sections also had higher moisture content with relatively higher levels of sulfate and chloride ions. However, accumulation of the sulfate ions in the top segments was significantly higher than the chloride ions which may be partly due to the higher concentrations of sulfate ions than the chloride ions in the mix water (2,000 ppm, 20,000 ppm, 150,000 ppm Na_2SO_4 vs 2,800 ppm, 7,000 ppm NaCl). In tendons with no added ions, as much as 25000 mg/kg sulfate accumulated in the top sections. Hard material in the lower sections of the tendons had higher compression and lower moisture, as well as lower sulfate and chloride ion concentrations.

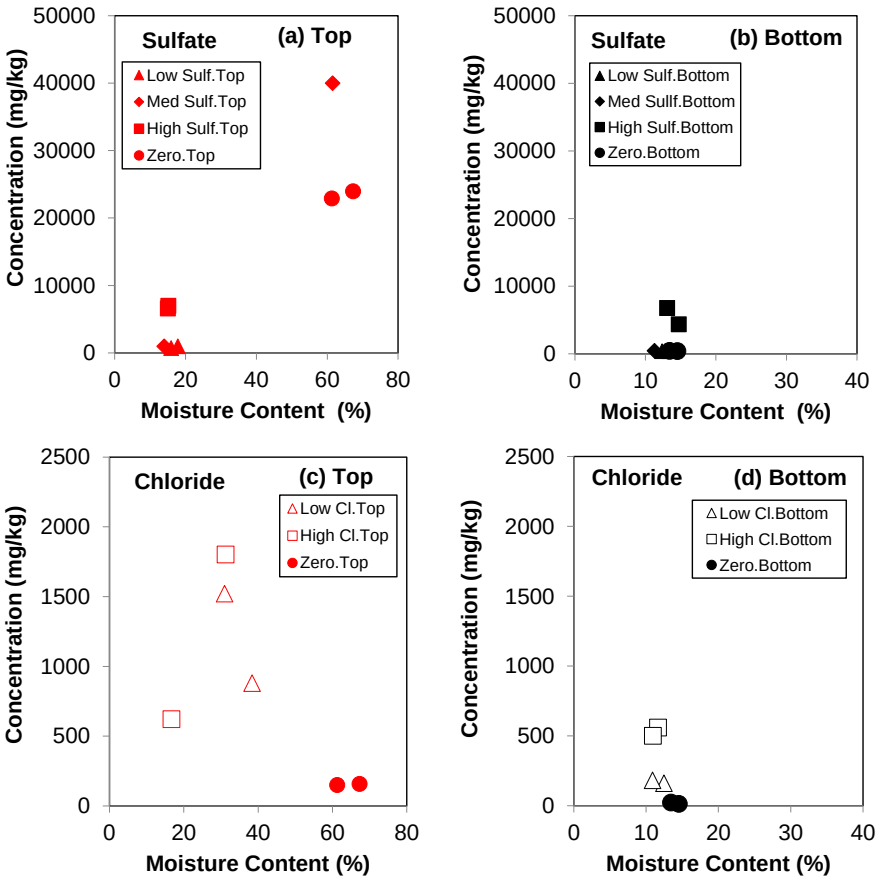

Figure 6.4. Variation in ion concentrations with moisture content in tendons prepared with different sulfate and chloride levels.
(a) and (b) sulfate levels in the grout samples collected after one year; (c) and (d) chloride levels in the grout samples collected after one year.

To quantify the ion stratification during the grout hydration and normalize the differences in the initial ion concentrations in the mix water, ion concentration factor (ICF) was defined as follows:

$$ICF = \frac{C_f}{C_i} \qquad (1)$$

where,
C_i: Ion concentration (as SO_4^{2-} or Cl^-) in the grout mix water (mg/L)
C_f: Ion concentration in leachate from the grout sample collected after one year (mg/L),

Figure 6.5a and 6.5 b present the ion concentration factor (ICF) for sulfate and chloride ions in the tendons with respect to the ion concentration in the grout mix water. There was no clear correlation between the ICF and the ion concentrations in the mix water. Fig. 5c and 5d presents the ion concentration factor (ICF) in the tendons for sulfate and chloride ions with respect to moisture content in the grout

samples collected from the tendons after one year. There was a direct correlation between ICF and moisture content in the grout samples which showed that higher moisture in the tendons also resulted in higher mobilization and stratification of ions in the tendons. The tendons with the high residual moisture after one year also had higher mobilization and increased concentrations of ions in top sections of the tendons, resulting in deficient grout conditions.

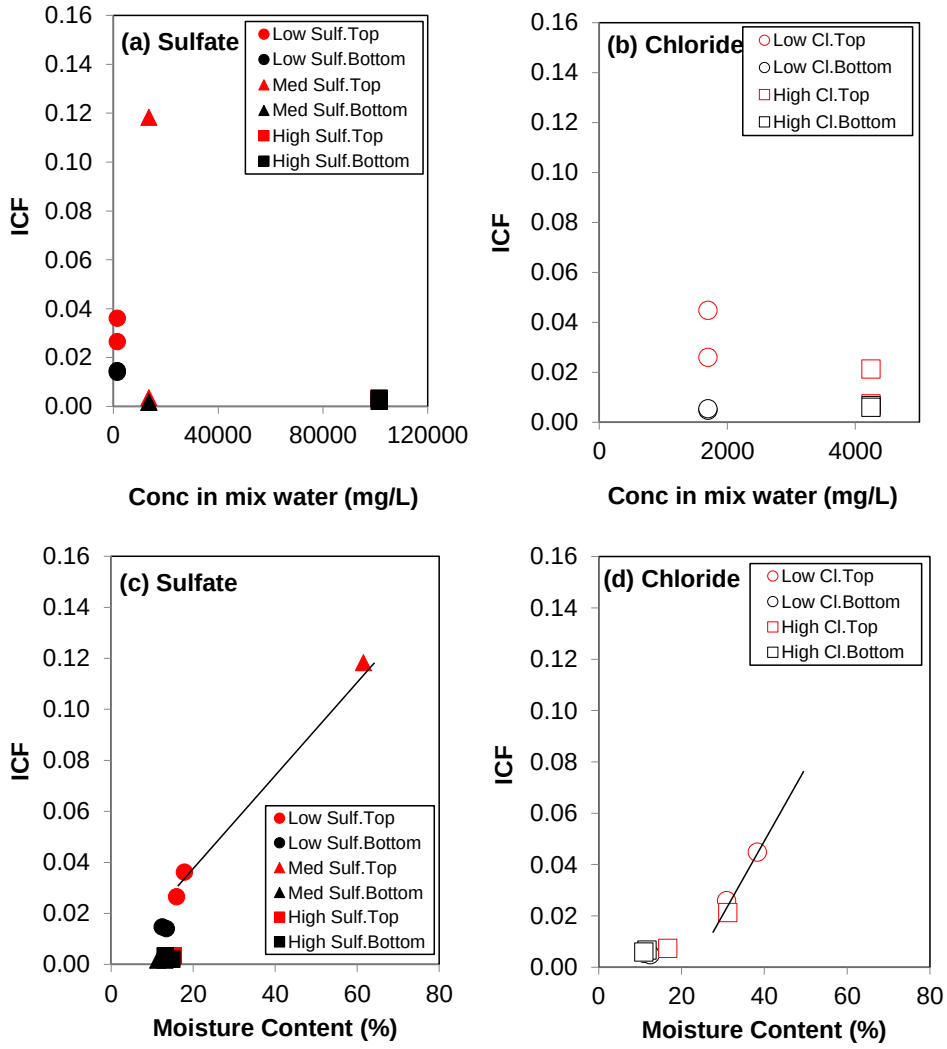

Figure 6.5. Variation in ion concentration factor (ICF) with ion concentration in the mix water and moisture content in the grout samples collected after one year. (a) variation of ICF for sulfate in the grout samples with sulfate concentration in the mix water; (b) variation of ICF for chloride in the grout samples with chloride concentration in the mix water; (c) variation of ICF for sulfate in the grout samples with moisture content after one year; (d) variation of ICF for chloride in the grout samples with moisture content after one year.

The structuring of water molecules around the ions affects their mobility and diffusion characteristics both in water and in concrete. Ions in solutions are classified as kosmotropes (structure makers) or chaotropes (structure breakers)

based on their relative abilities to interact and align with the water molecules around them. The degree of water structuring is determined by either the increase or decrease in viscosity of water due to added salt, or the entropies of ion solvation [53]. Table 6.1 presents the selected physico-chemical characteristics of the sulfate and chloride ions. Jones-Dole coefficient B is positive for kosmotropic ions and negative for chaotropic ions. Based on the Jones-Dole coefficient and entropy of salvation values, sulfate ions are kosmotropes, hence, result in structuring of water by aligning water molecules around them and creating a strong hydration shell around them. On the other hand, chloride ions are chaotropes and do not create a strong hydration shell around them.

Formation of strong hydration shells around the sulfate ions results in lower mobility and lower diffusion characteristics for sulfate ions in comparison to those for chloride ions. As shown in Table 6.1, diffusion coefficient of chloride ions in water is twice of that for sulfate ions (2.03×10^{-11} m^2/s for chloride vs 1.06×10^{-11} m^2/s for sulfate ions). In concrete, the diffusion coefficient of chloride ions is over 5,000 times higher than that for sulfate ions (0.28×10^{-8} to 4.00×10^{-8} m^2/s for chloride vs 3.0×10^{-12} to 4.2×10^{-12} m2/s for sulfate ions).

Under ideal conditions (i.e., uniform grout composition in the tendons), diffusion mechanisms would not play a role in ion transport. Experimental observations showed that mobilization of ions was enhanced by moisture transport during grout hydration. Moisture mobility caused by compression and grout hydration significantly increases the ion mobilization by advective transport (i.e., upward mobility of water in tendon) in addition to diffusive transport. As a result, tendons prepared using grouts prepared with excess mix water would result in deficient grouts due to stratification of ions and moisture as observed during this study.

Table 6.1. Characteristics of the ions studied in the cement mixture.

Parameter	Sulfate	Chloride
Ionic weight (Da)	96	35.5
Ionic radius (nm)	0.215 [a] to 0.230 [a]	0.181 [a,b]
Width of hydration shell (nm)	0.043[b]	0.043[b]
Hydrated radius (nm)	0.256 [b]	0.224 [b]
No of water molecules in hydration shell	3.1 [b]	2 [b]
Hydration free energy (kJ/mol) [c]	-1080 [b]	-340 [b] to -371 [a]
Solvation potential [c]	Likely to dissolve	Likely to dissolve
Jones-Dole coefficient B (dm^3/mol) [d,e,f]	+0.206 to +0.208 [a]	-0.007 [a]
Entropy of hydration (kJ/mol) [e]	-126 [a]	+6 [a]
Classification (based on potential for structuring water molecules) [f]	Kosmotrope (structure maker)	Chaotrope (structure breaker)
Mobility in water	Low	High
Diffusion coefficient in water (m^2/s)	1.06×10^{-11} [g]	2.03×10^{-11} [g]
Diffusion coefficient in concrete (m^2/s)	3.0×10^{-12} to 4.2×10^{-12} [h]	0.28×10^{-8} to 4.00×10^{-8} [i]

[a] Tansel, 2011 [53]
[b] Marcus, 1991 [54]
[c] A negative value for the hydration free energy corresponds to an ion that is likely to dissolve, whereas a high positive value means that solvation will not occur
[d] at 273 K
[e] Hribar et al., 2006 [55]
[f] Jones-Dole coefficient B is positive for kosmotropic ions and negative for chaotropic ions
[g] Samson et al., 2003 [56]
[h] Condor et al., 2011 [57]
[i] Zeng and Song, 2013 [58]

CHAPTER 7. CONCLUSIONS AND RECOMMENDATIONS

- Grout characteristics:
    - Different grout products have widely different propensity for segregation and accumulation of sulfate ions.
    - Adverse grout mixing practices such as the addition of 10% mix water above the manufacturer's recommendation and pre-hydration promote the development of grout deficiencies including the accumulation of sulfate ions.
    - Current commercially available grouts tested did not develop severe grout segregation in the form of soft grout and sulfate levels were within limits associated with corrosion.
    - Sulfate ion accumulation can occur without external sulfate ion sources. Sulfur content in the grout raw material showed modest correlation to the stratification of sulfate ions.
    - Grout flow restriction did not show appreciable effects on the accumulation of sulfate ions.
    - Mobilization of the sulfate ions was enhanced by moisture transport.

- Leaching Procedures:
    - Leaching of larger grout sample mass can yield higher leachate sulfate concentrations, but the concentrations were not commensurate to the larger grout mass. Leaching of a larger grout sample mass with a mass to water ratio of 1:10 was not shown to be efficient in the dissolution of sulfate ions.
    - Larger mass to water ratio (1:40) yielded higher leachate and normalized grout mass sulfate concentrations.
    - Predrying of grout samples to 100^{o}C for 24 hours was shown to incur losses in sulfate content.
    - The sulfate limits expressed as mass relative to the grout sample mass can be implemented to normalize leaching volume and mass size. Current FDOT specifications (30 ppm following current FM 5-618) can be expressed as 3 $mg_{sulfate}/g_{grout}$. Assessment of this limit to the corrosion data set developed is consistent with historic data from previous research.

- Recommended Modifications to FM 5-618

Preparation of Grout:

If necessary, crush the sample to approximately ¾"size using jaw crusher or other suitable device. Spread the sample in a thin layer on a clean tray and dry under ambient conditions until a constant mass is achieved, or dry in an oven at no higher than 140^{o}F (60^{o}C) for 24 hr or until a constant

mass is achieved. Pulverize sample with mechanical pulverizer or another suitable device until it passes through a No. 100 mesh (150um) sieve. Split the sample per AASHTO R76 to obtain 25 ± 1g.

Weigh 5 ± 0.1g of the dried powder into a clean 250 mL beaker. Add 200 mL of deionized water to obtain 1:40 leaching volume; stir and cover with a watch glass. Repeat for multiple samples.

Place the sample on a 135 ± 5^{o}F (57 ± 3^{o}C) hot plate. Remove the sample from the hot plate after 18-24 hr digestion time.

Set up a 500 mL filter flask for each sample solution. Place a funnel on top of each flask. Fold and place a No. 42 size filter paper in each funnel and connect the filter flask to the vacuum.

Using deionized water for all rinsing. Rinse any residue left on the stirring rod and on the underside of the watch glass into the funnel. Decant as much solution as possible through the filter.

Transfer the obtained solutions to 250 mL vials, and add deionized water to reach 250 mL for each solution.

Testing of Samples

Use FM 5-553 to obtain sulfate level from sample.

Comply with sections 2, 3 and 6 of FM 5-553.

The final sulfate ion concentration M associated with the leachate concentration determined by the test method can be calculated by the formula:

$$M = \frac{C\,V}{m}$$

where
M= SO_4^{2-} concentration in mg $_{Sulfate}$/g $_{Grout}$
C= SO_4^{2-} concentration of leachate in mg/L
V= Volume of sample in L (0.25 L)
m= dry mass of grout in gr (5 g)

REFERENCES

1. M.K. Hurst, Prestressed concrete design. 2nd Ed. CRC Press, New York, 2002.
2. K. Lau, I. Lasa, Corrosion of prestress and post-tension reinforced-concrete bridges, In: A. Poursaee, Corrosion of Steel in Concrete Structures, Woodhead Publishing., Cambridge 2016, pp. 37-57. https://doi.org/10.1016/B978-1-78242-381-2.00003-1
3. K. Lau, M. Paredes, and J. Rafols. Corrosion Evaluation of Post-Tensioned Tendons with Dissimilar Grout, CORROSION/2012. No.1738, NACE International, Salt Lake City, Utah (2012) 11-15 March; NACE International: Houston, TX, USA.
4. K. Lau, I. Lasa, M. Parades, Corrosion Development of PT Tendons with Deficient Grout: Corrosion Failure in Ringling Causeway Bridge. Florida Department of Transportation State Materials Office, Draft Report. (2011).
5. K. Lau, R. Powers, M. Paredes. Corrosion Evaluation of Repair-Grouted Post-Tensioned Tendons in Presence of Bleed Water. CORROSION/2013, Paper No. 2604, NACE International, Orlando, Florida (2013) 17-21March 2013; NACE International: Houston, TX, USA.
6. K. Lau, J. Rafols, M. Paredes, I. Lasa. Laboratory Corrosion Assessment of Post-Tensioned Tendons Repaired with Dissimilar Grout. CORROSION/2013, Paper No. 2602, NACE International, Orlando, Florida (2013) 17-21March 2013; NACE International: Houston, TX, USA.
7. K. Lau, M. Paredes, I. Lasa. Corrosion Failure of Post-Tensioned Tendons in Presence of Deficient Grout. CORROSION/2013, Paper No. 2600, NACE International, Orlando, Florida (2013) 17-21March 2013; NACE International: Houston, TX, USA.
8. K. Lau, I. Lasa, and M. Paredes, Bridge Tendon Failures in the Presence of Deficient Grout. Materials Performance, 52(2013) 64-68.
9. K. Lau, I. Lasa, and M. Paredes. Update on Corrosion of Post-Tensioned Tendons with Deficient Grout, CORROSION/2014. Paper No. 4225, NACE International, San Antonio, Texas (2014) 9-13 March; NACE International: Houston, TX, USA.
10. S. Permeh, K.K. Krishna Vigneshwaran, K. Lau, Corrosion of Post-Tensioned Tendons with Deficient Grout, Florida Department of Transportation, Final Report, Contract No. BDV29-977-04, October 20, 2016.
11. S. Permeh, K.K. KrishnaVigneshwaran, K. Lau, I. Lasa, and M. Paredes. Material and Corrosion Evaluation of Deficient PT Grout with Enhanced Sulfate Concentrations. CORROSION/ 2015, Paper No. 5828, NACE International, Dallas, Texas (2015) 15-19 March 2015; NACE International: Houston, TX, USA.
12. S. Permeh, K.K. KrishnaVigneshwaran, K. Lau, and I. Lasa. Anodic Behavior of Steel in Enhanced Sulfate Solutions. CORROSION/2016, paper No. 7712, NACE International, Vancouver, British Columbia, Canada (2016) 6-10 March 2016, NACE International: Houston, TX, USA.

13. K.K. Krishna Vigneshwaran, S. Permeh, I. Lasa, and K. Lau. Corrosion of Steel in Deficient Grout with Enhanced Sulfate Content. NACE Concrete Service Life Extension Conference 2015. Paper No. CCC15-6942; NACE International: Houston, TX, USA.
14. J.C. Rafols, K. Lau, I. Lasa, M. Paredes, and A. ElSafty. Approach to determine corrosion propensity in post-tensioned tendons with deficient grout. Open Journal of Civil Engineering, 3 (2012), Article ID: 36394.
15. S. Permeh, K. K.Krishna Vigneshwaran, K.Lau., and I.Lasa. Corrosion of PT Tendons in Deficient Grout in Presence of Enhanced Sulfate and Chloride Concentration. NACE Corrosion Risk Management Conference 2016, Paper No. 16-18751, NACE International: Houston, TX, USA.
16. V.K. Gouda, Corrosion, and corrosion inhibition of reinforcing steel: I. Immersed in alkaline solutions. British Corrosion Journal, 5(1970)198-203.
17. V.K. Gouda, and W.Y. Halaka, Corrosion and corrosion inhibition of reinforcing steel: II. Embedded in concrete. British Corrosion Journal, 5(1970) 204-208.
18. A.J. Al-Tayyib, S.K. Somuah, J.K. Boah, P. Leblanc, A.I. Al-Mana, Laboratory study on the effect of sulfate ions on rebar corrosion. Cement and Concrete Research, 18(1988) 774-782.
19. A.J. Al-Tayyib, M.S. Khan, Effect of sulfate ions on the corrosion of rebars embedded in concrete. Cement and Concrete Composites, 13(1991), 123-127.
20. C. Alonso Cobos, M. Acha, A. Perd, Corrosión bajo tensión de alambres de acero de pretensado, en medios alcalinos conteniendo sulfatos. Hormigón y Acero, 41(1990).
21. E. Blactot, C. Brunet-Vogel, F. Farcas, L. Gaillet, I. Mabille, T. Chaussadent, E. Sutter, Electrochemical behaviour and corrosion sensitivity of prestressed steel in cement grout. WIT Transactions on engineering sciences, 54 (2007).
22. A.H. Dehwah, M. Maslehuddin, S.A. Austin, S. A, Long-term effect of sulfate ions and associated cation type on chloride-induced reinforcement corrosion in Portland cement concretes. Cement and Concrete Composites, 24(2002), 17-25.
23. E. Blactot, C. Brunet-Vogel, F. Farcas, L. Gaillet, I. Mabille, T. Chaussadent, E. Sutter, Electrochemical behaviour and corrosion sensitivity of prestressed steel in cement grout. WIT Transactions on engineering sciences, 54 (2007).
24. K.K. Krishna Vigneshwaran, S. Permeh, M. Echeverría, K. Lau, and I Lasa, Corrosion of Post-Tensioned Tendons with Deficient Grout. Part 1. Electrochemical Behavior of Steel in Alkaline Sulfate Solutions, Corrosion 74 (2018) 362-371. https://doi.org/10.5006/2541
25. S. Permeh, K.K. KrishnaVigneshwaran, M. Echeverría, K. Lau, and I Lasa. Corrosion of Post-Tensioned Tendons with Deficient Grout. Part 2. Segregated Grout with Enhanced Sulfate, Corrosion 74 (2018) 457-467. https://doi.org/10.5006/2568
26. S. Permeh, K.K. Krishna Vigneshwaran, K. Lau., and I. Lasa, Corrosion of Post-Tensioned Tendons with Deficient Grout. Part 3: Segregated Grout with Elevated Sulfate and Vestigial .

27. S. Permeh, K. Lau, M. Duncan, and R. Simmons, Identification of Steel Corrosion in Alkaline Sulfate Solution by Electrochemical Noise, Materials and Corrosion, April 2021. https://doi.org/10.1002/maco.202112347
28. S. Permeh, K. Lau, M. Duncan, and R. Simmons , Initiation of Localized Steel Corrosion in Alkaline Sulfate Solution, Material and Structures, Under review. (2021)
29. H.R. Hamilton, Revised Draft Final Report to Florida Department of Transportation. Simulation of Prepackaged Grout Bleed under Field Conditions. Final Report, BDK75-977-59. April 2014.
30. HFW. Taylor, Cement chemistry. Vol. 2. London: Thomas Telford, 1997.
31. Section 938, Duct Filler for Post-Tensioned Structures, Florida Department of Transportation, Standard specification for road and bridge construction, Florida, July 2020.
32. FM 5-618, Florida Method of Test for Sampling of Post-Tensioned Tendon Grout, Florida Department of Transportation, Tallahassee, FL, 2018.
33. PTI M55.1-19. Specification for Grouting of Post-Tensioned Structures. Post-Tensioning Institute. Farmington Hills, MI.
34. R, Sonawane., Permeh, S., Garber, D., Lau, K., Simmons, R., and Duncan, M., Test Methods to Identify Robustness of Grout Materials to Resist Corrosion, CORROSION/2020, Paper No. 14820, NACE International, Digital proceeding, NACE International: Houston, TX, USA
35. S.Permeh, R, Sonawane, K.Lau, M. Duncan, R.Simmons, Update on the Evaluation of Grout Robustness and Corrosion by Accelerated Corrosion and Rapid Macrocell Testing, CORROSION/2021, Paper No. 16339, NACE International, Digital proceeding, NACE International: Houston, TX, USA
36. R, Sonawane, S.Permeh, K.Lau, M. Duncan, R.Simmons, Review on the Determination of Sulfate Ion Concentrations in Deficient Post-Tensioned Grouts, CORROSION/2021, Paper No. 16342, , NACE International, Digital proceeding, NACE International: Houston, TX, USA.
37. F.Y. Ma, Corrosive Effects of Chlorides on Metals. In Pitting Corrosion. Ed. N. Bensalah. 2012 http://www.intechopen.com/books/pitting-corrosion
38. C.M. Hansson, Corrosion of stainless steel in concrete. Chapter 4, 59-85 In: A. Poursaee, Corrosion of Steel in Concrete Structures. Woodhead Publishing., Cambridge 2016, pp. 59-85
39. Colajanni, P., Recupero, A., et al., Failure by Corrosion in PC Bridges: a case history of a viaduct in Italy., International Journal of Structural Integrity, 7(2), 181-193, March 2016.
40. Bertolini, Luca, and Maddalena Carsana. "High pH corrosion of prestressing steel in segregated grout." Modelling of corroding concrete structures. Springer Netherlands, 2011. 147-158.
41. HFW. Taylor, Cement chemistry. Vol. 2. London: Thomas Telford, 1997.
42. Essam A. Kishar, Doaa A. Ahmed, Maha R. Mohammed, Rehab Noury, “Effect of calcium chloride on the hydration characteristics of ground clay bricks cement

pastes" Beni-Suef University Journal of Basic and Applied Sciences,Volume 2, Issue 1,2013,Pages 20-30,
43. Lagerblad, Björn. Leaching performance of concrete based on studies of samples from old concrete constructions. SKB, 2001.
44. Corven, John, and Alan Moreton. Post-tensioning tendon installation and grouting manual. No. FHWA-NHI-13-026. 2013.
45. Ulf Håkansson, Lars Hässler, Håkan Stille, Rheological properties of microfine cement grouts,Tunnelling and Underground Space Technology, Volume 7, Issue 4, 1992, Pages 453-458
46. Schokker, A.J., Breen, J.E., and Kreger, M.E., "Grouts for Bonded Post-Tensioning in Corrosive Environments," ACI Materials Journal, Vol. 98 No. 4, July-August 2001, pp. 296-305.
47. PTI M55.1-19. Specification for Grouting of Post-Tensioned Structures. Post-Tensioning Institute. Farmington Hills, MI.
48. Lee, S. K., & Zielske, J. (2014). An FHWA special study: post-tensioning tendon grout chloride thresholds (No. FHWA-HRT-14-039).
49. R.S. Barneyback, Sidney Diamond,Expression and analysis of pore fluids from hardened cement pastes and mortars, Cement and Concrete Research, Volume 11, Issue 2, 1981, Pages 279-285,
50. Johnson, C. M., & Nishita, H. (1952). Microestimation of sulfur in plant materials, soils, and irrigation waters. Analytical chemistry, 24(4), 736-742.
51. Hamilton, H. R., Piper, A., Randell, A., & Brunner, B. (2014). Simulation of prepackaged grout bleed under field conditions (No. BDK75 977-59). University of Florida.
52. Hamilton, H.R., Torres, E., Aguirre, M., Ferraro, C. Final Report to FDOT. "Evaluation of Shelf Life in Post-Tensioning Grouts." BDV31-977-31. 2018.
53. B. Tansel, Significance of thermodynamic and physical characteristics on permeation of ions during membrane separation: Hydrated radius, hydration free energy and viscous effects. Separation and Purification Technology 86 (2011), 119–126.
54. Y. Marcus, Y., 1991. Thermodynamics of solvation of Ions: Part 5 Gibbs free energy of hydration at 298.15 K. , J. Chem. SOC., Faraday Trans., 1987,87(18), 2995-2999.
55. B. Hribar, N.T. Southall, V. Vlachy, A. Ken, K.A. Dill. How Ions Affect the Structure of Water. J. Am. Chem. Soc. 124 (2002), 12302–12311.
56. E. Samson, J. Marchandl, K.A. Snyder. Calculation of ionic diffusion coefficients on the basis of migration test results. Materials and Structures. 36 (2003), 156-165.
57. J. Condor, K. Asghari, and D. Unatrakarn. Experimental results of diffusion coefficient of sulfate ions in cement type 10 and class G.Energy Procedia 4 (2011): 5267-5274.
58. L. Zeng, R. Song, 2013. Controlling chloride ions diffusion in concrete, Scientific Reports 3, 3359. https://doi.org/10.1038/srep03359

APPENDIX: INT GROUT SPECIMENS

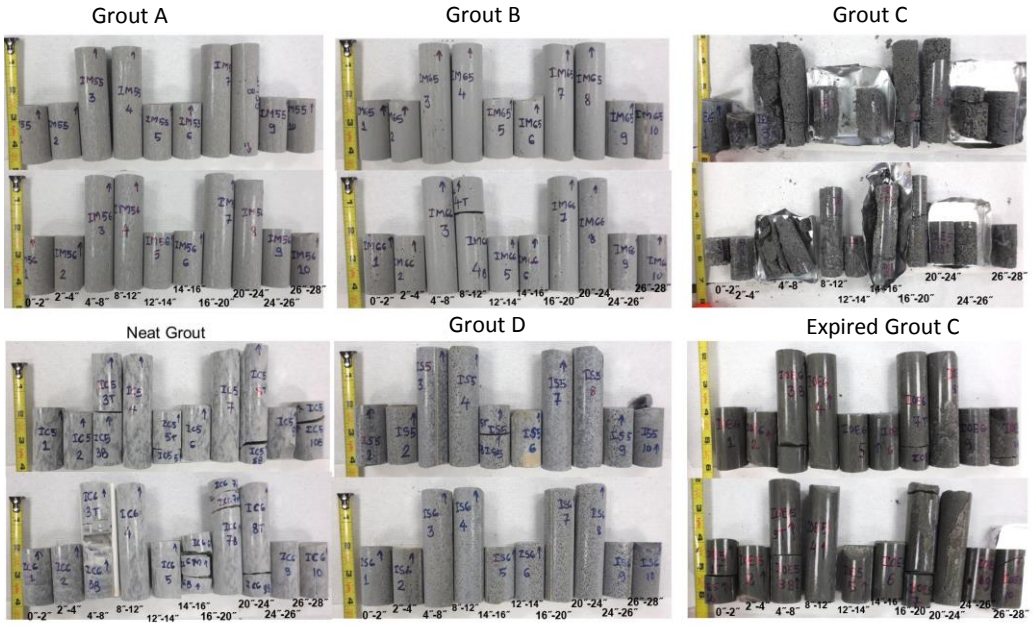

Figure A1. INT Tee-header test specimen after opening, cast with extra 10% mix

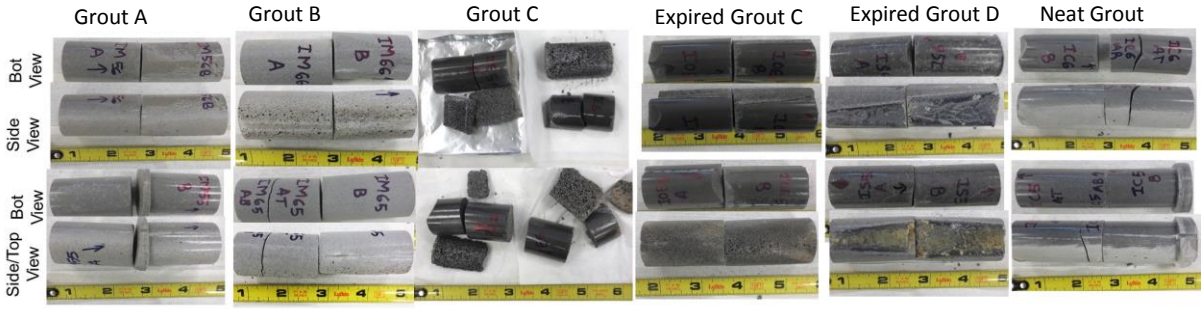

Figure A2. INT Tee-body test specimen after opening, cast with extra 10% mix water

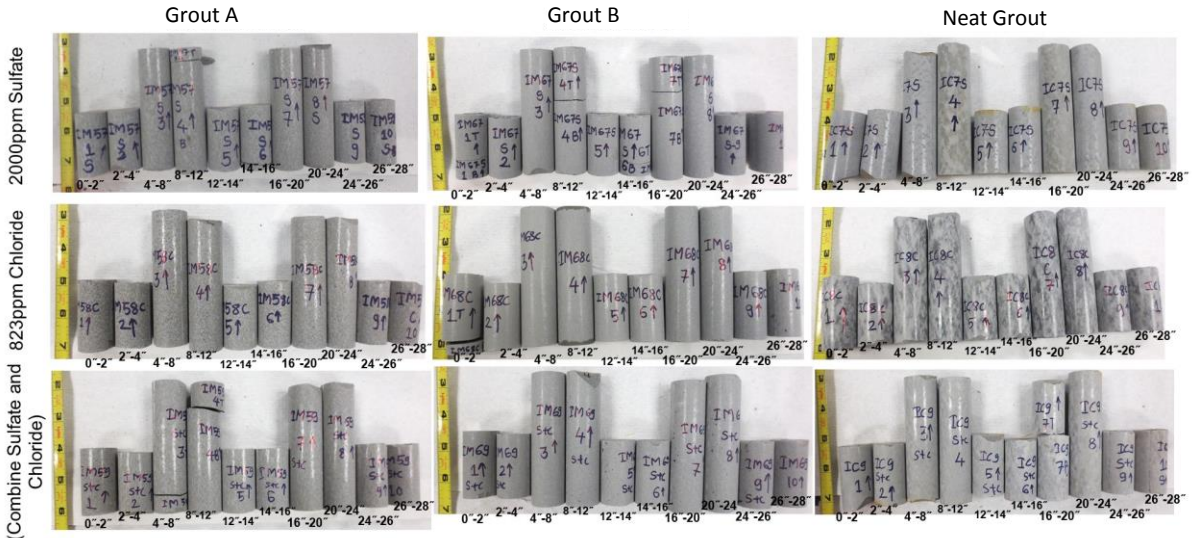

Figure A3. INT Tee-header test specimen after opening, cast with external ion contamination and extra 10% mix water

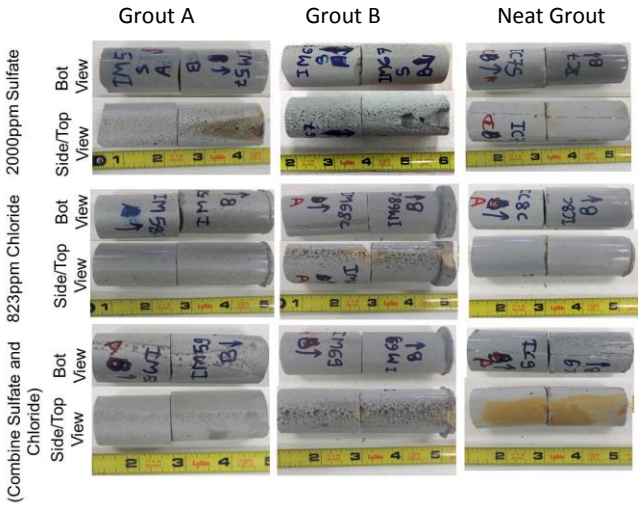

Figure A4. INT Tee-body test specimen after opening, cast with external ion contamination and extra 10% mix water

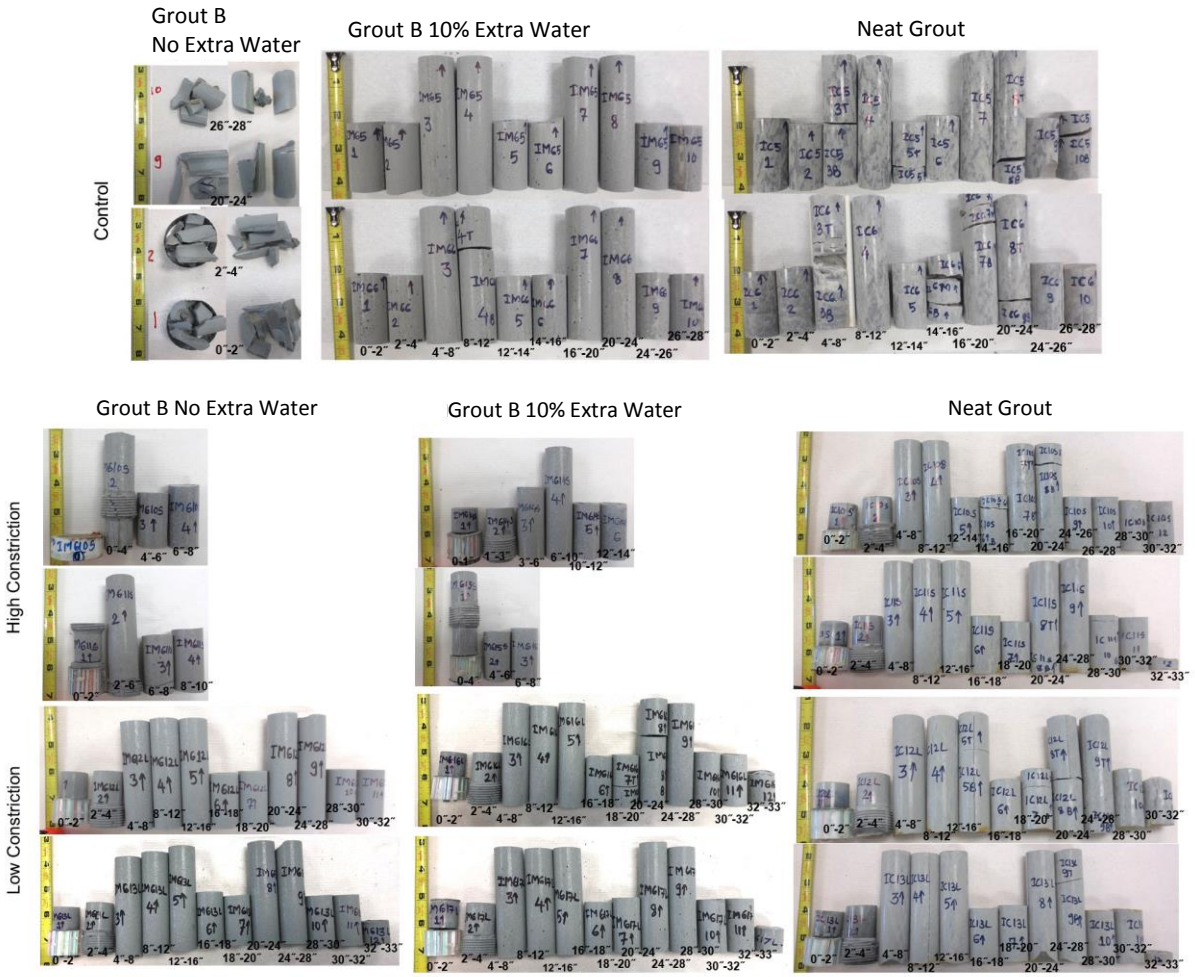

Figure A5. INT Tee-header test specimen after opening, cast with control and physical confinement condition

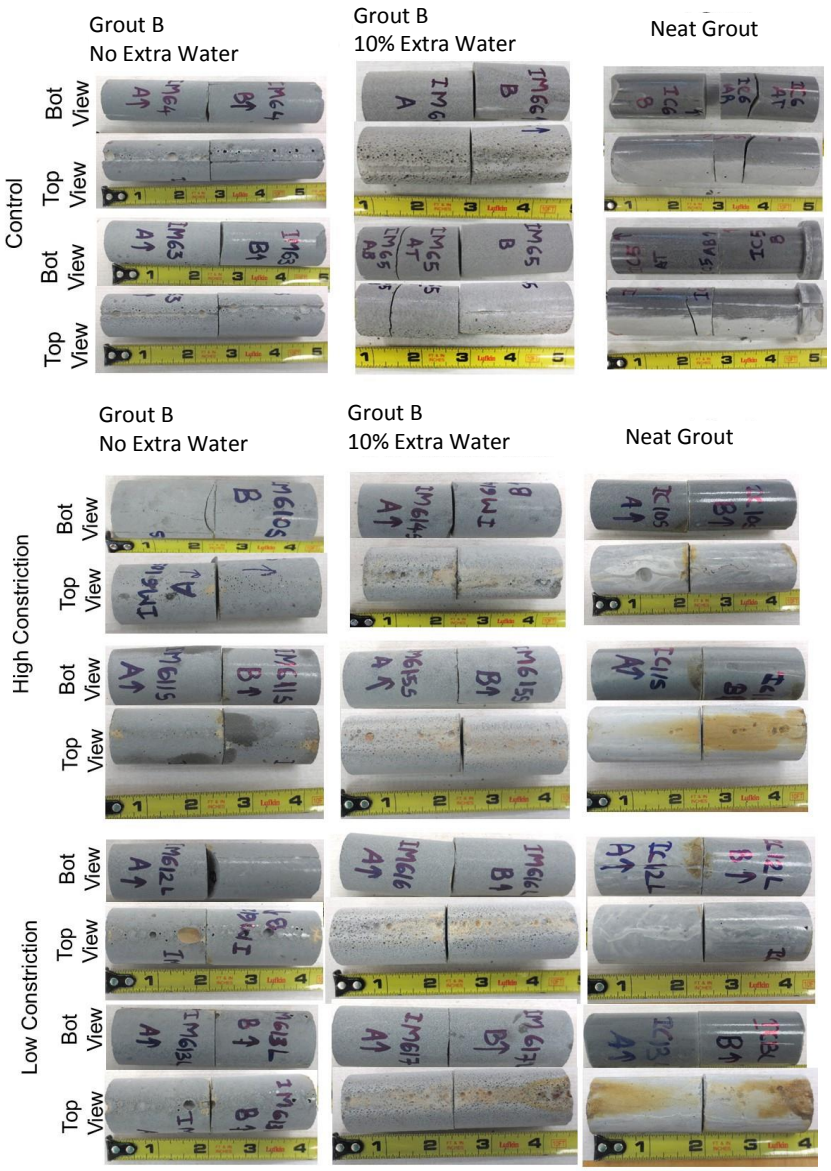

Figure A6. INT Tee-body test specimen after opening, cast with control and physical confinement condition